

WIGGLE Room

AD-A198 845

卷之三

ZEPHYRUS
UNIVERSITY OF TORONTO LIBRARY

卷之三

ANNUAL REPORT PERIOD SEPTEMBER 1965 TO NOVEMBER 1967

RECORDED AND INDEXED BY COMPUTER

The logo for Defense Technical Information Center (DTIC) features the acronym "DTIC" in large, bold, serif capital letters at the top. Below it, the words "DEFENSE TECHNICAL INFORMATION CENTER" are written in a smaller, all-caps serif font. A circular seal is positioned to the right, containing a stylized eagle with wings spread, perched atop a shield, with the word "SECURITY" visible at the bottom of the circle.

62 8-09 197

CONFIDENTIAL INFORMATION CHECKLIST

CONFIDENTIAL

**ALL INFORMATION CONTAINED HEREIN IS UNCLASSIFIED AND IS
EXEMPT FROM EXEMPTION 1, 3, 4, AND 5 OF THE FOIA.**

THIS PAGE IS UNCLASSIFIED AND IS EXEMPT FROM EXEMPTION 1, 3, 4, AND 5 OF THE FOIA.

CONFIDENTIAL

CONFIDENTIAL

UNCLASSIFIED
SECURITY CLASSIFICATION OF THIS PAGE

Form Approved
OMB No. 0704-0188

REPORT DOCUMENTATION PAGE			
1a. REPORT SECURITY CLASSIFICATION UNCLASSIFIED		1b. RESTRICTIVE MARKINGS	
2a. SECURITY CLASSIFICATION AUTHORITY		3. DISTRIBUTION/AVAILABILITY OF REPORT Approved for public release, distribution is unlimited	
2b. DECLASSIFICATION/DOWNGRADING SCHEDULE			
4. PERFORMING ORGANIZATION REPORT NUMBER(S)		5. MONITORING ORGANIZATION REPORT NUMBER(S) AAMRL-TR-88-016	
6a. NAME OF PERFORMING ORGANIZATION Biomedical Engineering Laboratory		6b. OFFICE SYMBOL (If applicable)	
7a. NAME OF MONITORING ORGANIZATION Harry G. Armstrong Aerospace Medical Research Laboratory		7b. ADDRESS (City, State, and ZIP Code) Wright-Patterson AFB OH 45433-6573	
8c. ADDRESS (City, State, and ZIP Code)		8b. OFFICE SYMBOL (If applicable)	
9. PROCUREMENT INSTRUMENT IDENTIFICATION NUMBER		10. SOURCE OF FUNDING NUMBERS	
11. TITLE (Include Security Classification) Human Auditory and Visual Unimodal and Bimodal Continuous Evoked Potentials (U)		PROGRAM ELEMENT NO. 62202F	PROJECT NO. 7184
12. PERSONAL AUTHOR(S) Goldman, Zvi Z.		TASK NO. 14	WORK UNIT ACCESSION NO. D6
13a. TYPE OF REPORT Summary	13b. TIME COVERED FROM Sept 83 TO Nov 87	14. DATE OF REPORT (Year, Month, Day) 1988 March	15. PAGE COUNT 188
16. SUPPLEMENTARY NOTATION			
17. COSATI CODES	18. SUBJECT TERMS (Continue on reverse if necessary and identify by block number) Evoked Potentials, Lock-In Amplifier Application Sensory Integration: Human Steady-State EP Audio-Visual Interaction		
19. ABSTRACT (Continue on reverse if necessary and identify by block number) This research has adapted the phase-lock technique in recording of Continuous Evoked Potentials (CEPs, also referred to as "steady-state" potentials) for monitoring of the auditory and visual sensory channel engagement and for stimulus parameter-space characterization of the Auditory-Visual Interaction effect (AvV). Sensory interaction was concluded whenever response variations of one sensory channel could be attributed to parameter changes of an additional stimulus, simultaneously presented to another sensory channel.			
The stimuli consisted of sinusoidally modulated, 100% amplitude-modulated tone and spot-light signals. The independent variables were the stimulus modality (audio, visual or both), Modulation Frequency (MF, 5-61 Hz), intensity (24 dB range) and subject attentiveness. CEPs were recorded from Cz-A1 (auditory) and Oz-A1 (visual) sites. The CEP dependent variables were the magnitude and phase of the evoked potential component phase-locked to (continue on reverse)			
20. DISTRIBUTION/AVAILABILITY OF ABSTRACT <input checked="" type="checkbox"/> UNCLASSIFIED/UNLIMITED <input type="checkbox"/> SAME AS RPT. <input type="checkbox"/> DTIC USERS		21. ABSTRACT SECURITY CLASSIFICATION UNCLASSIFIED	
22a. NAME OF RESPONSIBLE INDIVIDUAL Dr Andrew M. Junker		22b. TELEPHONE (Include Area Code) 513-255-8747	22c. OFFICE SYMBOL AAMRL/HEG

19. ABSTRACT (Continued)

the stimulus fundamental or 2nd harmonic MF. The CEPs were characterized in terms of their magnitude, phase and latency Modulation Transfer Functions, background EEG, repeatability, linearity, and stimulus intensity and subject attentiveness dependencies.

CEP magnitude peaks were obtained at 5-6 Hz (major), 8-14 Hz, 18-22 Hz and 40-50 Hz (only auditory) MF regions. Estimated from linear models fitted to the magnitude data, these peaks were associated with averaged latency/delay values of 205 msec/60 msec, 200 msec/80 msec, 70 msec/30 msec and 25 msec/10 msec, respectively, suggesting cortical origins. Most of the results were derived from two MF regions, "Beta" (16-25 Hz) and "Theta" (5-6 Hz). Responses elicited from these MF regions were consistent, exclusively evoked, repeatable and easily detectable. In comparison to the auditory CEPs, the visual CEPs were associated with higher signal/noise magnitude ratio, higher inter-subject variability and lower intra-subject variability.

Genuine AxV effects of 5.5 dB magnitude-gain and 40 degree phase-shift were found. Magnitude inhibition and phase lag were generally associated with, and induced by, the short-latency Beta MF region. Magnitude data was primarily affect by "Internal" parameters (intra-modality stimulus intensity or MF) and phase data by "External" parameters (cross-modality stimulus intensity). Attention allocation did not play a major role.

This line of investigation can lead to further understanding of human sensory-channel transfer function and sensory information integration, and, may help in designing more effective man-machine communication channels.

PREFACE

This report is based on doctoral research, initially and partially supported by the Armstrong Aerospace Medical Research Laboratory under contract number F33615-81-K-0510 (half-time Research Assistant position over a time period of approximately two years). During that time an auditory response equivalent to the visual "steady-state" response was explored with the goal of obtaining an on-going "secondary-task" response to be utilized in monitoring human-operator performance on a primary visual task.

The additional, non-sponsored material presented in this report includes characterization and comparison of the auditory and visual responses and a pilot investigation of the parameter-space of the electrophysiological human auditory-visual integration process.

I wish to thank Dr. R. Northrop, the director of the Biomedical Engineering Laboratories in the University of Connecticut, for his support and guidance, and, A. M. Junker, the contract monitor, for his enthusiastic involvement.

Accession For	
NTIS GRA&I	<input checked="" type="checkbox"/>
DTIC TAB	<input type="checkbox"/>
Unannounced	<input type="checkbox"/>
Justification	
By _____	
Distribution/ _____	
Availability Codes	
Dist	Avail and/or Special
R'	

QUALITY
INSPECTED
2

Table of Contents

PART I: INTRODUCTION	1
Background	2
1.1 Motivation	2
1.2 Brain potentials	3
1.2.1 EEG and evoked potentials	3
1.2.2 Evoked potential methodologies	5
1.2.2.1 Ensemble averaging approach	6
1.2.2.2 Single-trial approach	7
1.2.2.3 Lock-in approach	7
1.3 Auditory-visual interaction	8
1.3.1 Supporting behavioral phenomena	8
1.3.2 Possible neural basis	10
Research Objectives	13
Assessment	15
3.1 Outline of experiment	15
3.2 Working hypotheses	16
3.3 Common resources	16
3.3.1 Subject participation	16
3.3.2 Research system hardware description	18
3.3.2.1 Stimulus generation	18
3.3.2.2 Data recording and processing	18
3.4 Common methodology	22
3.4.1 Stimulation procedure	22
3.4.2 Recording procedures	23
3.4.3 Data analysis	27
PART II: UNISENSORY CONTINUOUS EVOKED POTENTIALS	30
Modulation Transfer Functions of Continuous Evoked Potentials	31
4.1 Literature review	31
4.1.1 Visual continuous evoked potentials (CEPs)	33
4.1.1.1 CEP archetype and important stimulation parameters	33
4.1.1.2 CEPs in response to 4-12 Hz modulation frequency stimuli	34
4.1.1.3 CEPs in response to 12-25 Hz modulation frequency stimuli	36
4.1.1.4 CEPs in response to 45-60 Hz modulation frequency stimuli	37
4.1.2 Auditory continuous evoked potentials	37
4.2 Methodology	39
4.2.1 Data acquisition paradigm	39
4.2.2 Data analysis	40
4.2.2.1 Latency estimation	40
4.2.2.2 Neural delay estimations	41
4.3 Results	43
4.3.1 Spontaneous EEG spectrums	43
4.3.2 Lock-in amplifier raw data output example	43
4.3.3 CEP magnitude modulation transfer functions	46

4.3.4 CEP phase modulation transfer functions	46
4.3.5 CEP latency modulation transfer functions	47
4.3.6 CEP modeling and neural delays	47
4.4 Discussion	61
4.4.1 CEP validity	61
4.4.2 Evoked and spontaneous potentials	62
4.4.3 CEP latency and delay estimations	63
4.4.4 Modulation transfer functions of visual CEPs	64
4.4.5 Modulation transfer functions of auditory CEPs	66
4.4.6 CEP overview	67
Continuous Evoked Potentials at Beta and Theta Modulation Frequency Regions	70
5.1 DISC experiment: CEP harmonics and trends	72
5.1.1 Introduction	72
5.1.1.1 Short-term CEP trends	72
5.1.1.2 1st and 2nd harmonics of CEPs	72
5.1.2 Methodology	73
5.1.3 Results	74
5.1.3.1 Raw data example	74
5.1.3.2 CEP stability	74
5.1.3.3 CEP harmonics	76
5.1.4 Discussion	81
5.1.4.1 CEP trends	81
5.1.4.2 CEP harmonics	83
5.2 INT experiment: stimulus intensity level effect	84
5.2.1 Introduction	84
5.2.2 Methodology	84
5.2.3 Results	85
5.2.4 Discussion	90
5.3 ATT experiment: subject attentiveness effect	93
5.3.1 Introduction	93
5.3.2 Methodology	93
5.3.3 Results	94
5.3.4 Discussion	95
PART III: BISENSORY CONTINUOUS EVOKED POTENTIALS	100
Introduction for The Bisensory Continuous Evoked Potentials Experiment	101
6.1 Terminology and approach comparison	101
6.2 Auditory-visual interaction in evoked potentials	103
Methodology for The Bisensory Continuous Evoked Potentials Experiment	107
7.1 Experiment paradigm and variables	107
7.2 Auditory-visual interaction assessment	111
Results of The Bisensory Continuous Evoked Potentials Experiment	114
8.1 Raw data and results outline	114
8.2 Data description of the runs	115
8.3 Noise level absolute magnitudes	122
8.4 Bimodal - unimodal relative auditory CEPs	123
8.4.1 Analysis of variance	123
8.4.1.1 Auditory relative magnitudes	125
8.4.1.2 Auditory relative phases	125
8.4.2 Trend analysis	130

8.4.2.1	Auditory magnitude trends	131
8.4.2.2	Auditory phase trends	131
8.5	Bimodal - unimodal relative visual CEPs	133
8.5.1	Analysis of variance	133
8.5.1.1	Visual relative magnitudes	133
8.5.1.2	Visual relative phases	137
8.5.2	Trend analysis	137
8.5.2.1	Visual magnitude trends	138
8.5.2.2	Visual phase trends	138
Discussion of The Bisensory Evoked Potentials Experiment		140
9.1	Data validity and reliability	140
9.2	Auditory and visual bisensory responses	141
9.2.1	Trend interpretation	141
9.2.2	Trend detectability	142
9.2.3	Magnitude and phase data comparison	143
9.2.4	Modeling of the auditory-visual interaction process	143
PART IV: SUMMARY AND CONCLUSIONS		145
Summary and Conclusions		146
REFERENCES		152
Appendix A. Summary of Individual Responses		158
Appendix B. Alphabetic List of Abbreviations		177

LIST OF FIGURES

<u>FIGURE</u>	<u>TITLE</u>	<u>PAGE</u>
I 3.1	: The Research System	19
I 3.2	: The Visual Stimulation Setup	24
II 4.1	: Phase Unfolding and Latency Derivation Procedures .	42
II 4.2	: Spontaneous EEG Magnitudes	44
II 4.3	: Lock-In Amplifier (LIA) Output Example	45
II 4.4	: CEP Magnitudes	48
II 4.5	: Visual Cyclic Phase MTF	49
II 4.6	: Visual Individuals and Averaged Cyclic-to-Continuous Converted Phases	49
II 4.7	: Visual Continuous and Cyclic-to-Continuous Converted Average Phases	49
II 4.8	: CEP Continuous Phases	50
II 4.9	: CEP Latencies	51
II 4.10	: Linear Models of CEP Regions	53
II 4.11	: Summary of Individual Responses (Appendix A)	158
II 5.1	: CEP Harmonics Example	75
II 5.2	: Stability of CEP Magnitudes and Phases	77
II 5.3	: CEP Magnitude and Phase Versus Stimulus Intensity .	86
II 5.4A	: Attention Effects on CEP Magnitudes	96
II 5.4B	: Attention Effects on CEP Phases	97
III 8.1	: AxV Experiment Paradigm and Independent Variables .	109
III 8.2	: Run Example of The AxV Experiment	116
III 8.3	: AxV CEP Magnitudes	117
III 8.4	: AxV CEP Phases	118
III 8.5	: Magnitude SF * CF Effect	119
III 8.6	: Magnitude SI * CI Effect	120
III 8.7	: Magnitude CF * CI Effect	121
III 8.8	: Magnitude SI * CI * ATT Effect	128
III 8.9	: Phase SI * CF Effect	129
III 8.10	: Stimulus Parameters Inducing The Auditory Peak AxV Trends	132
III 8.11	: Magnitude SF * CF * ATT Effect	136
III 8.12	: Stimulus Parameters Inducing The Visual Peak AxV Trends	139

LIST OF TABLES

TABLE	TITLE	PAGE
I 3.1	: Subject Description	17
I 3.2	: PAR EG&G MOD: 5204 Lock-In Amplifier	21
I 3.3	: Experiment Specifications	25
II 4.1	: Auditory and Visual CEP Comparison	52
II 4.2	: Estimation of CEP Delays and Latencies	60
II 5.1	: Auditory and Visual CEP Trends	76
II 5.2	: CEP Fundamental and 2nd Harmonic Comparison	81
II 5.3	: Intensity Effects on Auditory and Visual CEPs	90
II 5.4	: Attention Effect on Visual CEPs	98
III 8.1A	: AxV Experiment Independent Variable Definitions ..	110
III 8.1B	: AxV Experiment Dependent Variable Definitions	112
III 8.2	: AxV Noise Level Magnitudes	124
III 8.3	: Relative (Bimodal-Unimodal) Auditory CEP Vectors ..	126
III 8.4	: Auditory AxV Univariate Statistics	127
III 8.5	: Relative (Bimodal-Unimodal) Visual CEP Vectors ..	134
III 8.6	: Visual AxV Univariate Statistics	135

Part I: Introduction

Chapter 1

Background

1.1 Motivation

The motivation for this research was to develop an Event Related Cortical Potential (ERCP) methodology for non-invasively monitoring the auditory and visual sensory channel engagement and interaction (AxV) in humans. Sensory interaction is inferred whenever response variations of one sensory channel can be attributed to parameter changes of an additional stimulus, simultaneously presented to another sensory channel. This type of on-line continuous monitoring and parameter-space characterization of the AxV process has never been attempted before. This approach can be utilized in many existing disciplines and promote new research directions: providing further understanding of human sensory channel transfer functions and sensory information integration, investigating the unaccounted for intra-subject unisensory ERCP variability by applying an exhaustive multisensory input stimulus, facilitating the effectiveness of audio-visual trainers, monitoring sensory channel engagement and alerting against overloading tasks

that might deteriorate human-operator performance, and designing more effective and efficient man-machine communication channels.

1.2 Brain potentials

1.2.1 EEG and evoked potentials

The human brain and its marvelous complexity is regarded by many scientists as the "last frontier". Although extensively investigated, there is the valid reservation of whether the human brain can ever reveal itself. Ever advancing technology often provides analogies and metaphors to theorize how the brain "works", i.e. "holographic" type memory, "distributed-computational network" type cognitive information processing, etc. The research described in this study also incorporates metaphors, terminology and analysis techniques common in engineering and computer science fields. Although never completely valid or accurate, these "mental tools" can simplify problems and facilitate intuitive understanding of their solutions.

One obvious function of the human brain is encoding and processing environmental information. External cues (detectable features in our environment) undergo energy transformation at the receptor level and their neural codes are deployed and mediated to the cortical level through specific and diffused sensory channels. Each specific sensory channel is a neural pathway comprised of a chain of neuronal aggregates. The contact between two neurons is accomplished mostly through chemical-coupled synapses. The informational "bit" passed through a synaptic gap is believed to be the Action-Potential (AP), an electrical biphasic pulse (1-2 msec duration) capable of propagating along the neuron axon. A synchronized response from a group of excited neurons is referred to as a compound-potential. With bipolar far-field recording (differential amplification of scalp potentials), the compound-potentials reflect the dipole-

equivalent model of either the propagating volley of APs or the post-synaptic potentials of the targeted neuronal population (Childers, 1977; Vaughan, 1982). The cortical pyramidal cell layer is a good example of the latter. When neurons in this homogenously-architected layer are synchronously activated, the far-field potential gradient across this layer can be differentially recorded from the scalp (Vaughan, 1982). The magnitude of this response is a function of the source strength, distance and orientations relative to the recording electrode sites.

The brain is never "quiet". Even without any apparent input, an on-going electrical activity, termed background EEG (electroencephalogram) is always present. This background activity has been related to many processes (cortical activation level, system "noise-level", cognitive information processing indicator, etc.) and found to be affected by many behavioral and physiological factors. When an input stimulus is presented, a different, stimulus-related Evoked Potential (EP) can be recorded. Scalp potential distributions and frequency response comparisons of background EEG and EP signals reveal that different sources (or subsystems) contribute to each signal (Childers and Perry, 1971).

It will be helpful to pause here and formally define and characterize the ERCP signal. ERCP is the total causal brain electrical activity, mostly from cortical origins, which follows a defined administered stimulus. It can be recorded non-invasively in response to auditory, visual or somatosensory stimuli. The stimulus can be transient (click, flash) or continuous (sinusoidal or sinusoidally modulated carrier signal) and the ERCP data can be processed both in time and frequency domains. In most cases, the input stimulus can be precisely controlled and characterized, or in other words, a defined input feature vector can be constructed.

Some of the more important features of a single ERCP are:

1. It has small magnitudes (0.5-50 microvolt) with low Signal/Noise Ratio (SNR);
2. Noise (EEG, EMG, ECG, instrumental artifacts, etc.) and ERCP signals frequently share a common frequency band;
3. It is a highly variable compound-response (produced by an unlikely linear, time-variant, complex neural system);
4. It reflects both the system "hardware" (structural response) and "software" (cognitive response); the latter is more likely to be detected in longer latency ERCP components.

Apart from the single-trial ERCP methodology using a pattern recognition approach (Vidal, 1977; Horst and Donchin, 1980), several methods, from averaging and correlation methods to special adaptive filtering methods, have been employed to optimally extract the ERCP (Aunon and Sencaj, 1978; Sencaj et al. 1979).

1.2.2 Evoked potential methodologies

EP methodologies were developed under subjective ad-hoc hypotheses with various intended applications in mind. These methods can be ranked and compared by the following criteria: neural response acquisition-time, size of the targeted or responding neuronal population (observation unit) and degree of observation unit spatial distribution disclosed and displayed. For the purpose of example and reference, the methodology of traditional ensemble averaging of Transient Evoked Potentials (TEPs) is reviewed in the following paragraphs.

1.2.2.1 Ensemble averaging approach

The major assumption behind ensemble averaging is that identical stimulus vectors under the same controllable experimental conditions are translated through the same neural pathways in the same manner, yielding exactly the same spatial and temporal distribution of the ERCP. In other words, the sensory channel is treated as a time-invariant system, triggered by an adequate transient signal. The same type of reasoning also linked the ERCP to the associated behavioral observation. As the ERCP is "time-locked" to the input stimulus, so is the behavioral pattern "feature-locked" to the ERCP. This conceptual approach provided the rationale for studies in which the expected future behavior was extrapolated from the ERCP, or the unknown past input stimulus vector was interpolated from the present behavior (Callaway et al., 1978; Begleiter, 1979). The descriptive ERCP features used in these studies were: means and variances of amplitudes and latencies, cross-correlations, wave areas, principal components, power spectrums and others.

Most of the ERCP studies investigated the sensory channel response to a limited, single modality stimulus vector (Callaway et al., 1978). Inter- and intra-subject ERCP variability were often cited as the major obstacles which prevented more significant ties between the ERCP features and the input stimulus vector. Treating the brain as a time-variant system and pre-processing the whole ERCPs ensemble (posterior adaptive filtering preceding the averaging), the "best" representative ERCP, free of temporal "jitters" in its components, was derived (de Weerd, 1981; de Weerd and Kap, 1981). The advantages of this method are obvious, as are the drawbacks. A computer is needed for data storage, digital filtering and processing, and more important, the resultant ERCP lacks valuable information regarding the dynamics of the ERCP components throughout

the recording session. In simple ensemble averaging, described previously, this information is partially expressed by the ERCP variance.

In summary, ensemble averaging methodology utilizes long acquisition-times (in order of minutes) to obtain a limited average potential distribution of ERCPs, probably generated in large and distributed neuronal populations.

1.2.2.2 Single-trial approach

A faster acquisition-time method must be used to allow detection and faithful monitoring of parameter changes in smaller Time-Constant (TC) EPs (produced by a sensory channel with a wide frequency response bandwidth). This can be implemented by dichotomizing key features of the stimulus (digitizing the selected features), and/or by restricting its response interpretation (collapsing the EP data-base). These principles have been utilized in many single-trial EP studies, where pattern-recognition algorithms and other statistical analysis techniques were employed to detect gross features within an EP generated for a single stimulus (Squires and Donchin, 1976; Vidal, 1977; Gevins, 1980; Childers et al., 1982; McGillem and Aunon, 1977, 1983, 1985). Vidal (1977) was able to correctly classify single-trial TEPs generated by high feature-contrast stimuli (stimulating different halves of the retina). This conceptual approach necessitates an exhaustively defined and controlled input stimulus and utilizes adaptive signal-extraction techniques to cope with the intra-subject variability.

1.2.2.3 Lock-in approach

Other implementations of these principles are the use of phase-lock techniques (also referred to as complex or synchronous demodulation, lock-in, or Fourier analysis techniques) in recording Continuous Evoked Potentials (CEPs) (Regan, 1966; Levine et al., 1972). When a target feature within the input vector stimulus is periodically modulated

(intensity modulation, phase modulation, etc.), a CEP vector component phase-locked to the Modulation Frequency (MF) can be tracked and monitored with recording TCs of 3-30 sec. Generally, this technique provides faster EP acquisition-time and better SNR enhancement than do the ensemble averaging and single-trial techniques, respectively. The narrower the Bandwidth (BW) of the "reacting" MFs (MFs for which the EP data validates or negates the research hypotheses), the more efficient this technique becomes. The drawback, however, is the loss of direct EP temporal information, implicitly obtained in single-trial or ensemble averaging techniques.

In light of the above, the phase-lock technique is suitable for the purpose of continuously monitoring the sensory channel engagement. CEPs can be simultaneously recorded from one or more sensory channels under unimodal or multimodal stimulus conditions. Due to the high frequency resolution of the phase-lock technique, the effects of cross-modal, similar MF stimuli can be investigated. The following section provides the rationale for investigating such effects, specifically between the auditory and visual sensory channels.

1.3 Auditory-visual interaction

1.3.1 Supporting behavioral phenomena

It is well known that auditory and visual information supplement and complement each other in daily human communications. Speech intelligibility was greatly enhanced when supplemented by visual cues from a speaker's lip movements (Sumby and Pollack, 1954). Also, visual recognition of a word was enhanced when presented simultaneously with a matched spoken word (Smith, 1965). On the other hand, early auditory deprivation in children impaired the temporal pattern-reproduction ability in auditory, and visual tasks as well (Sterrit et al., 1966). These three examples help to substantiate an

intuitive notion about the Auditory-Visual interaction (AxV) mechanism in humans and its importance.

There is some evidence that the auditory input in AxV tasks is dominant. Auditory intermittent stimulation drove the perceived visual stimulus flicker rate, making it almost independent of the actual visual flash rate. The visual flicker rate, on the other hand, could not drive the perceived auditory flutter rate (Knox, 1945). Auditory flutter increased the Critical Flicker Frequency (CFF) (Oglove, 1965) and it was much harder to match with a stable flicker rate than vice versa (Gebhard and Mowbray, 1959). Sensitivity indices (differences between expected values of the responses to noise alone and noise + signal) and Reaction Time (RT) tests consistently showed that the detection of a bimodal signal was better than the auditory signal alone, which was better than the visual signal alone (Loveless, et al., 1970).

Some experiments have demonstrated the specific nature of the AxV phenomenon. Maruyama (1959) investigated the effects of tones with different frequencies and intensities on the absolute visual threshold at various times during a 4 second period of auditory stimulation. For foveal vision, the threshold shift effect was immediate, lasted for 3 seconds, and was proportional to the tone's intensity level. For peripheral vision, the peak effect was obtained about 2 seconds after tone onset. High frequency tones facilitated the effect while lower frequency tones (below 50-100 Hz) inhibited it. Further, Maruyama (1961) demonstrated that stimulating the right peripheral vision increased the sensitivity of the left ear only, and when that ear was stimulated, a contralateral effect on half of the visual field sensitivity was observed.

1.3.2 Possible neural basis

As previously indicated, language and speech ability in humans requires bisensory convergence of auditory and visual information. Human neuroanatomy studies provide structural evidence about the auditory and visual afferent systems converging in points along fast-conducting channels (Colliculi, Geniculate Body, Thalamus and associated non-specific cortical areas, etc.) as well as onto diffused, slow-conducting neuronal masses (Reticular Formation, etc.).

Walter (1964) investigated the convergence of auditory, visual and tactile responses in the human non-specific cortex, recorded both from implanted microelectrodes and surface scalp electrodes. Habituation characteristics and differences inflicted by the recording techniques, led him to conclude that scalp-recorded EPs were comprised of specific and nonspecific responses, the latter predominant. Specific and non-specific responses originated from the primary and the associative cortical areas, respectively. He found that signals in all studied modalities converged at the frontal cortex (a non-specific area) and were widely dispersed therein. Intracranial recording from the same sites showed that each modality had its own "signature". Distinguished-featured, modality-dependent auditory and visual EPs were recorded from this area with latencies of 25 and 35 msec, respectively.

The convergence of sensory inputs was demonstrated also at longer latency responses. Davis et al. (1972) recorded TEPs in response to "comfortably strong" and approximately equal subjective magnitude audio, tactile, shock and flash stimuli. Similar latencies, waveforms, amplitudes and recovery periods of these so-called "vertex-potentials" (recorded from Cz-M1/Forehead with a 1-15 Hz BW amplifier) were found

in all modalities. In summary, it has been suggested that the auditory and visual systems have, or share, common "hardware" facilities or coding mechanisms.

Using a "holistic" approach in analyzing the sensory neural codes in feature extraction, Erickson (1974) suggested that:

The neural possibilities afforded to one sense by the structure and physiology of its neurons and their connections are also available to other senses, and thus the encoding parameters available to one are also, to some degree, available to another.

Using solely the neuronal activity attributes of quality, intensity and duration formulated in the nineteenth century, Erickson defined classes of change in neural activity related to these attributes. Intensity was coded by change in the amount of neural activity without change in the appearance of this activity, while quality (i.e. sound spectrum, object position in space, color, etc.) was coded by change in the appearance of the neural activity (shifting to a new population of neurons or an across-fiber pattern change of activity within the same neuronal population). In this respect, an Amplitude Modulated (AM) tone was comparable to an AM spotlight (intensity modulation of a quality feature) and a Frequency Modulated (FM) tone was comparable to the position modulation of the spotlight (quality modulation in a given intensity).

The quality attribute was coded topographically (spatial position in the retina, ascending tracks, and the primary cortex) by narrowly tuned neurons or non-topographically (color coding) by a smaller population of broadly tuned neurons. Erickson suggested that,

Each neuron may be sensitive along many broadly tuned (non-topographic) dimensions but sensitive to only one narrowly tuned (topographic) dimension, which is in accordance with the conflicting principles of necessary neural redundancy and neural volume reduction.

A plausible interpolation of Erickson's analysis is that for a given quality, the intensity and quality related neuronal activities (or populations) are orthogonal. So, a narrowly tuned, topographically-arranged neuronal sub-population, engaged in a specific quality feature extraction, may at the same time participate in other, very broadly tuned, diffused or distributed neuronal populations encoding intensity of other different qualities. Another possibility is that a very broadly tuned neuronal population participate in intensity coding of more than one quality feature.

Direct EP evidence regarding the auditory-visual bisensory interaction is provided in the introduction section of the AxV experiment in this study.

Chapter 2

Research Objectives

The purpose of this investigatory study was to adapt the phase-lock methodology for recording and characterizing Continuous Evoked Potential (CEP) variations induced by the Auditory-Visual bisensory interaction process (AxV). The specific AxV aspect investigated here was the dependency of single sensory channel CEP variations on cross- or inter-modality stimulus parameters. The research goal, obtaining the effective AxV stimulus parameter-space for future investigation, was translated into the following objectives:

1. Developing the hardware-system needed for continuous generation, recording and processing of the CEPs; Including: unimodal and bimodal stimulus generation with programmable gate control, sensitive and stable acquisition of CEPs over long recording sessions and providing for on-line and off-line data processing.
2. Obtaining and optimizing on-line detection of auditory and visual CEPs; Exploring stimulus conditions, experiment paradigms, recording sites and CEP processing.

3. Characterizing the CEPs in terms of their magnitude, phase, estimated latency and delay, 2nd harmonic component, response stability and the effects of stimulus intensity and subject attentiveness.
4. Demonstrating an AxV process on a selected stimulus parameter-space; CEP magnitude and phase variations were associated with specific stimulus conditions (modulation frequencies, intensities and attention allocation).

Chapter 3

Assessment

3.1 Outline of experiment

The main hypothesis of this research was studied in the AxV experiment, where attention, stimulus modalities and intensity effects on magnitude and phase of the Continuous Evoked Potentials (CEPs) were investigated. All preceding experiments were designed to determine optimal values for the Independent Variables (IVs) or provide controls for the Auditory-Visual Interaction (AxV) experiment. Results from the MTF experiment were used to derive 5-61 Hz range, magnitude, phase and latency Modulation Transfer Functions (MTFs). Best Modulation Frequency (MF) regions, excluding the Alpha EEG peak activity frequency regions, were selected for further detailed investigation. Results from the following DISC and INT experiments facilitated choice of optimal MF values. Based on response magnitude and stability characteristics, two optimal MFs (from Theta and Beta MF regions) were chosen for each subject to be used in the AxV experiment. Utilizing the IVs selected in the DISC and INT experiments,

CEP magnitude and phase dependencies on subject attentiveness under unimodal stimulation conditions were studied in the ATT experiment.

3.2 Working hypotheses

The feasibility of detecting CEP variations induced by the AxV process depends on the validity of the following ad-hoc assumptions:

1. Integration of auditory and visual information is partially "hardwired". The two inputs physically converge upon a common, multimodal neuronal population, rather than being just "observed" and merged by cognitive "software".
2. The AxV effects are consistent and durable, at least for the duration of the bisensory stimulations used in this study.
3. The AxV process affects the compound potentials (or EPs) generated by the multimodal neuronal population.
4. The ratio of the polysensory to unisensory neuronal population is quantitatively significant to allow detection of the AxV effect.
5. Common, cross-subject general AxV trends can be observed (tolerable low inter-subject variability).

3.3 Common resources

3.3.1 Subject participation

Ten students, all reporting normal hearing and normal or corrected vision, participated in this research. Description of these subjects is presented in TABLE I 3.1 (notation: TABLE/FIGURE < part I, II or III > < chapter 1-10 > . < running number >).

One subject, distinguished by a very poor raw CEP data Signal/Noise Ratio (SNR), could not be processed and was excluded from further statistical analysis.

SUBJECT DESCRIPTION

TABLE I 3.1 : All subjects were students at the University of Connecticut. Notation : 1st TABLE in chapter 3 in part I, N : normal, C : corrected to normal, P : paid, V : volunteer.

SUBJECT	AGE years	SEX M/F	HANDED R/L	VISION N/C	INCENTIVE V/P	DATA USEABLE yes/no
AM	25	F	R	N	V	yes
CR	21	F	R	N	P	yes
EW	26	F	R	N	V	yes
KC	27	F	R	C	V	yes
MR	22	M	R	N	P	yes
PM	21	M	R	N	P	yes
RT	20	M	R	N	P	yes
SC	22	F	L	C	P	yes
TN	30	M	R	N	V	yes
FL	27	M	R	C	V	no

For most of the subjects, the data was collected in three recording sessions, about four to five hours each, over a period of two to three weeks. Sessions and experiments were standardized through subject conditioning (acquaintance, information, motivation) and experiment procedures (instructions, involvement, trials, breaks). The research was presented as a Reaction Time (RT) study and subjects were not disclosed the real goals of the experiment nor the hypotheses involved, prior to completing their research engagement.

3.3.2 Research system hardware description

3.3.2.1 Stimulus generation

A program selector module ("Home Made", HM) drove and controlled a digital sum of sines synthesized module (HM), producing pre-programmed, experiment-dependent stimulus (ASIG, VSIG), reference (AREF, VREF) and control (AGATE, VGATE) signals (FIGURE I 3.1). GATE signals, reflecting stimulus "on" and "off" conditions, were digital (TTL) signals. All other signals were digital-to-analog converted (DAC), filtered sinusoidal, or sum of sinusoidal signals (1 RMS volt per sine waveform) with a 2nd harmonic attenuation better than -70 dB. The continuous REF and gated SIG signals were the modulation frequencies and modulated carriers (915 Hz for audio stimuli and 0 Hz for visual stimuli), respectively. ASIG and VSIG signals were transferred through Logarithmic Attenuator and Power Driver modules (HM) and converted to sound and light stimuli by a headphone set (TELEPHONICS, TDH-49P) and a Glow-tube (METCOM, tube #7920253), respectively. The physical stimulus 2nd harmonic attenuation was better than -60 dB.

3.3.2.2 Data recording and processing

The EP or EEG signals were differentially amplified and bandpassed between 0.5-570 Hz using first-order, cascaded High-Pass and Low-Pass Filters (HPF-LPF). The front-end in each of the Differential Amplifiers (DA, HM modules) was a Medical Isolation Amplifier (INTRONICS, IA-297 or IA-296), characterized by high Common Mode Rejection Ratio (CMRR > 120 dB) and input impedance (> 100M ohms), low input noise (< 1.5 microvolt) and a driven reference.

THE RESEARCH SYSTEM

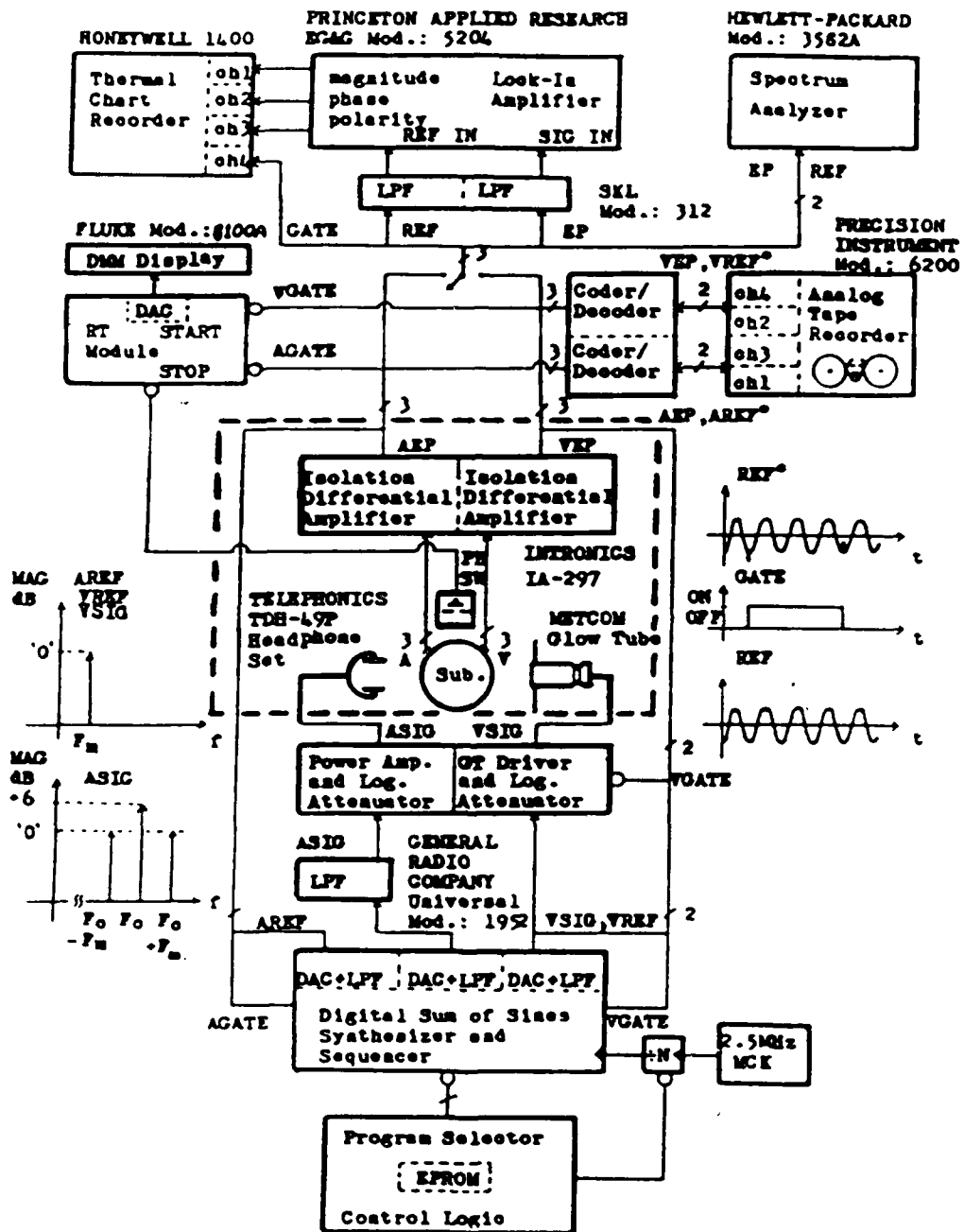


FIGURE I 3.1 : HARDWARE MODULES USED FOR STIMULUS GENERATION, DATA RECORDING AND DATA PROCESSING. DOTTED SECTION : THE RECORDING CHAMBER. SEE TEXT FOR FURTHER DETAILS.

CEP and gated-REF (REF*) signals were recorded on an Analog Tape Recorder (PRECISION INSTRUMENTS MOD: 6200) set on FM recording and 1 KHz cutoff frequency, and were available for off-line data processing. Since only a 4-channel recorder was available, GATE signals were superimposed (ac-coupled) on the REF signals using coder/decoder (HM) modules generating the REF* signals. CEP and REF (on-line) or REF* (off-line) signals were routed to the Lock-In Amplifier's (LIA, PRINCETON APPLIED RESEARCH EG&G MOD: 5204) REF IN and SIG IN inputs, respectively. In order to enhance the LIA input SNR, both CEP and REF or REF* signals were passed through matched LPFs (SKL MOD: 312) set on an 80 Hz corner frequency.

An LIA is a device that extracts the magnitude and phase of a frequency component (coherent with a reference frequency applied to REF IN input) within a noisy signal (applied to SIG IN input). The LIA technique is extremely sensitive in detecting low-amplitude and poor SNR periodic signals (Kaufman and Price, 1967; Regan and Cartwright, 1970; Euler and Kiessling ,1981; Nelson et al., 1984). Analog LIA output signals, proportional to the magnitude and phase of the coherent component, are obtained through a single-Time-Constant (TC) LPF. Increasing the LIA output TC reduces the output signal variance and prolongs the response time to a step change in MF (or modulation depth).

The LIA equivalent frequency response is of a very sharply tuned Band-Pass Filter (BPF). Within the frequency range of 5-61 Hz, the LIA used in this study (PAR, MOD: 5204) exhibited average Equivalent Noise Bandwidth (ENBW) and "Q" factor values of 0.035 Hz and 530, respectively (TABLE I 3.2). Note that the stimulus period was always made longer than the LIA step-function response-time (0 to 95% of the full-scale LIA output). With an internally-generated square waveform reference signal, only odd har-

monics, weighted by their harmonic numbers, contributed to the LIA vector output. These characteristics make the LIA a powerful tool in detection of very low SNR, fundamental and 2nd harmonic driven responses (i.e. CEPs). Also, its high frequency resolution enabled "locking-in" on the response from one sensory channel while the other sensory channel was excited with a MF of slightly different value.

PAR EG&G MOD: 5204 LOCK-IN AMPLIFIER

TABLE I 3.2 : LIA measured performance. TC : Time Constants of the pre- and output-amplifiers, ENBW : Equivalent Noise Bandwidth, "Q" factor : BPF sharpness, T : response time, 0 to 95% of the full-scale LIA output.

TC sec	ENBW Hz	FREQUENCY RANGE Hz	"Q" FACTOR (Average)	T sec
1 + 10	0.02	5 - 15	430	30
1 + 3	0.05	16 - 61	625	15

With a CEP amplification of 20K-50K, the LIA full scale sensitivity was set to 100-250 millivolt. An output TC of 1-10 sec was selected. Hard copies of the LIA output and GATE signals were obtained from a 4-channel Analog Chart Recorder (HONEYWELL MOD: 1400). A Spectrum Analyzer (HEWLETT-PACKARD MOD: 3582A) was used off-line to measure the EEG spectrums (on 64 RMS averaged epochs).

The system's overall magnitude and phase transfer functions were measured between the stimulus input and the LIA output. The phase difference between the REF frequency and the physical stimulus MF was found to be: Phase (degrees) = 24 - LOG10 (MF), where MF is the modulation frequency in Hz. The corresponding magnitude transfer function displayed a maximum error of +/- 0.5 dB over the 5-61 Hz MF range.

All phase and magnitude results presented in this study were corrected for and should be regarded as final, system-error-free results.

In addition to brain potential data, RT data were on-line measured and collected using an RT module (HM). GATE signal transitions (High-to-Low or Low-to-High) required subjects' responses, and turned on a digital counter. By pressing a low-pressure push-button switch (270 gr) held in their preferred hand, the subjects stopped the counter. The analog-converted, digital number from the counter was monitored on a Multimeter and was recorded manually.

3.4 Common methodology

3.4.1 Stimulation procedure

Subjects were seated in a small closed room wearing a headphone set (TELEPHONICS TDH-49P) or optometrist trial frames (AMERICAN OPTICAL CORPORATION MOD: 11072) or both, holding a push-button switch in their preferred hand and facing a Visual Stimulator (HM). Background light intensity was 130 lux and average noise level did not exceed 40 dB Sound Pressure Level (SPL) in the test room.

The audio stimuli (a 915 Hz carrier, 100% sinusoidally Amplitude Modulated, AM) were monaurally delivered to the subject's left ear. The highest average stimulus intensity level (defined as "0" dB audio stimulus level) delivered through the headphone set was 108 dB SPL.

Visual stimuli (100% sinusoidally AM white light) were delivered by the Visual Stimulator (VS) and binaurally viewed. The VS was made of a 2.3 cm diameter, diffused

surface Glow tube light source mounted in the center of a 61 cm wide x 49.5 cm high black board, and viewed from a distance of 33 cm (3.6 degrees of visual angle).

During visual stimulation, subjects wore artificial pupils (mounted on the trial frames) through which they focused on a small black dot painted on the exposed Glow tube lens. Artificial pupil diameter was 1.7 and both pupils were adjusted to allow an unobstructed view of the Glow tube surface, binaurally viewed from comfortable head posture (see FIGURE I 3.2 for further details). The highest average stimulus intensity level (defined as "0" dB visual stimulus level) delivered by the VS was 44 lux.

For both audio and visual stimuli, an MF waveform given by $-\text{COS}(2\pi f \times MF \times t)$, and a complete number of MF cycles were delivered in order to eliminate onset/offset transients. A condensed overview of all the experiments' paradigms is presented in TABLE I 3.3. Specific stimulus parameters are detailed separately for each experiment.

3.4.2 Recording procedures

Three types of data were recorded from each subject: EEGs and CEPs, RTs and post-experiment subjective performance evaluation. EEG and CEP data were collected in accordance with the research hypotheses. The other data were generated and collected to promote control over the experiment paradigm, to verify response strategy and induce motivation and involvement. In addition to task-specific instructions and trials, a general set of instructions was stressed before each experiment. Subjects were asked to minimize their voluntary muscle activity and relax, attend and concentrate on the relevant stimulus and response cue, then react and recover as quickly as possible.

THE VISUAL STIMULATION SETUP

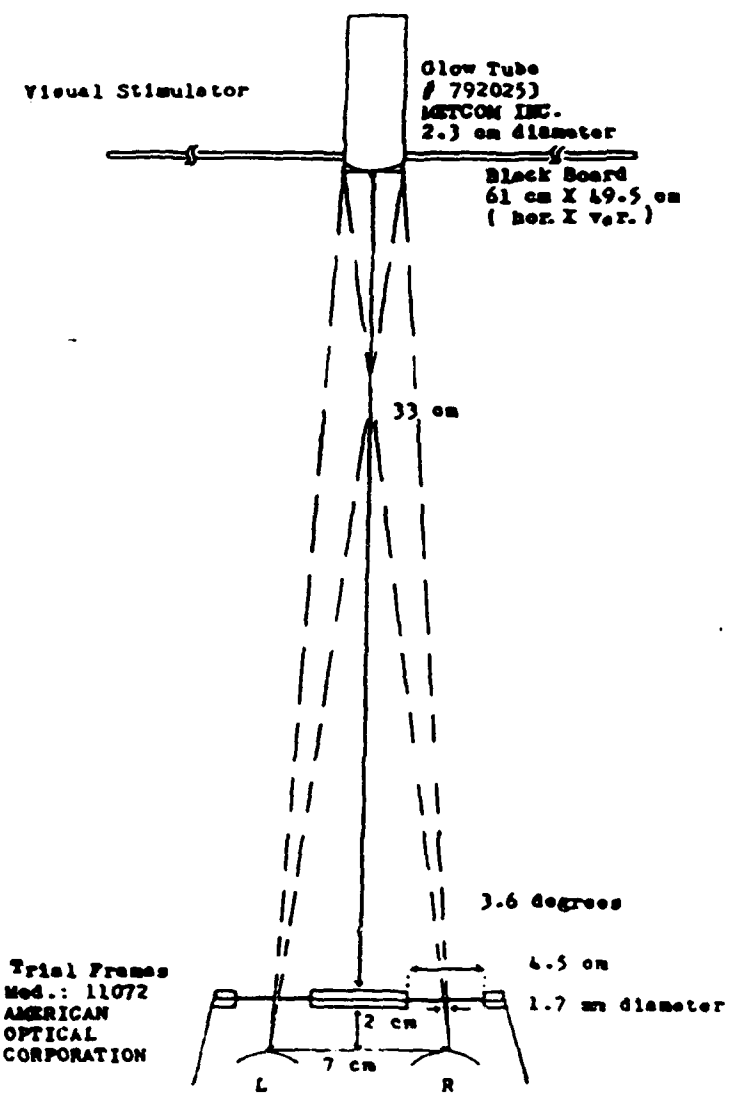


FIGURE I 3.2 : THE VISUAL STIMULATOR AND THE ARTIFICIAL PUPILS.

SPECIFICATIONS OF EXPERIMENTS

TABLE I 3.3 : Summary of the experiment purposes, stimulus parameters and recording procedures. See text for further details.

Experiment Purpose	Session Duration (hours/exp. (# of sub./exp.))	Stimuli A:Audio V:Visual	Stimuli GATE/run Freq. bin repetition/run: RT to GATE transition: S: "on" L: "off"	Stimuli(s) duration S: MF-dependent Freq. ranges: -po: 5-6.5Hz -pu: 16.1-27.7Hz
<u>MF</u> Best magnitude & latency MF regions	1st 4 hours (9)	A,V	 S: MF-dependent RT: variable, x2/Freq. bin ISI: 1.2 sec. AVD: 1.2 sec.	$E_p = 32.5 \pm 2\%$ $E_p = 32.5 \pm 1\%$ $E_p = 32.5 \pm 1\%$ $E_p = 32.5 \pm 1\%$
<u>MF</u>	1st/2nd (9) 1/2 hour	None	None	None
<u>MF</u> Neural to repeatability optimal points harmonics	2nd 3 hours (9)	A,V	 S: MF-dependent RT: fixed, 4, 16/Freq. bin ISI: 1.4 sec. AVD: 1.4 sec.	$E_p = 32.5 \pm 2\%$ $E_p = 32.5 \pm 1\%$
<u>INT</u> Intensity effect, durability	2nd 1 hour (6)	A,V	 S: MF-dependent RT: fixed, 4, 15, 23/Freq. bin ISI: 1.4 sec.	$E_p = 32.5 \pm 2\%$ $E_p = 32.5 \pm 1\%$
<u>ATT</u> Attention effect	2nd 1 hour (6)	A and V. Non-overlapping	 S: MF-dependent RT: s:fixed, x2/Freq. bin ISI: 0.5, fixed AVD: 0.5, fixed	$E_p = 32.5 \pm 2\%$ $E_p = 32.5 \pm 1\%$
<u>INT</u> modality x attention x intensity x MF effect	2nd 3 hours (9)	A and V. Overlapping	 S: MF-dependent RT: s:fixed, x2/Freq. bin ISI: 0.5, fixed AVD: 0.5, fixed	$E_p = 10.9 \pm 7\%$ $E_p = 10.4 \pm 2\%$

SPECIFICATIONS OF EXPERIMENTS

TABLE I 3.3 : Continued.

	RF points/run (# of points, run duration, in min.)	Stimuli: Intensity/run E:-0°43 L:-1243	Run order/ scans/ channel	LIA output TC, sec	Comments
M17	W: 5-8.5 (8, 12.5', 9-15.3 (1), 19' P: 16.1-22 (9.8', 23.5-61 (6.9', 25.7-18 Hz)	E, fixed	1 3 2 4	10 10 3 3	Non-monotonic # sweep: maximizing pair distance in each run. x) repeat at the beginning
M18	None	None	AMBI 1st VERO 2nd	None	None runs, raw data averaging.
M19	W1 best of W's W2 (1, 8') W3, (1, 8') P1 best of P's P2 (1, 8') P3, (1, 8')	E, fixed	1 3 5, (7) 2 4 6, (8)	1, 10 All	# was uniformly distributed over the percentile range.
M20	W ₀ : optimal (1, 8') P ₀ : optimal (1, 8')	Variable -24 → -0°43 6dB/step	1 2	10 All	Same as above.
A11	W ₀ -2 (A) post W ₀ -4 (V) P ₀ -2 (A) post P ₀ -4 (V) (1, 8')	INTENSITYS E/L A/V : E/E L/L E/E	3 4 1 2	10 All	Same as above. Transition seq- ence between gates was randomized. last 5% of the preceding value.
A12	W ₀ , W ₁ , W ₂ , W ₃ repeated sequence for each intensity level. W ₀ -W ₂ , P ₀ -P ₂ All A/V (1, 8')	INTENSITYS E/L A/V : L/E E/L E/E	1, 2, 3, 4, 11 2, 6, 10, 14 3, 7, 11, 15 4, 8, 12, 16	10 All	# was uniformly distributed over the percentile range.

CEPs were recorded for audio and/or visual stimuli. Referring to the 10/20 electrode system (Jasper, 1958) auditory CEPs were recorded between Cz(+ IN)-A1(-IN)/Nose (driven reference) ipsilaterally to the stimulated ear, and visual CEPs were recorded between Oz(+ IN)-A1(-IN)/F3 (driven reference). EEG potentials were recorded simultaneously from both CEP recording sites to opened-eyes condition without any stimulus or required response. Skin impedance was kept below 5K ohms. It was checked periodically and for most of the subjects it measured between 1.5K-3K ohms. Ag/AgCl electrode leads (IN VIVO METRIC SYSTEM, E201) were mounted on the skin (using HM accessories) in a manner designed to ensure long-term recording stability.

Reacting to stimuli offset engaged the subject's attention and RT data was collected to subjectively verify subject concentration and alertness level during the experiments. Subjects were required to press a push-button switch (held in their preferred hand), as quickly as possible in response to stimuli offset (additional onset responses were required only during the ATT experiment). At the end of each run and after submitting their subjective performance evaluation, subjects were informed of their actual scores. The subjective evaluation consisted of grading quickness, attention and degree of difficulty. In addition, at the end of the AxV experiment, subjects were asked to describe their response strategy.

3.4.3 Data analysis

EEG raw data was RMS averaged off-line (64-128 epochs were averaged per run), and subjected to further statistical analysis. All CEP raw data was recorded on the analog tape recorder and most of it was processed on-line by the LIA. In all the experiments, single Stimulus duration (S, or S/3 in AxV experiment) and the choice of stimulus repetition factor were the outcome of trade-off between performance and practical considerations. In a pilot study, the TCs of the CEP responses to a step

function input stimulus were estimated to be less than 1 sec. Due to the poor CEP SNR, LIA TCs greater than 3 sec had to be applied. On the other hand, it was desired to lower the LIA TC in order to minimize run duration and resource expenditure (subject fees, number of tapes, etc.). Consequently, LIA TCs of 3 and 10 sec were used in this study.

Magnitude and phase values were measured using the following criteria:

1. Values were accountable only for the stimulus "on" period of time, exceeding at least 2 LIA output TCs.
2. Magnitude values were recorded only if they were accompanied by stable phase responses (CEP phase spread of less than 180 degrees).

Final values were obtained by averaging across the repetitions in each experiment (x2 or x3) for each subject. Linear averaging was applied for magnitude values and cyclic averaging (minimizing the Standard Deviation, SD, around the mean value) for phase values. Data processing used in specific experiments will be described later. In light of the high inter-subject variability observed in this study, cross-subject averages (MEANs) were often supplemented with the SD measures (bars in the figures) or the individual data.

Processed data was statistically analyzed and presented graphically using SAS and SAS/GRAPH software packages (SAS INSTITUTE, INC.). Result significance was ascertained by utilizing parametric tests (t-test, F-test, ANOVA, MANOVA, regression, etc.). The original or transformed experiment data sets (i.e. magnitude in dB, etc.) were all checked for normality. In most cases, the normal data distribution assumption could not be conclusively rejected due to border-line significance level, and a symmetrical distribution was observed (low absolute skewness values). With symmetrical data distribution, non-parametric tests, utilizing rank procedures, testing the median rather than the

mean, should yield comparable results to parametric tests. After trying both tests on several data sets, and in light of the general similarity found between the results, parametric tests were chosen for convenience.

Part II: Unisensory Continuous Evoked Potentials

Chapter 4

Modulation Transfer Functions of Continuous Evoked Potentials

4.1 Literature review

This review will provide the reader with background information regarding the specific type of Continuous Evoked Potentials (CEPs) recorded in this study. A CEP archetype response will be characterized in terms of methodological parameters, origin, peak magnitudes and latencies. The visual CEP review was based solely on comparable CEP studies, while the auditory CEP review was supplemented by additional information from Transient Evoked Potential (TEP) studies.

The physical origin of scalp-recorded CEPs is generally deduced from their potential distributions and neural delays. Since temporal information is not retained in frequency domain methods (lock-in technique, Fourier analysis, etc.), response delay can only be estimated from the CEP phase Bode plot, under restricting assumptions.

If a linear, minimum-phase plus a fixed delay system is assumed, the recorded CEP phase is: $P = (2\pi f \times MF \times D) + P_0 + Pf(f)$. In this equation MF is the Modulation Frequency in Hz, D is the CEP delay in seconds, P_0 is the fixed initial phase in radians and $Pf(f)$ is the frequency-dependent, neural filter phase-shift in radians. The CEP delay can be computed from: $D = d(P) / d(MF \times 2\pi f) - d(Pf(f)) / d(MF \times 2\pi f)$. The first derivative term was referred to as the response "apparent-latency" (Regan, 1972) or simply "latency" in other studies. When the second derivative term (the "group-delay" of the equivalent neural filter) is negligible or estimable, the response delay (D) can be obtained.

The second derivative term is negligible only when the delay is estimated at frequency regions remote from the poles and zeros of the equivalent filter modeling the peak CEP magnitude. This approach, in which the peak delay is approximated from "noisier", peak-adjacent data (having lower magnitudes and more variable and unreliable phases), should not be utilized in Bode plots with multiple overlapping magnitude peaks since the approximated delays (if at all related to their designated peaks) would consequently be underestimated. Nevertheless, this easy-to-apply approach was used by many researchers (Spekreijse, 1966; Regan, 1972, etc.).

The second derivative term can be estimated at the peak magnitude by fitting an equivalent linear model to the CEP magnitude response data. It is possible to challenge the validity of both approaches, but delay estimations of the second approach (modeling) should at the least be more accurate. This is the approach that has been utilized in this study.

4.1.1 Visual continuous evoked potentials (CEPs)

4.1.1.1 CEP archetype and important stimulation parameters

Visual CEPs, recorded in response to amplitude-modulated light stimuli, have been extensively investigated and applied in various fields: system identification studies (Tweel and Lunel, 1965; Spekreijse, 1966; Reits, 1975; Spekreijse and Reits, 1975; Spekreijse et al., 1977), normative and clinical studies (Regan, 1966, 1972, 1977) and human-operator monitoring studies (Wilson and O'Donnell, 1981; Junker and Peio, 1984; Levison et al., 1985; Moise, 1985;). In these studies, changes in CEP parameters (magnitude, phase,- latency, coherence, etc.) were attributed to the following experimental variables:

1. Stimulus intensity measures (source and background luminance, retinal illumination), spatial pattern, color, MF and modulation depth;
2. Visual angle, stimulus field, adaptation, accommodation and pupil aperture;
3. Externally or internally imposed subject attitude (stimulus relevance, work-load, attention allocation, etc.).

The remainder of this review will concentrate on a specific class of CEPs, namely those recorded in response to sinusoidally amplitude modulated diffused (unpatterned) light stimuli. Generally, when response magnitude was plotted against MF, three major peaks at 10 Hz (highest), 18 Hz and 50 Hz (lowest), were typically found. These potentials were recorded under the following general experimental conditions:

1. Large stimulus field and visual angle (7-30 degrees, larger than the fovea centralis field angle);
2. Photopic stimulation (luminance of 20-2000 cd/m², retinal illumination of 50-5000 troland) following dark or stimulus-averaged intensity adaptation (1 troland is defined as the retinal illumination caused by a 1 candela/m² luminance surface viewed through an exit pupil area of 1 mm²);
3. High stimulus intensities and large Signal/Noise Ratio (SNR) enhancements for the high MF region (since high modulation frequency stimuli of 30-60 Hz generated the lowest CEP magnitudes);
4. Binocular and Maxwellian views for low and high stimulus intensities respectively;
5. Natural pupil (natural focal depth control);
6. CEPs recorded differentially between the occipital and the vertex area or the earlobe;
7. No attempt made to control subject attitude (attention, vigilance, etc.), except when directly investigated.

4.1.1.2 CEPs in response to 4-12 Hz modulation frequency stimuli

CEPs recorded for 4-12 Hz MF stimuli showed a very sharp fundamental magnitude peak at the Alpha EEG frequency (around 10 Hz). The potential distributions of these CEPs and the Alpha EEG spontaneous activity were similar. It was therefore generally accepted that these CEPs, like the Alpha EEG spontaneous potentials, originated from a substantial part of the non-specific cortical area (Spekreijse et al., 1977).

Within this frequency range, CEP latency estimations were difficult to assess due to the following obstacles: (1) The wide-spread CEP scalp potential distribution could have been generated by multiple, synchronized sources. Consequently, the estimated latency of the recorded compound potential would be affected by the recording sites. (2) The

degree to which the spontaneous Alpha EEG and Alpha CEP responses are interrelated is still controversial (Childers and Perry, 1971), thus making the interpretation of the CEP magnitude and phase Bode plots unreliable. In light of the above, latencies of the Alpha CEP were broadly estimated and ranged between 100-220 msec (Regan, 1972; Diamond, 1977; Spekreijse et al., 1977; Junker and Peio, 1984). CEPs recorded to 4-7 Hz MF stimuli (typically low magnitude, highly non-linear responses) were estimated from the authors' figures, to have a latency of 220 msec (Regan, 1966) and 145 msec (Spekreijse, 1966).

A two-input (noise, stimulus) one-output (recorded cortical potentials) sequential model was derived by Spekreijse (1966) and Spekreijse et al. (1977), based on the following observations:

1. High ratios of 2nd harmonic/fundamental components that were found in CEPs recorded to 4-7 Hz MFs (even for modulation depth as low as 1%) indicated a non-analytic non-linear processing stage. Based on further analysis, transfer function of this stage was modeled by an asymmetric full-wave rectifier.
2. The fundamental and 2nd harmonic CEP components at the Alpha EEG MF region had similar Bode-plots and scalp potential distributions. This behavior was modeled by a cortical equivalent BPF, sharply tuned at the Alpha EEG frequency and subjected to visual and cerebral noise input.
3. Saturation of CEP magnitudes, induced by an increase in modulation depth, was found to be MF-dependent and binocularly additive. This analytic non-linear processing stage was modeled by a "soft"-saturation element, limiting the binocularly-merged rectifier stage output.
4. Superimposed auxiliary signals (noise or other sinusoidally Amplitude Modulated, AM, signal) linearized the responses evoked for stimuli with MF of Alpha EEG

frequency/2 (increasing the fundamental/2nd harmonic component ratio). The dependency of the linearizing effect on the auxiliary signal frequency indicated a linear processing stage preceding the non-linear rectifier stage. This linear stage was modeled by a retinal equivalent BPF with a center frequency of 18 Hz and low and high frequency asymptotes of -6 and -18 dB/octave, respectively.

This working-model (Spekreijse, 1966) was formulated under the following assumptions: retina-cortex sequential information processing (no feedback, no parallel pathways, etc.), single output system (the recorded potentials originated from a cortical single source), time-invariant sensory channel, zero-memory non-linear elements and non-interactive sensory pathway (unaffected by cross-sensory input, subject attitude, etc.). Some of these assumptions will be contested later in the discussion of the MTF experiment.

4.1.1.3 CEPs in response to 12-25 Hz modulation frequency stimuli

CEP magnitudes at the 12-25 Hz MF region were maximal at the occipital, 4 cm right or left off the midline, ipsilateral to the stimulated visual field. It has not yet been resolved whether these CEPs were actually generated in, or just favorably recorded from, the ipsilateral hemisphere. Regan (1972) and Spekreijse et al. (1977) concluded that the equivalent dipole source of these CEPs resided in the secondary visual cortex (Brodmann areas 18 and 19; the "secondary response"). The estimated latency range of these CEPs was 60-140 msec (Regan, 1966; Regan, 1972; Diamond, 1977; Spekreijse et al., 1977, Junker, 1984).

The "secondary response" CEPs were characterized by the following observations: the responses were color-dependent and relatively undistorted (high fundamental/harmonic component ratios); the spontaneous EEG spectrum did not show

any 12-25 Hz frequency band equivalent selectivity (the response could not be modeled by a cortical equivalent filter subjected to cerebral noise). The distal, linear transfer function, of the "secondary response" was modeled by a linear equivalent BPF with a center frequency of 18 Hz and low and high frequency asymptotes of -6 and -12 to -18 dB/octave, respectively (Spekreijse et al., 1977).

4.1.1.4 CEPs in response to 45-60 Hz modulation frequency stimuli

CEP magnitudes at the 45-60 Hz MF region were maximal around the occipital region, topographically corresponding to the projected retinal map of the stimulated fovea centralis (Spekreijse, 1966; Spekreijse et al., 1977). The primary visual cortex (Brodmann 17) was suggested as the equivalent dipole source for these low level CEPs (the "primary response"). Estimated latency range for these CEPs was 30-60 msec (Tweel and Lunel, 1965, for MFs > 35 Hz; Regan, 1972; Spekreijse et al., 1977).

4.1.2 Auditory continuous evoked potentials

Contrary to the visual system, few comparable CEP studies have been carried out on the human auditory system. Utilizing amplitude modulated tone or noise and click stimuli, CEPs recorded for 4-15 Hz, 15-25 Hz and 40-55 Hz MF stimuli were associated with latency ranges of 60-200 msec (Rodenburg et al, 1972; Rickards and Clark, 1984), 30-100 msec (Rees, 1981; Rickard and clark, 1984; Stapells et al., 1984) and 10-50 msec (Galambos et al., 1981; Galambos, 1982; Rees, 1981; Rickards and Clark, 1984; Stapells et al., 1984), respectively. Some of the latency measures cited here were not provided by the above authors, but were estimated from their phase plot data. A common feature in all the cited studies is that subject attitude was not formally controlled. The subjects were reading a book, relaxing or dozing.

Rickards and Clark (1984) obtained averaged CEPs (recorded from the vertex-mastoid) for 0.25-8 KHz tones, 94% modulation depth, 4-512 Hz sinusoidally amplitude-modulated stimuli, at average sound levels of 20-108 dB SPL. They found that the fundamental magnitude, generally the dominant CEP component, was carrier-frequency-dependent. Maximal magnitudes at low and high MFs (relative to 20 Hz) were obtained with low and high carrier frequencies (relative to 1 KHz), respectively. Bode plots of CEPs recorded from one of their subjects showed two similar magnitude peaks at 15 and 40 Hz, superimposed on an LPF-like response (60 Hz corner frequency and -8dB/octave high frequency attenuation). Estimated latencies of the CEPs recorded for the 4-12 Hz, 15-35 Hz and 40-140 Hz MF ranges were 150, 50 and 15 msec, respectively.

Rees (1981) obtained averaged CEPs (recorded from F4-A2), for a 1 KHz carrier tone, 100% modulation depth, 1-500 Hz sinusoidally amplitude-modulated stimuli, at intensities up to 70 dB Sound Level (SL). Magnitude peaks were found at 4 Hz (major peak, in one subject) and 40 Hz (minor peak, in two subjects). Average estimated latencies of the CEPs recorded at the 5-5.5 Hz, 18-21 Hz and 40-55 Hz MFs were 300, 110 and 50 msec, respectively.

Rodenburg et al. (1972) obtained averaged CEPs (recorded from C3-F3,4) for white noise sound, 5-100% modulation depth, 4-11 Hz sinusoidally amplitude-modulated stimuli, at an intensity level of 55 dB SL. They demonstrated (in two subjects) a single fundamental magnitude peak (the dominant harmonic in their recorded CEPs) at the 8-10 Hz MF range. Neither of the previously cited studies (Rees, 1981; Rickards and Clark, 1984) revealed a similar peak. Galambos et al. (1981) obtained averaged CEPs (recorded from the forehead-earlobe) for 10-60/sec, click or tone burst stimuli, at intensity levels up to 50 dB SL. They plotted response amplitude against stimulus rate and

found two magnitude peaks at stimulus rates of 15-20 (minor) and 35-45 (major) stimuli/sec. It was not clear how the amplitudes of the transient evoked responses were defined and measured. This kind of ambiguity can be resolved by using a Lock-In Amplifier (LIA), working in the frequency domain.

4.2 *Methodology*

4.2.1 Data acquisition paradigm

The investigated MF range of 5-61 Hz was divided into four sections (runs) presented in the following order: 5-8.5 Hz (8 MF values, 12.5' run duration in minutes), 16.1-27.7 Hz (9 MF values, 8' run duration), 9-15.3 Hz (13 MF values, 19' run duration) and 30.5-61 Hz (6 MF values, 9' run duration). The combinations of stimulus duration--LIA output Time-Constant (TC) setting were a function of MF : 30-51 sec--10 sec, 16-28 sec--3 sec, 29-50 sec--10 sec and 18-36 sec--3 sec for the first, second, third and fourth runs, respectively. Within a run, MF values were non-monotonically stepped (1st, middle (m), 2nd, m+1, 3rd, m+2,.. etc.) to reduce possible temporal interaction between adjacent MF values. This type of interaction was demonstrated and reviewed in Kay (1982) and others for the auditory system. Inter Stimulus Interval (ISI) was set at 3.2 sec and every MF value was repeated twice (or three times if it was the first MF of the run). The entire "MTF" and "EEG" recording session, auditory first and visual second, lasted four hours, including rest breaks taken between runs (more details in TABLE I 3.3).

In order to maximize the CEP magnitudes, high stimulus intensities were utilized (108 dB SPL or 730 cd/m² luminance level, defined as "0" dB). Modulation Transfer Functions (MTFs) of cross-repetition-averaged magnitude and continuous-phase values plotted against MF, were generated for each subject. Following the CEP session,

spontaneous EEG was recorded simultaneously from the same two recording sites under opened-eyes, no-stimulus and no-required-response conditions. EEG spectrums were estimated from RMS-averaged spontaneous EEG activity.

4.2.2 Data analysis

4.2.2.1 *Latency estimation*

Assuming a linear, minimum-phase plus a fixed delay system, CEP latencies (and consequently latency MTFs) were estimated for each subject from the continuous-phase MTF slope. Regression and correlation coefficients were computed on a 5 phase-point-wide sliding window. CEP latencies (regression coefficients/2Pi) and their reliabilities (correlation coefficients) were assigned to the windows' center frequencies. The chosen sampling window width enabled sensitive detection of latency variations with reasonable regression coefficient significance levels. Note that shorter latencies obtained for higher MFs will be more affected by a fixed margin error phase plot, imposed by the recording system and measurement process. Therefore, demonstrating the dissimilarity of shorter latency populations is difficult using this data analysis technique.

For latency estimations, the LIA cyclic-phase output data (-180 degrees to +180 degrees) had to be unfolded into continuous-phase MTFs. Although an important stage, phase unfolding has been usually conducted informally and intuitively. A more objective procedure was used by Levison et al. (1985). Their phase data was fitted to a linear filter model, estimated from the magnitude MTF. The underlying assumptions were of a minimum-phase, sequential processing system and high inter-/intra-subject variability ratio. A more heuristic, less restrictive approach was applied in the current study (FIGURE II 4.1). The unfolded, cross-subject-averaged cyclic-phase plot was used as a "template" against which the individual cyclic-phase plots were matched and unfolded. Complementary and redundant data (from other experiments in this study)

helped to determine the phase values of the noisier measurements (applied to less than 5% of the data).

4.2.2.2 Neural delay estimations

Neural delays were estimated for the auditory and visual, Alpha, Beta and Theta frequency region magnitude peaks. Linear, minimum-phase plus a fixed delay neural system was assumed, and the CEP magnitude distributions were modeled by two conjugate poles, LPF or BPF, for simplicity.

In order to increase their reliability, models were fitted to preprocessed magnitude data sets:

1. Theta, Alpha, Beta and "40 Hz" MF regions were rejected from the magnitude data set if no distinct magnitude peak was visually recognized within the 5-8 Hz, 8-12 Hz, 14-28 Hz and 32-61 Hz frequency ranges, respectively.
2. Each regional magnitude MTF was expressed in dB gains relative to its peak magnitude value and plotted against frequency ratios relative to its peak frequency value. This alignment procedure was employed in order to obtain a more accurate description of the neural equivalent filter model (reducing the inter-subject variability).
3. In each of the signal x MF region groups, only the data of magnitude values exceeding some threshold level were modeled. The threshold level was arbitrarily defined as the lower quartile value of the data distribution. This procedure insured against the inclusion of noisier, less reliable data values in the analysis.

PHASE UNFOLDING AND LATENCY DERIVATION PROCEDURES

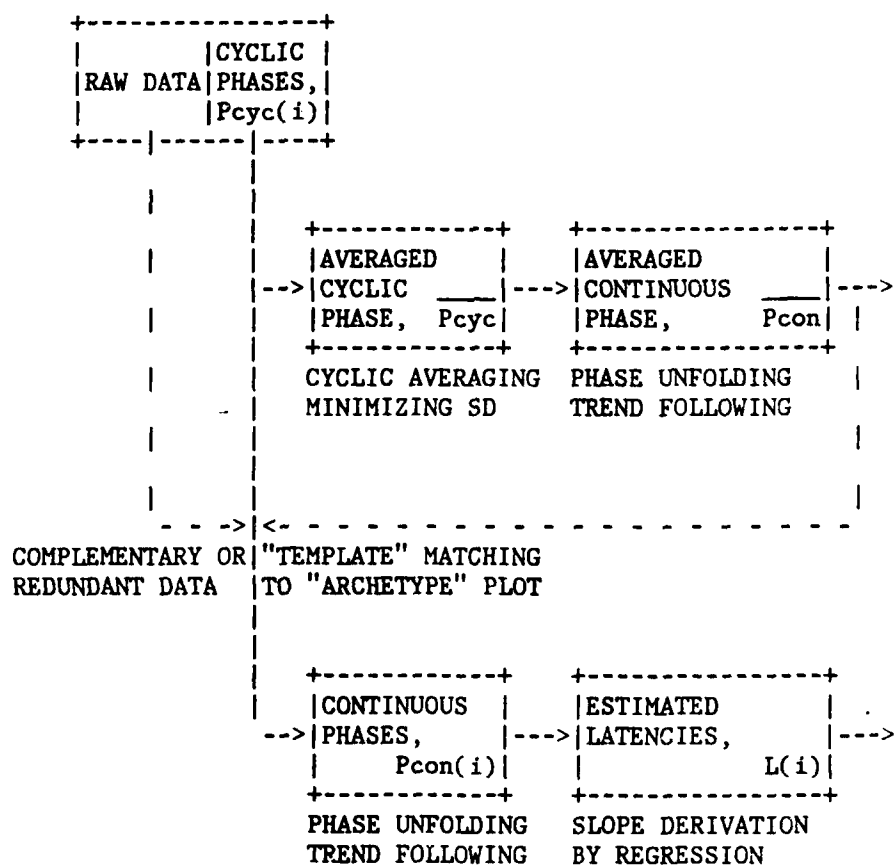


FIGURE II 4.1 : STEPS TAKEN IN GENERATING THE PHASE AND LATENCY MODULATION TRANSFER FUNCTIONS (MTFs). THE CYCLIC PHASE (Pcyc) WAS UNFOLDED INDEPENDENTLY OF THE MAGNITUDE MTF, GENERATING THE CONTINUOUS PHASE (Pcon).
 SD : STANDARD DEVIATION.

Filter parameters (LPF or BPF and damping coefficients) were optimized in the Mean Square Error sense (MSE, errors being the model - data gain differences). As previously described (in section II 4.1), it is possible to estimate the neural delay from the difference between the data and the model phase slopes measured at the peak magnitude. The slopes were derived from regression coefficients calculated for the frequency range of 1/1.15 to 1.15 of the frequency region's center frequency (0.85 to 1.17 range was used for the "40 Hz" MF region). Center frequencies were obtained by averaging the individual peak magnitude frequencies.

4.3 Results

4.3.1 Spontaneous EEG spectrums

Cross-subject averages of spontaneous EEG spectrums recorded from Oz-A1 and Cz-A1 sites (FIGURE II 4.2) were significantly different only at frequencies below 10 Hz (Alpha EEG), where larger vertex potentials were recorded. Both spectrums are characterized by a similar, inter-subject highly-variable peak at Alpha EEG frequency, absence of additional higher frequency peaks and similar Coefficient of Variability (defined as: CV = MEAN / Standard Deviation, SD).

4.3.2 Lock-in amplifier raw data output example

One of the better CEP sets processed by the LIA, is demonstrated in FIGURE II 4.3. This data was recorded in four runs covering the 5-61 Hz MF range. The data of each run details the MFs, stimulus durations and LIA fundamental component vector output. These LIA outputs were used to generate the magnitude, phase and latency MTFs presented in the following sections.

SPONTANEOUS EEG MAGNITUDES

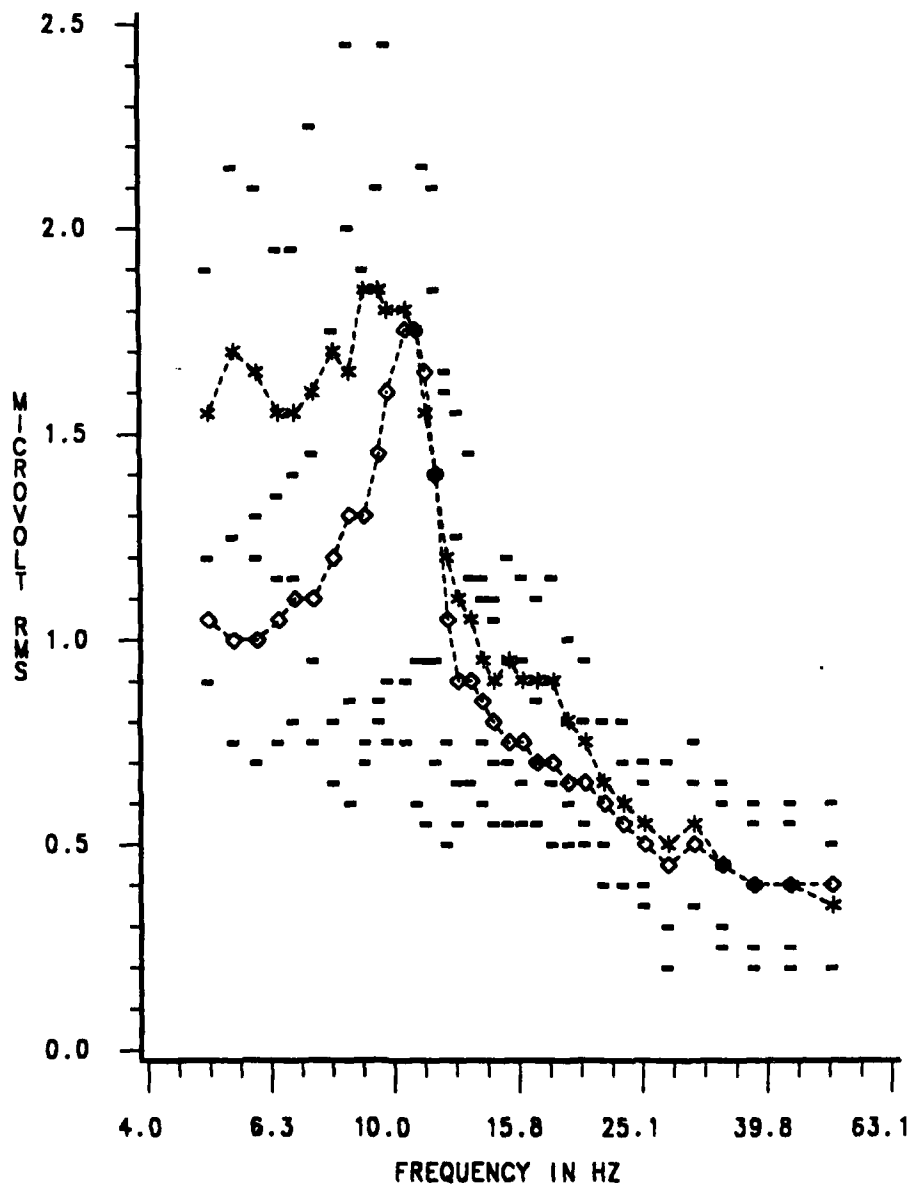


FIGURE II 4.2 : EEG SPECTRUMS, AVERAGED (MEAN AND SD) OVER 9 SUBJECTS.
STAR : RECORDED FROM CZ-A1/NOSE (AUDITORY CEP) SITES.
DIAMOND : RECORDED FROM CZ-A1/F3 (VISUAL CEP) SITES.
HORIZONTAL BARS : SD OF THE MEAN VALUES.

LOCK-IN AMPLIFIER (LIA) OUTPUT EXAMPLE

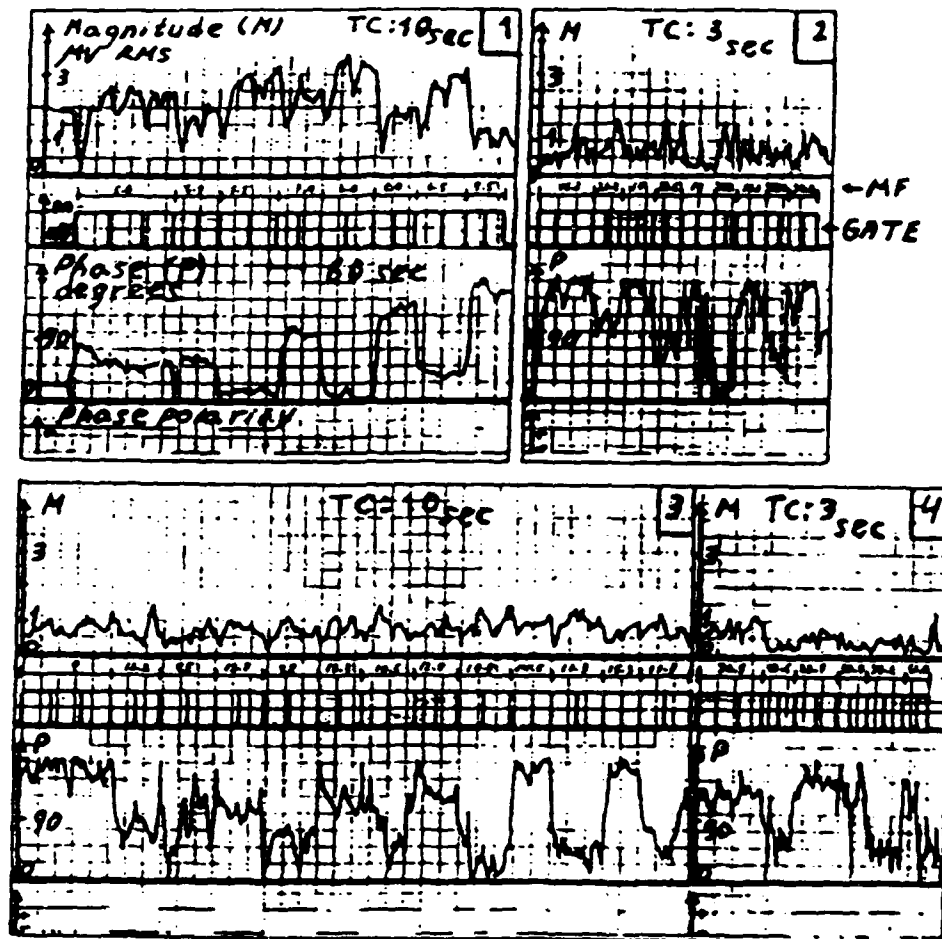


FIGURE II 4.3 : LIA OUTPUT OF 4 CONSECUTIVE RUNS OF VISUAL CEP RAW DATA OBTAINED FROM SUBJECT SC UNDER "0" dB INTENSITY LEVEL AND LIA OUTPUT TIME CONSTANTS (TCs) OF 3 AND 10 SECONDS. EACH RUN CONTAINS MAGNITUDE AND PHASE CEPs, PHASE POLARITY AND MODULATION FREQUENCIES (MFs) AND THEIR GATES. EACH MAJOR DIVISION EQUALS 30 SECONDS.

4.3.3 CEP magnitude modulation transfer functions

Auditory and visual cross-subject averages of magnitude MTFs (FIGURE II 4.4) have a similar general shape, different from the corresponding spontaneous EEG spectrums. Both averaged MTFs exhibit a primary peak (1.5-2.5 microvolt RMS) at 5-6 Hz and a secondary peak (0.5-1 microvolt RMS) at 16-25 Hz (Theta and Beta MF regions, respectively). The lower-magnitude auditory MTF, shows additional peaks (0.6-0.9 microvolt RMS) at 10.5 Hz and 50 Hz (Alpha and "40 Hz"MF regions, respectively). In general, the auditory MTF demonstrates smaller absolute (SD) and relative (SD / MEAN) inter-subject variabilities.

When t-tested for Beta and Theta MF regions, auditory and visual averaged MTFs significantly differed in absolute values, but were similar in relative values (magnitude ratio of Theta/Beta; TABLE II 4.1). A further full-frequency scale comparison of magnitude dynamic range (95%-5% of the magnitude range) and magnitude median (MEDIAN) revealed an obvious trend of larger visual averaged CEPs. This trend was not significant for the means ($P > |t|$ of 0.093-0.14), although the distributions were found to be significantly different ($P > F$ of 0.009-0.0004).

4.3.4 CEP phase modulation transfer functions

Demonstrations of the previously described phase processing stages (FIGURE II 4.1), "template" generation --> alignment procedure --> "match goodness" test, are presented in FIGUREs II 4.5, 4.6 and 4.7, respectively. Auditory and visual cross-subject averages of the continuous-phase MTFs are shown in FIGURE II 4.8. The overall visual phase response dynamic range (6Pi radians) was significantly smaller, due to a significant auditory - visual high-frequency phase difference (TABLE II 4.1). Other inter-sensory significant differences were found at Alpha and Beta MF regions ($P > |t|$

of < 0.0001). Both average MTFs exhibited small variance at Beta and Theta frequency regions, and larger variance at Alpha MF region.

4.3.5 CEP latency modulation transfer functions

Auditory and visual cross-subject averages of the latency MTFs and their confidence levels are presented in FIGURE II 4.9 and compared in TABLE II 4.1. Generally, longer latencies were associated with responses elicited for lower MFs and vice versa. Cross-modality averages of latency MTFs at the Theta, Alpha, Beta and "40 Hz" MF regions were 220 msec, 160 msec, 70 msec and 25 msec, respectively (FIGURE II 4.9, TABLE II 4.1). Auditory and visual MTFs exhibited similar latency MTFs at Beta and higher MF regions.

4.3.6 CEP modeling and neural delays

Linear models of the pre-processed auditory and visual CEPs (see section II 4.2.2.2 for details) at Theta, Alpha, Beta and "40 Hz" MF regions are presented in FIGURE II 4.10 and described in TABLE II 4.2. A "40 Hz" MF region model for the visual CEPs was not constructed since only two subjects exhibited magnitude MTF peaks at MF above 32 Hz. A LPF model was justified (MSE-wise) only for the auditory Alpha MF region. In general, the auditory data were fitted with sharper filters (higher Q factor), and the Alpha MF region filters in both modalities were the sharpest. Also, longer and more reliable delays were estimated for the visual CEPs, where longest and shortest delays were found in both modalities at Alpha and Beta MF regions, respectively. Cross-modality averages of neural delays were 59 msec, 82 msec, 31 msec and 10 msec for the Theta, Alpha, Beta and "40 Hz" (auditory CEP only) MF regions, respectively.

CEP MAGNITUDES

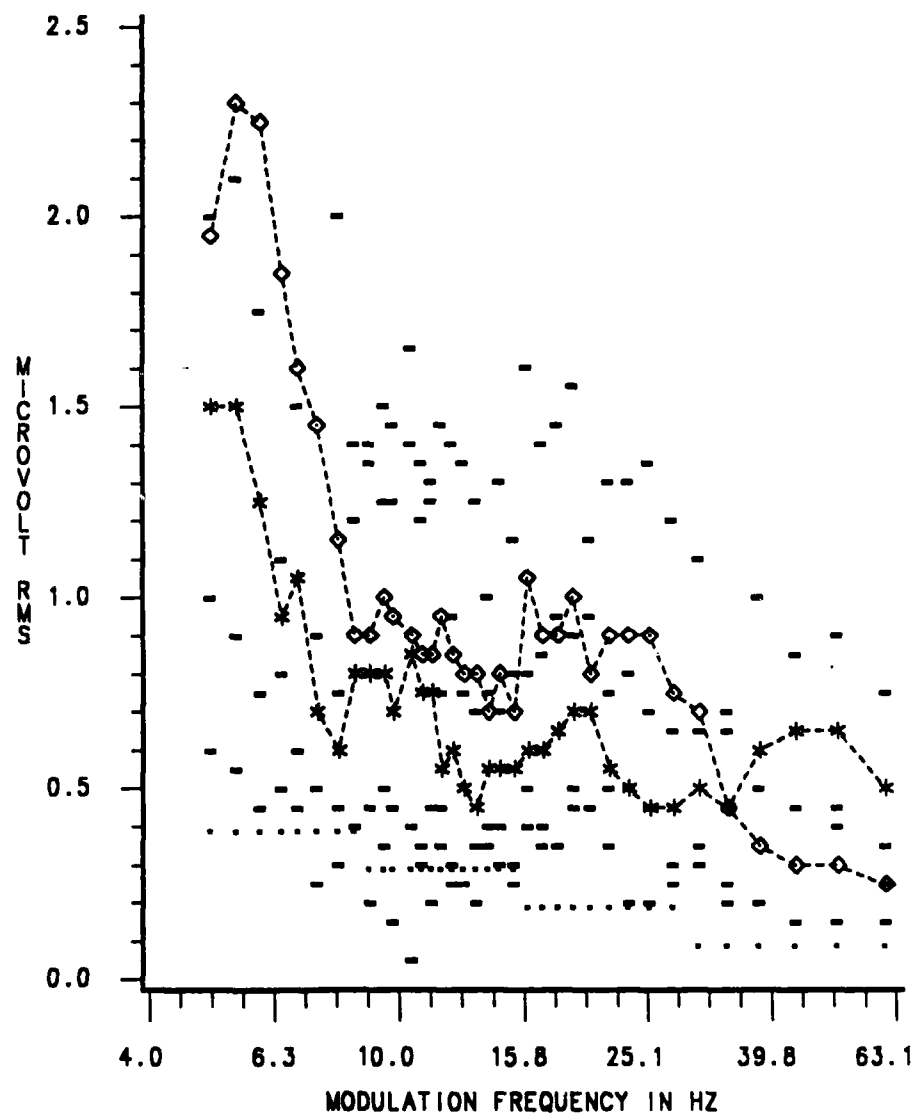


FIGURE II 4.4 : MAGNITUDE RESPONSES, AVERAGED (MEAN AND SD) OVER 9 SUBJECTS.
DOTTED LINE : NOISE LEVEL IN MICROVOLT RMS,
STAR : AUDITORY CEP (RECORDED FROM CZ-A1/NOSE SITES),
DIAMOND : VISUAL CEP (RECORDED FROM OZ-A1/F3 SITES),
HORIZONTAL BARS : SD OF THE MEAN VALUES.

VISUAL CYCLIC PHASE MTF

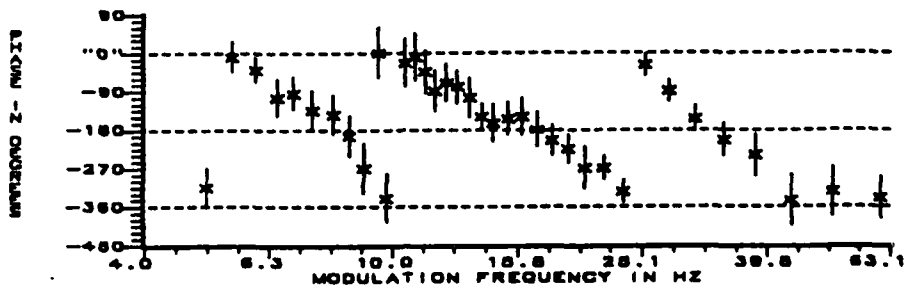


FIGURE II 4.5 : AVERAGE PHASE RESPONSE OVER 8 SUBJECTS, STAR : AVERAGE (SD MINIMIZING MEAN) CYCLIC PHASE, VERTICAL LINE : STANDARD DEVIATION SPREAD.

VISUAL INDIVIDUALS AND AVERAGED CYCLIC-TO-CONTINUOUS CONVERTED PHASES

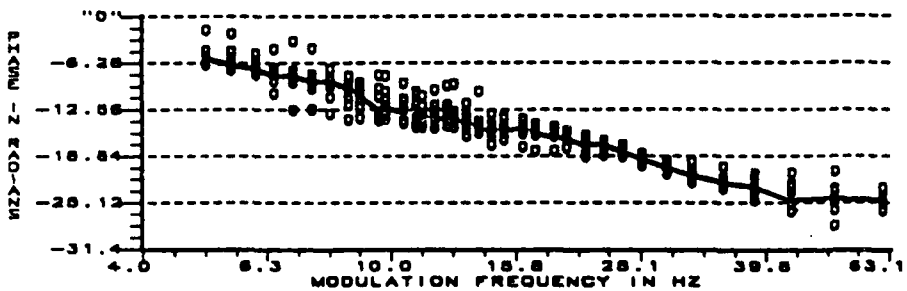


FIGURE II 4.6 : PHASE RESPONSE OF 8 SUBJECTS, LINE : AVERAGED CYCLIC, CONVERTED TO CONTINUOUS PHASE, CIRCLES : INDIVIDUALS, CYCLIC-TO-CONTINUOUS CONVERTED PHASE

VISUAL CONTINUOUS AND CYCLIC-TO-CONTINUOUS CONVERTED AVERAGE PHASES

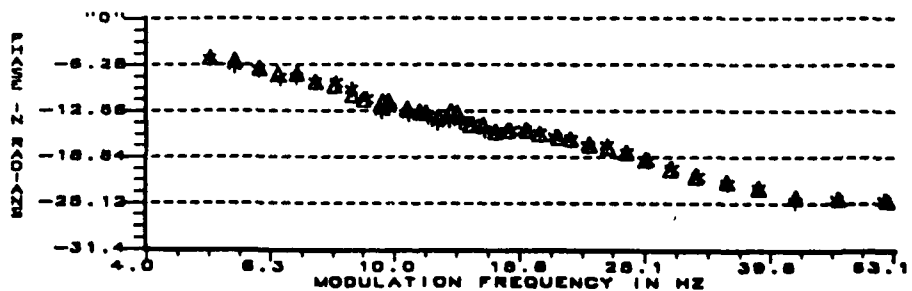


FIGURE II 4.7 : AVERAGE PHASE RESPONSE OVER 8 SUBJECTS, STAR : AVERAGED CYCLIC, CONVERTED TO CONTINUOUS PHASE, TRIANGLE : AVERAGED, CYCLIC CONVERTED TO CONTINUOUS PHASE.

CEP CONTINUOUS PHASES

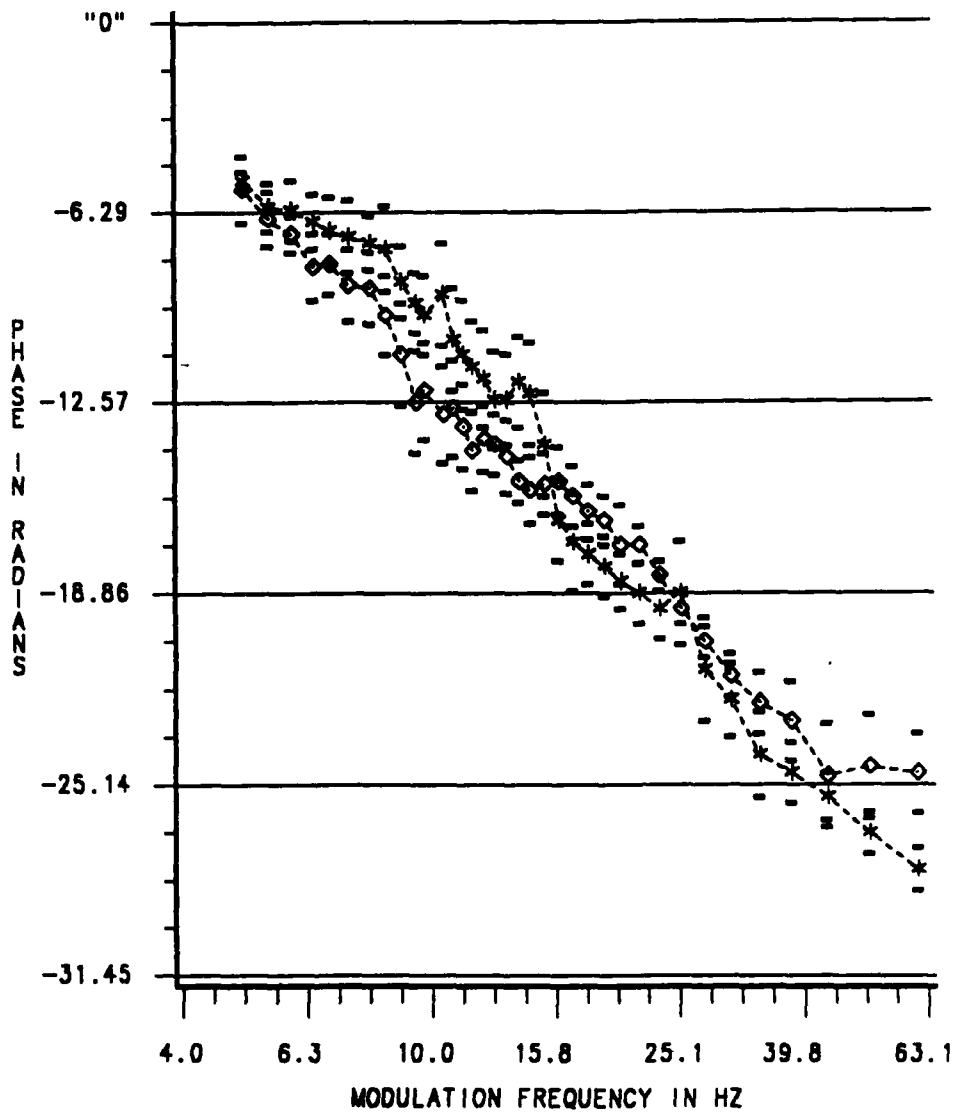


FIGURE II 4.6 : PHASE RESPONSES, AVERAGED (MEAN AND SD) OVER 9 SUBJECTS.
AVERAGED CYCLIC PHASE WAS CONVERTED TO CONTINUOUS PHASE.
STAR : AUDITORY CEP (RECORDED FROM (+)CZ-(+)A1/NOSE SITES),
DIAMOND : VISUAL CEP (RECORDED FROM (+)OZ-(+)A1/T3 SITES).
HORIZONTAL BARS : SD OF THE MEAN VALUES.

CEP LATENCIES

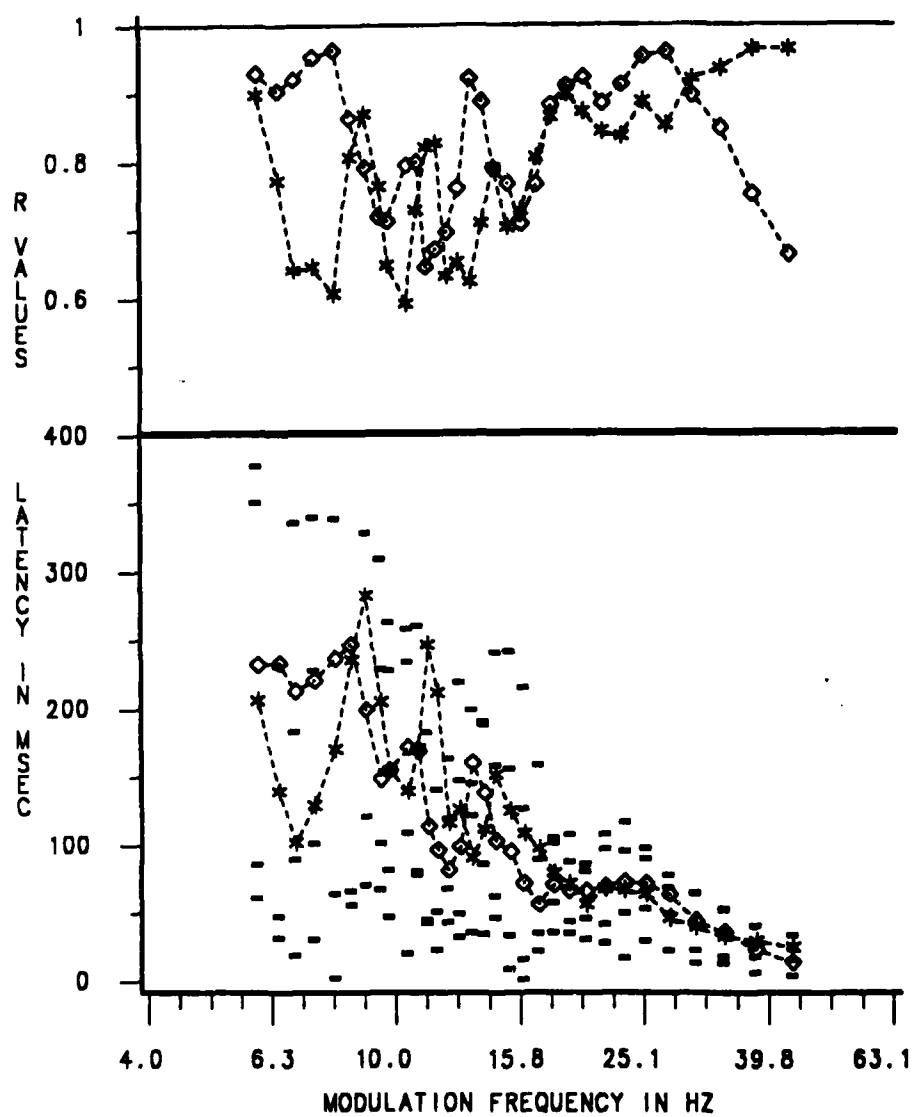


FIGURE II 4.9 : AVERAGED CONFIDENCE (TOP) AND LATENCY (BOT) OVER 9 SUBJECTS.
 LATENCY (REGRESSION COEFF/6.29) AND CONFIDENCE (CORRELATION COEFF)
 WERE ESTIMATED FROM 5 PHASE-POINT-WIDE SLIDING WINDOW.
 STAR : AUDITORY CEP (CZ-A1/NOSE RECORDING SITES).
 DIAMOND : VISUAL CEP (OZ-A1/F3 RECORDING SITES).
 HORIZONTAL BARS : SD OF THE MEAN VALUES.

AUDITORY AND VISUAL CEP COMPARISON

TABLE II 4.1 : t-test, F-test and descriptive statistics. MEAN : averaged value over N observations, SD : Standard Deviation, MF : Modulation Frequency, MTF: Modulation Transfer Function, BETA: 18, 19.1, 20.3 and 21.8 Hz MF values, THETA : 5, 5.5 and 6 Hz MF values.

PARAMETERS	N	AUDITORY	VISUAL	P>F	P> t
<hr/>					
MEAN±SD of Magnitudes in microvolt RMS					
THETA MF region	27	1.41±0.53	2.16±1.57	0.000	0.026
BETA MF region	36	0.64±0.23	0.90±0.46	0.000	0.004
THETA / BETA	9	2.42±1.10	2.47±1.48	0.42	0.94
MTF MEDIAN	9	0.60±0.13	0.83±0.35	0.009	0.09
MTF 95%-5% range	9	1.43±0.34	2.24±1.47	0.000	0.14
<hr/>					
MEAN±SD of con- tinuous phases in radians					
THETA MF region	27	-6.07±1.1	-5.98±1.3	0.33	0.79
BETA MF region	36	-18.22±1.05	-16.83±0.97	0.65	0.000
THETA - BETA	9	12.15±0.85	10.85±1.81	0.047	0.07
MTF 95% value	9	-5.97±0.69	-5.82±1.38	0.07	0.78
MTF 5% value	9	-26.22±1.55	-24.41±1.4	0.79	0.019
MTF 95%-5% range	9	20.95±1.5	18.59±1.63	0.82	0.038
<hr/>					
MEAN±SD of latencies in msec					
THETA MF region (at 6 Hz)	9	206±143	233±145	0.96	0.70
BETA MF region (over all)	36	69±32	67±28	0.40	0.73

LINEAR MODELS OF CEP RESPONSES
 SIG=AUDIO REGION=THETA CF=5.45 HZ THRESH=0.70 MICROVOLT RMS

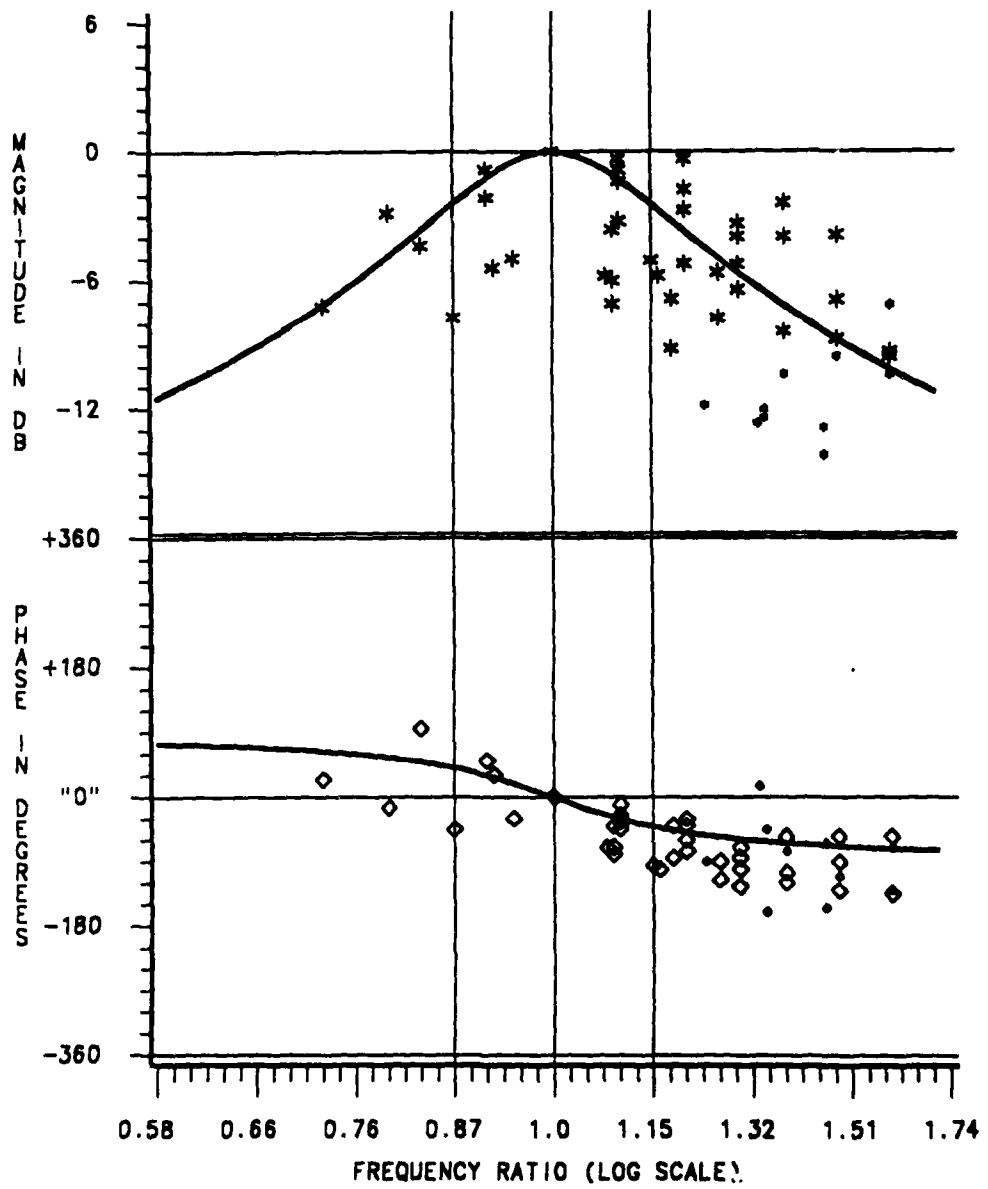


FIGURE II 4.10 : LINEAR MODELING AT ALPHA, BETA AND THETA ALIGNED MF REGIONS.
 LEAST-MSE QUADRATIC BPF MODELS WERE FITTED TO THE MAGNITUDE DATA.
 CF: CENTER FREQUENCY, THRESH: DATA DISTRIBUTION LOWER QUARTILE.
 LARGER CHARACTERS: DATA EXCEEDING THE THRESHOLD LEVEL (MODELED DATA).

LINEAR MODELS OF CEP RESPONSES
 SIG=AUDIO REGION=ALPHA CF=10.35 HZ THRESH=0.40 MICROVOLT RMS

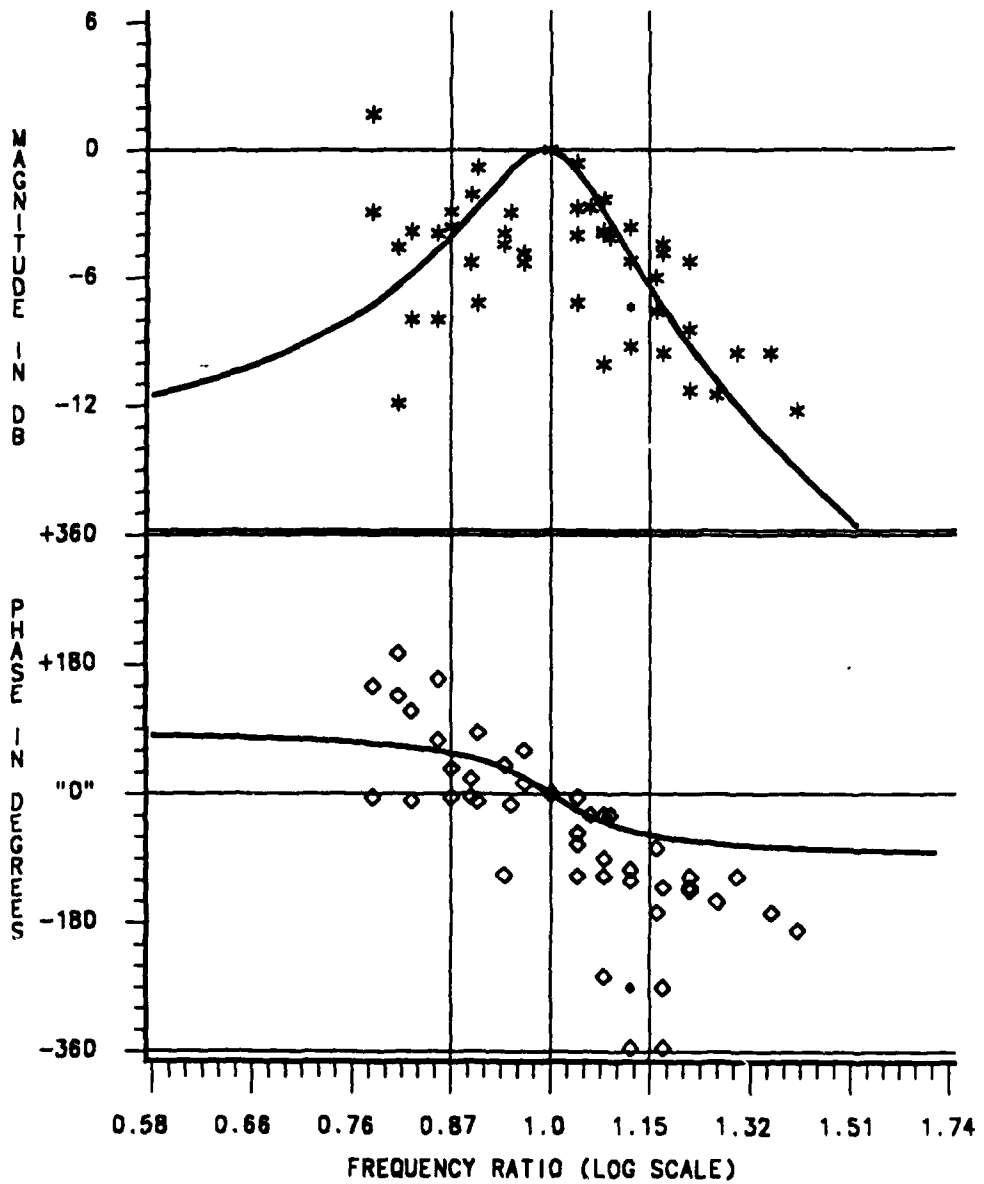


FIGURE II 4.10 : LINEAR MODELING AT ALPHA, BETA AND THETA ALIGNED MF REGIONS.
 LEAST-MSE QUADRATIC BPF MODELS WERE FITTED TO THE MAGNITUDE DATA.
 CF: CENTER FREQUENCY, THRESH: DATA DISTRIBUTION LOWER QUARTILE.
 LARGER CHARACTERS: DATA EXCEDING THE THRESHOLD LEVEL (MODELED DATA).

LINEAR MODELS OF CEP RESPONSES
 SIG=AUDIO REGION=BETA CF=18.85 HZ THRESH=0.40 MICROVOLT RMS

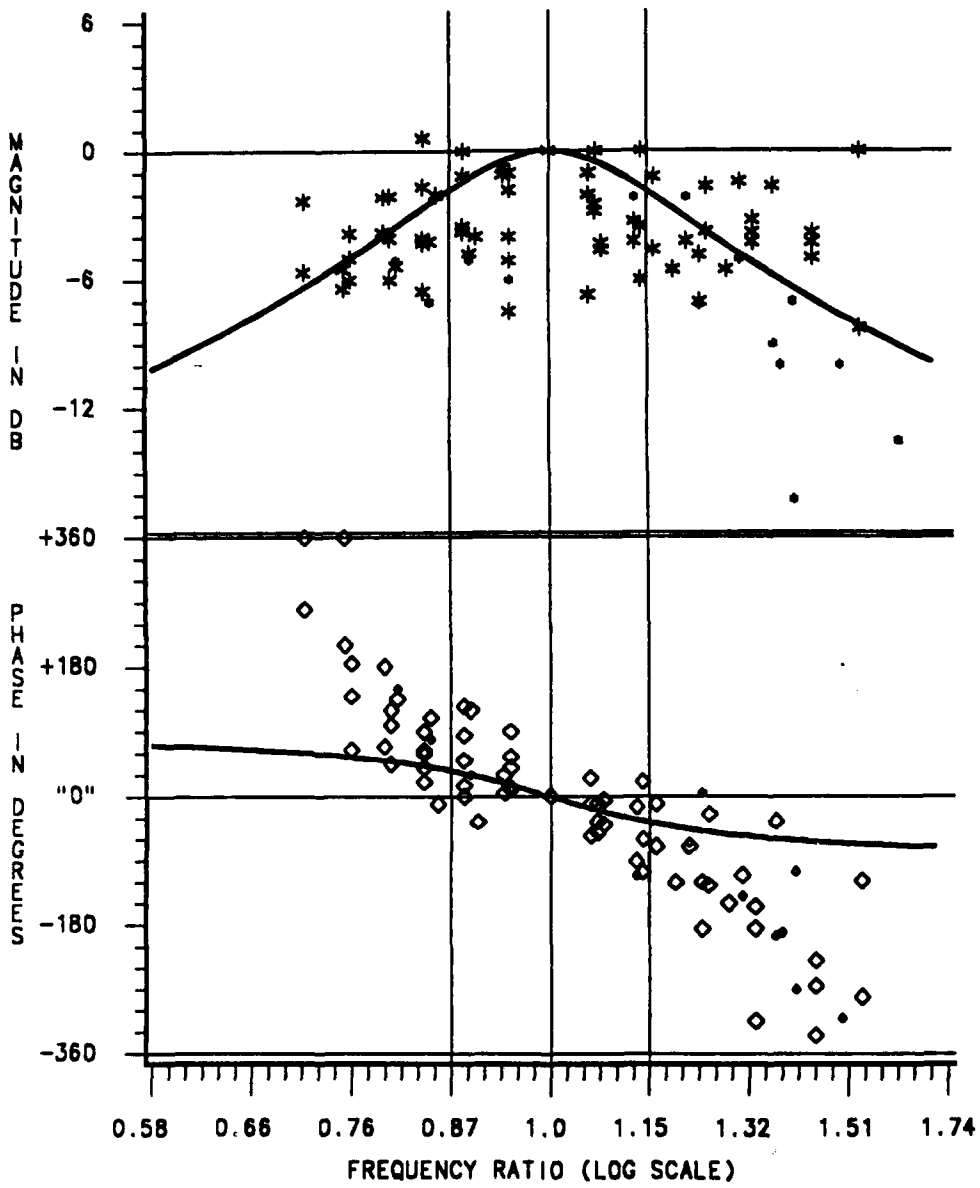


FIGURE II 4.10 : LINEAR MODELING AT ALPHA, BETA AND THETA ALIGNED MF REGIONS.
 LEAST-MSE QUADRATIC BPFF MODELS WERE FITTED TO THE MAGNITUDE DATA.
 CF: CENTER FREQUENCY, THRESH: DATA DISTRIBUTION LOWER QUARTILE,
 LARGER CHARACTERS: DATA EXCEEDING THE THRESHOLD LEVEL (MODELED DATA).

LINEAR MODELS OF CEP RESPONSES
SIG=AUDIO REGION="40 HZ" CF=45 HZ THRESH=0.40 MICROVOLT RMS

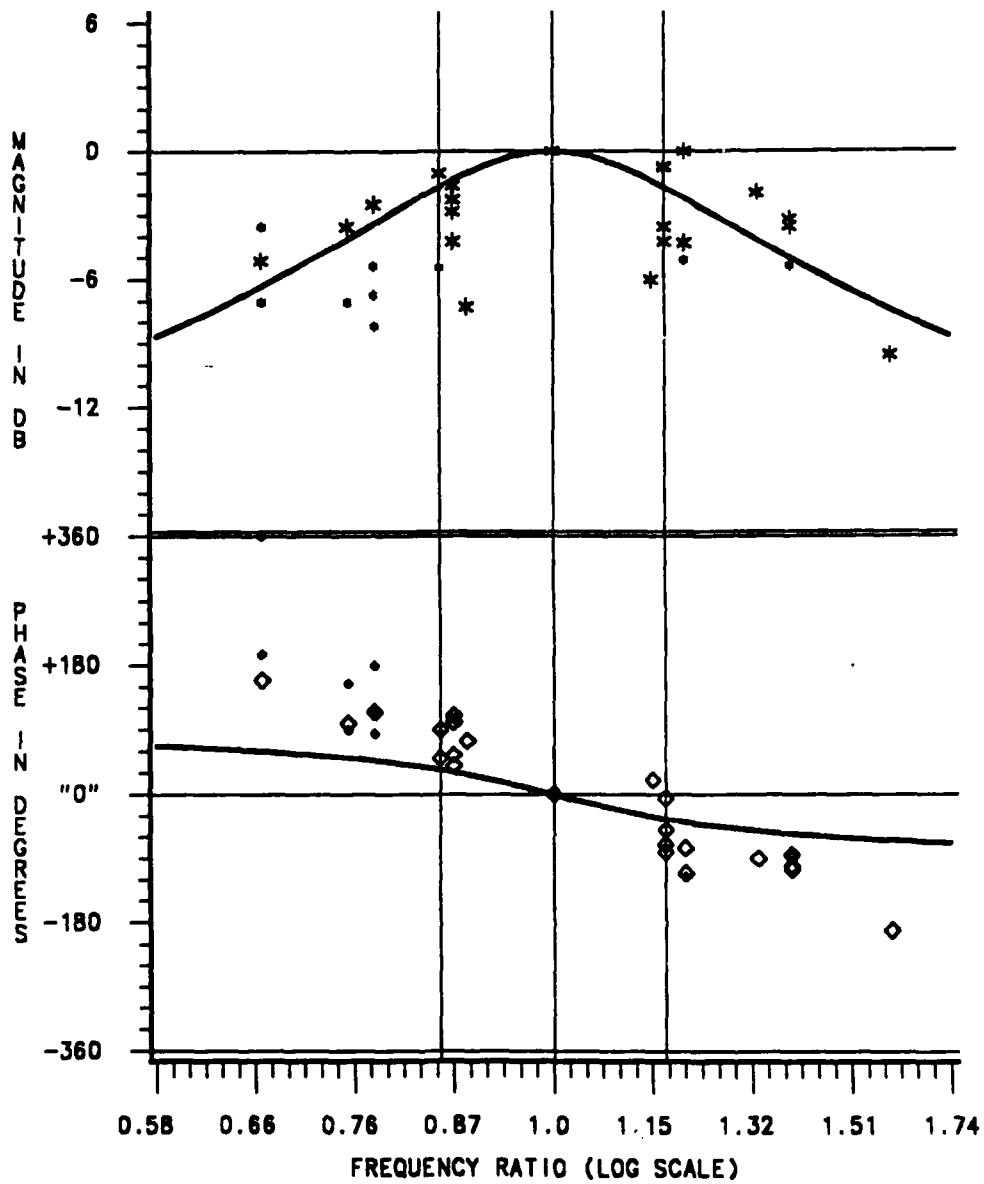


FIGURE II 4.10 : LINEAR MODELING AT HIGH FREQUENCY ("40 HZ") ALIGNED MF REGION.
LEAST-MSE QUADRATIC BPF MODEL WAS FITTED TO THE MAGNITUDE DATA.
CF: CENTER FREQUENCY, THRESH: DATA DISTRIBUTION LOWER QUARTILE,
LARGER CHARACTERS: DATA EXCEEDING THE THRESHOLD LEVEL (MODELED DATA).

LINEAR MODELS OF CEP RESPONSES
SIG=VISUAL REGION=THETA CF=5.40 HZ THRESH=0.70 MICROVOLT RMS

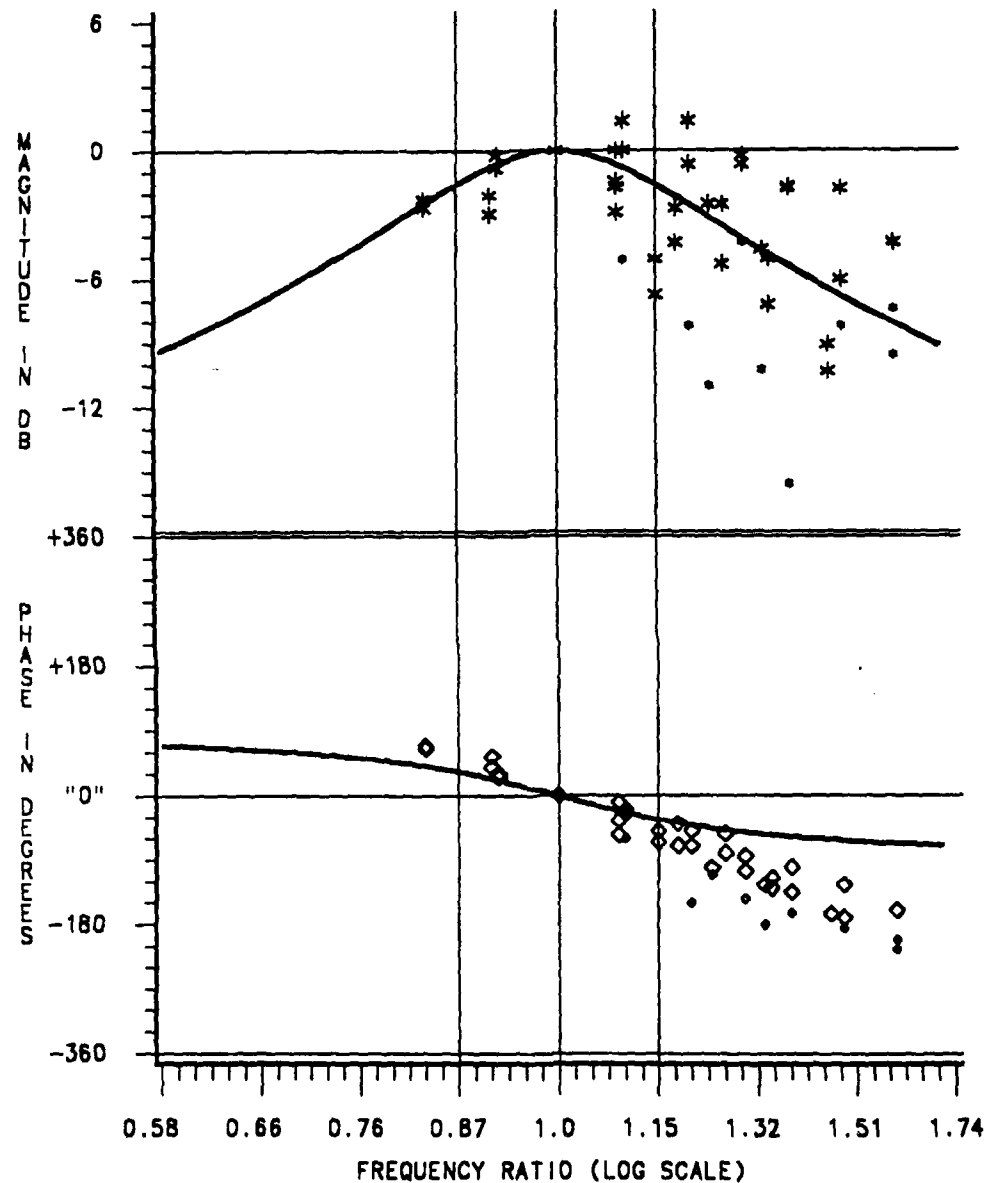


FIGURE II 4.10 : LINEAR MODELING AT ALPHA, BETA AND THETA ALIGNED MF REGIONS.
LEAST-MSE QUADRATIC BPF MODELS WERE FITTED TO THE MAGNITUDE DATA.
CF: CENTER FREQUENCY, THRESH: DATA DISTRIBUTION LOWER QUARTILE,
LARGER CHARACTERS: DATA EXCEEDING THE THRESHOLD LEVEL (MODELED DATA).

LINEAR MODELS OF CEP RESPONSES
 SIG=VISUAL REGION=ALPHA CF=10.35 HZ THRESH=0.55 MICROVOLT RMS

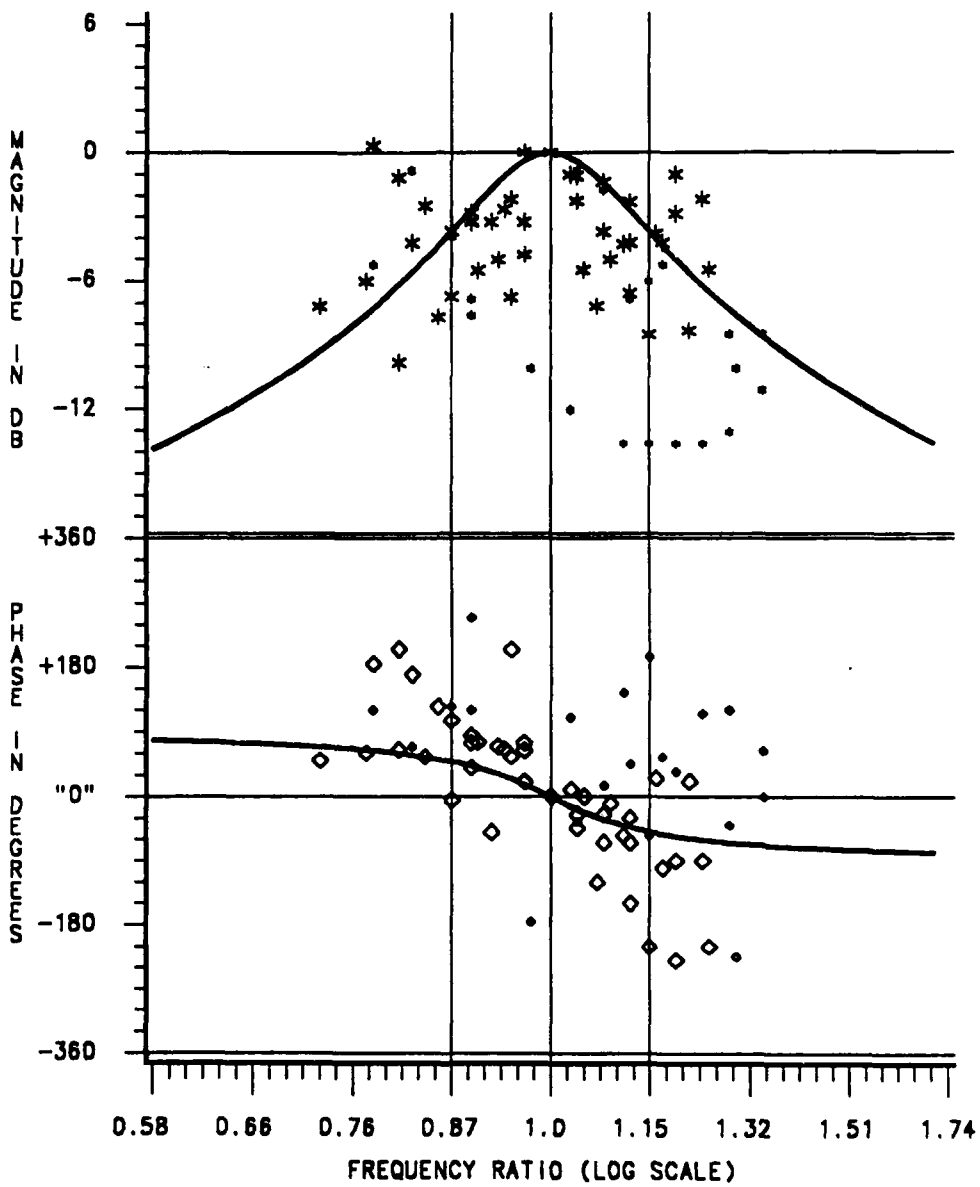


FIGURE II 4.10 : LINEAR MODELING AT ALPHA, BETA AND THETA ALIGNED MF REGIONS.
 LEAST-MSE QUADRATIC BPF MODELS WERE FITTED TO THE MAGNITUDE DATA.
 CF: CENTER FREQUENCY, THRESH: DATA DISTRIBUTION LOWER QUARTILE,
 LARGER CHARACTERS: DATA EXCEEDING THE THRESHOLD LEVEL (modeled data).

LINEAR MODELS OF CEP RESPONSES
 SIG=VISUAL REGION=BETA CF=20.65 HZ THRESH=0.55 MICROVOLT RMS

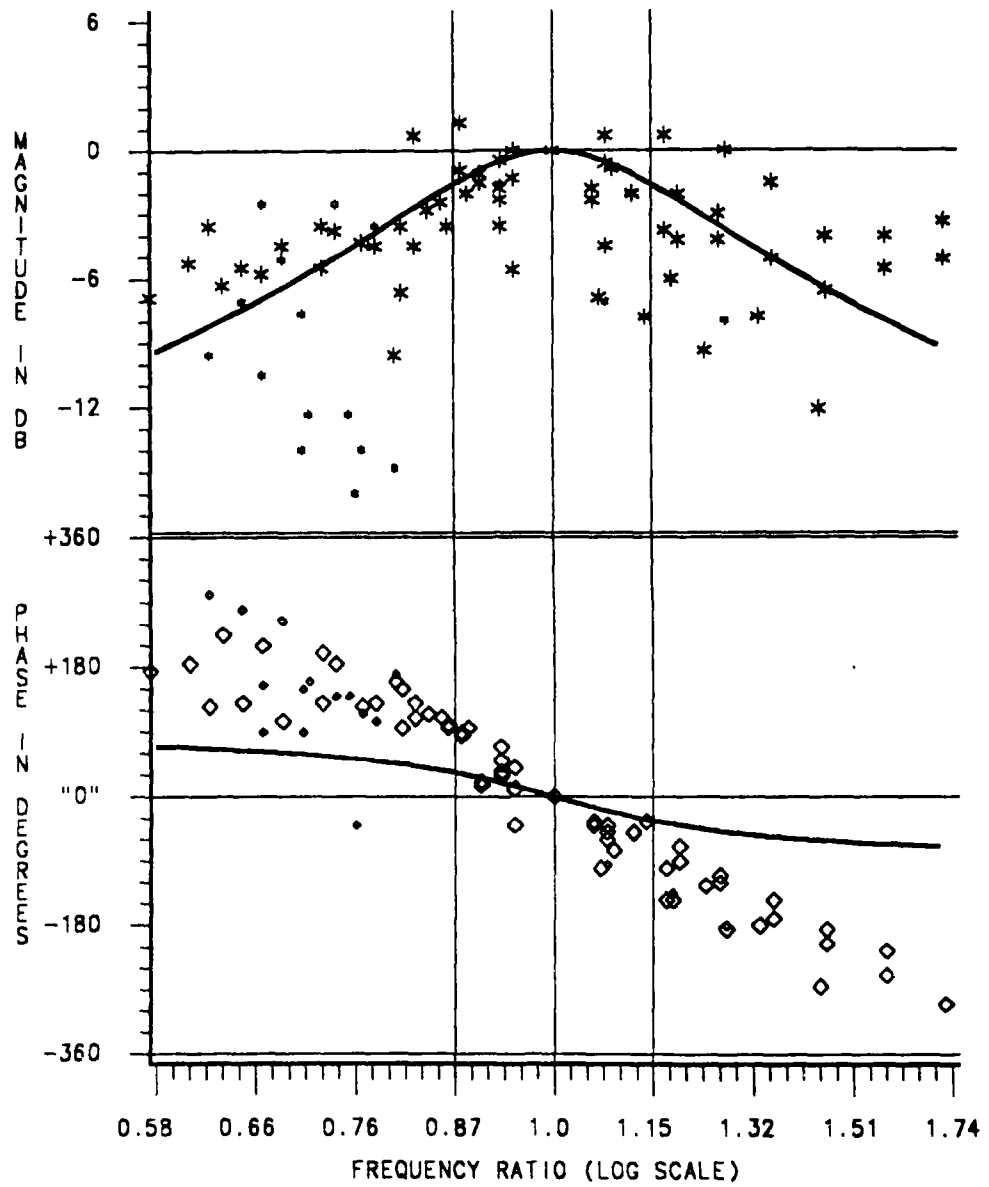


FIGURE II 4.10 : LINEAR MODELING AT ALPHA, BETA AND THETA ALIGNED MF REGIONS.
 LEAST-MSE QUADRATIC BPN MODELS WERE FITTED TO THE MAGNITUDE DATA.
 CF: CENTER FREQUENCY, THRESH: DATA DISTRIBUTION LOWER QUARTILE,
 LARGER CHARACTERS: DATA EXCEEDING THE THRESHOLD LEVEL (MODELED DATA).

ESTIMATION OF CEP DELAYS AND LATENCIES

TABLE II 4.2 : Estimated CEP delays and latencies from band-pass or low-pass quadratic filter models. Max group delay : filter's largest phase-shift slope, SD/SE : Standard Deviation/Standard Error, MF: Modulation Frequency, RMSE: Root Mean Square Error.

PARAMETERS	AUDITORY CEP MF REGIONS			
	THETA	ALPHA	BETA	"40 Hz"
Frequency Range, Hz	5-8	8-12	14-28	32-61
Number of Cases (N)	8	5	8	8
Peak Frequency \pm SD, Hz	5.4 \pm 0.7	10.4 \pm 0.8	18.9 \pm 1.2	45 \pm 4.4
Peak Mag \pm SD, microV RMS	2.0 \pm 0.4	1.7 \pm 0.8	0.9 \pm 0.3	0.8 \pm 0.3
Model-Data RMSE, dB	2.7	3.1	2.5	1.9
Damping Factor	0.16	0.09	0.19	0.23
Max "Group Delay", msec	163	128	40	14
CEP Latency \pm SE, msec	223 \pm 38	203 \pm 47	62 \pm 12	24 \pm 3
R ² of The Estimation	0.64	0.38	0.45	0.72
CEP Delay \pm SE, msec	60 \pm 38	75 \pm 47	22 \pm 12	10 \pm 3
VISUAL CEP MF REGIONS .				
PARAMETERS	VISUAL CEP MF REGIONS .			
	THETA	ALPHA	BETA	"40 Hz"
Frequency Range, Hz	5-8	8-12	14-28	
Number of Cases (N)	7	7	8	2
Peak Frequency \pm SD, Hz	5.4 \pm 0.5	10.4 \pm 0.8	20.7 \pm 3.5	
Peak Mag \pm SD, microV RMS	2.7 \pm 1.4	1.3 \pm 0.4	1.4 \pm 0.6	
Model-Data RMSE, dB	2.3	2.9	2.7	
Damping Factor	0.21	0.12	0.21	
Max "Group Delay", msec	131	106	34	
CEP Latency \pm SE, msec	188 \pm 23	195 \pm 30	73 \pm 9	
R ² of The Estimation	0.81	0.56	0.71	
CEP Delay \pm SE, msec	57 \pm 23	89 \pm 30	39 \pm 9	

4.4 Discussion

4.4.1 CEP validity

Before addressing the results, the response (CEP) must first be proved to be exclusively and physiologically related to the stimulus (AM signal). Based on their equivalent filter models, the CEP TC ranged between 40 to 180 msec (TABLE II 4.2). Since the LIA output TC was much larger (10 sec), the CEP vectors obtained between 2-3 LIA output TCs were assumed to be at their "steady-state" levels. The following supporting observations were obtained under stimulus on/off conditions, while the stimulus MF (REF signal) and the raw CEP were input to the LIA. Under stimulus-off condition and independently of the MF value, only low magnitudes and random phases (status defined as noise level) were recorded (clearly shown in the next set of experiments). Under stimulus-on condition, similar repetitive stimuli produced a non-random variable response vector (FIGURE II 4.3). Also, since the resultant magnitude and phase MTFs were significantly different from the recording system transfer functions, the non-physiological-"CEP" possibility was rejected.

The most prominent peak was found at the lowest MF scale (5-8 Hz), an active frequency region also of the myogenic responses (EMG). Since voluntary muscle activity was required only at the end of each attended-to stimuli (the Reaction Time, RT, test), and the long ISIs (3.2 sec each) provided ample time for the myogenic and related neurogenic transient potentials to die out, these low MF potentials were concluded to be genuine CEPs. It was therefore concluded that the recorded CEPs were valid, representing neural activity exclusively evoked by the stimuli.

4.4.2 Evoked and spontaneous potentials

The CEPs were extracted from the spontaneous EEG and other biological noise sources (EMG, ECG, etc.). The spontaneous EEG, with an equivalent noise bandwidth similar to that of the CEPs was considered to be the primary noise source. SNRs of CEP/spontaneous EEG (in dB of mean square values) were calculated for Alpha, Beta and Theta frequency regions. The visual SNRs (recorded from Oz-A1 sites) were 29, -12 and 5.7 dB at Theta, Alpha and Beta MF regions, respectively (from FIGUREs II 4.2, 4.4). The corresponding auditory SNRs (recorded from Cz-A1 sites) were -2.2, -14.3 and -2.3 dB. Overall lower auditory CEP magnitudes made their SNRs smaller than the corresponding visual SNRs. The greatest inter-sensory SNR difference occurred at the Theta frequency region, partially due to high low-frequency background activity picked up at the Cz-A1 recording sites. The more frontal vertex electrode might have picked up additional signals from myogenic sources (eyeball and facial muscles).

The worst SNRs were obtained in the Alpha frequency region. In contrast to the dominant Alpha EEG spontaneous activity, only minor CEPs were evoked at this MF region. A reverse situation occurred at Beta and higher frequency regions. Contrary to distinct MTF peaks, no visible EEG spectrum peaks were detected. Thus, as Spekreijse et al. (1977) pointed out for the Beta MF region visual CEPs, these responses could not have been generated by spontaneous EEG-equivalent filters.

Spontaneous EEG was recorded in this current study under opened-eyes, no-stimulus and no-required response conditions. The degree to which this background "noise" was task-engagement-independent (an assumption made in calculating the previous SNRs) has not been established here. Other studies (Koles and Flor-Henry, 1981; Sterman, 1984), investigating the task-engagement effects on the EEG Theta and Alpha frequency

regions, provided mixed results. Koles and Flor-Henry (1984) demonstrated a decrease of Alpha frequency region power-density (the commonly accepted trend) and an increase of Theta/Alpha frequency region power ratio (> 1), in subjects engaged in verbal or motor tasks. Since motor responses were required during the entire task-engagement sessions, the Theta frequency region power-density was correctly attributed to myogenic responses. Contrasting results, obtained by Sterman (1984), showed a general (recording-site-dependent observation) increase of Alpha frequency region power-density and a decrease of Theta/Alpha frequency region power ratio (< 1), in subjects engaged in a flight simulation task. In summary, utilizing the Lock-In method, the CEP variance (and not the mean value) will reflect the recording SNR, where the noise itself (background EEG), like the signal (CEP), may be stimulus- or task-dependent.

4.4.3 CEP latency and delay estimations

The Bode plots presented in FIGURE II 4.11 (in Appendix A) should not be perceived as traditional "black-box" frequency responses. The values at each frequency point represent a compound potential vector, averaged over multiple, complexly-connected sources responding with various latencies. Therefore, even if linearity and time-invariance properties can be assumed, a singular neural delay and latency cannot be calculated for the entire phase plot since the phase and magnitude Bode plots are not uniquely related. However, if small isolated regions of the Bode plots can justifiably be analyzed separately, regional latency and delay estimations can be obtained.

This approach was utilized to estimate the CEP neural delays and latencies at Alpha, Beta and Theta MF regions. The following assumptions were made: CEPs at each MF region were generated predominantly by a single, time-invariant source; each source could be modeled by a transmission-line delay followed by a linear equivalent filter, partially disclosed on the Bode plots (the center frequency and the high frequency

asymptote); each equivalent filter could be modeled by a two conjugate pole LPF or BPF with various degrees of tuning. These assumptions will be examined after the presentation of additional experimental results. The significance of the models' parameters, summarized in TABLE II 4.2, is discussed in section II 4.4.6.

4.4.4 Modulation transfer functions of visual CEPs

Cross-subject averages of the fundamental CEP component latencies at Theta, Alpha, Beta and 45-60 Hz ("40 Hz") MF regions were 233, 160, 67 and 20 msec, respectively. Excluding the Theta MF region, these results confirm the latency estimations of other researchers (Twael and Lunel, 1965; Regan, 1966, 1972; Spekreijse, 1966; Spekreijse et al., 1977; Diamond, 1977; Junker, 1984; Junker and Peio, 1984). When a restricted (more reliable) data set was used (data set used in the neural delay estimation, TABLE II 4.2), the Theta MF region latency results were also confirmed. With the exception of the Beta MF region, the cross-subject average of magnitude MTFs do not, however, comply with the results in the majority of the above cited studies (reviewed in section II 4.1.1.2-4). These differences will be discussed in the following section.

The major fundamental magnitude peak at the Theta MF region was detected in 75% of the visual MTFs obtained in this current study (FIGURE II 4.11). It was generated for low to medium average luminance, 100% amplitude-modulated, attended-to, spotlight stimuli. Magnitude peaks at this temporal frequency range (Theta) have been typically obtained for a high spatial-frequency, pattern-reversal stimulation method (Regan, 1977). Utilizing diffused light and unattended-to stimuli Spekreijse (1966), Spekreijse et al. (1977) and Regan (1966, 1972) obtained predominantly 2nd harmonic component responses. The contrasting results of high fundamental/2nd harmonic component ratios, obtained in this current study (the results of this and the following ex-

periments) may be attributed to (1) a response-linearizing phenomenon, and/or, (2) the fact that the stimuli were attended-to.

(1) Utilizing the Spekreijse "retina-cortex low-frequency subsystem" model (reviewed in section II 4.1.1.2), the response of the essentially non-linear stage (a 2nd harmonic generator modeled by an asymmetric full-wave rectifier) would have been linearized by an added high-frequency auxiliary signal. The auxiliary signal could be comprised of harmonic components generated in a preceding stage (non-linear gain, magnitude saturation, etc.) or carried along with the fundamental input signal. The large-signal input applied in this current study (100% modulation depth stimuli) might have generated such early higher harmonic auxiliary signals, linearizing the following rectifier transfer function. Such a linearizing effect is expected of fixed stimulus-rate, flash stimuli input. This input can be regarded as a fundamental frequency input signal accompanied by auxiliary, higher harmonic components. And indeed, Perry and Childers (1969) and others, obtained a predominant fundamental component TEP recorded for 4-6/sec flash stimuli.

(2) The low MF, attended-to stimuli may have been perceived as discrete flashes rather than continuous signals. TEPs in response to flash stimuli exhibited a major magnitude peak (peak "P VII") at a 180-220 msec latency (Perry and Childers, 1969). Therefore, if CEP and TEP data are comparable, the high magnitude, 188-233 msec latency (TABLEs II 4.1-?), Theta MF region CEPs obtained in this current study can be attributed to that P VII TEP peak. Attention effects are described in the following ATT experiment.

The Alpha MF region peaks, detected in 75% of the MTFs obtained in this current study, were of less significance when compared to results of other studies (section II

4.1.1.2). These differences may be attributed to (1) subject's engagement effect and/or (2) the driven-reference, CEP recording method.

(1) Although not believed to be totally unrelated, the dependency between the spontaneous EEG and the CEP magnitudes at Alpha frequency region (Alpha EEG and Alpha CEP, respectively), is still controversial (Childers and Perry, 1971; Spekreijse et al., 1977 and others). If these responses positively correlate to some degree (in peak magnitudes and frequencies), task-engagement that attenuates the Alpha EEG magnitudes (see section II 4.4.2) must decrease the Alpha CEP response as well.

(2) A driven-reference differential amplifier device, the recording system's front-end amplifier used in this current study, is characterized by a very high CMRR of 150 dB. Therefore it is possible that the widespread Alpha EEG potentials were rejected more efficiently than in other studies where conventional 60-80 dB CMRR devices were used.

None of the MTFs obtained in this current study showed the High Frequency MF region peak, obtained by others. These low-magnitude potentials can be generated only for high retinal-illuminations (typically on the order of 1,000-10,000 troland; Spekreijse, 1966; Regan, 1972), higher levels than those utilized in this current study (approximately 1400 troland).

4.4.5 Modulation transfer functions of auditory CEPs

Cross-subject averages of the fundamental CEP component latencies at Theta, Alpha, Beta and "40 Hz" MF regions were 206, 160, 69 and 30 msec, respectively. Magnitude peaks at Theta (major), Alpha, Beta and "40 Hz" frequency regions were detected in approximately 85%, 55%, 85% and 85% of the individual MTFs, respectively (FIGURE II 4.11). In comparison to the visual CEPs, the auditory CEPs were

associated with lower signal/noise magnitude ratio, lower inter-subject variability and higher intra-subject variability.

CEP magnitude and latency results obtained in this study for MFs greater than 15 Hz, roughly agree with those of other studies (Galambos et al., 1981; Rees, 1981; Rickards and Clark, 1984; Stapells et al., 1984). (See review of these studies in section II 4.1.2). Since these studies did not apply an adequate frequency resolution at lower MF regions, further comparison was not meaningful.

The degree to which subcortical neural structures (from the receptor level to the Geniculate Body of the Thalamus) contributed to the recorded compound CEPs is believed to be negligible. Each of the "primary sensory" cortical areas (Brodmann 17, 42) contains at least two-orders more excitable neurons than any subcortical afferent nucleus, with the exception of the relatively remote retinal structures.

4.4.6 CEP overview

It was found that the lower the MF of the amplitude modulated stimuli, the larger the CEP magnitudes and the longer the latencies. This trend reflects the expected general transfer function of an afferent neural pathway. Successively larger neuron populations generate larger compound potentials with lower frequency response and longer latencies. The cross-modality averaged CEP latencies increased from 35-45 msec (at 50-60 Hz) to 200-240 msec (at 5-6 Hz).

Both auditory and visual magnitude MTFs deviated from a monotonic plot description, showing distinct magnitude peaks at non-harmonically-related specific MF regions. Since Theta and Beta regions exhibited the most detectable and reliable re-

sponse vectors in both modalities, they were the center of investigation in this and the following experiments.

CEPs at Beta MF region had latencies of 60-70 msec and delays of 30-40 msec. Latencies of the initial compound-potentials originating from the "primary-sensory" auditory and visual cortical areas were found to be 10-25 msec (Regan, 1972; Celesia, 1976). Other CEP and TEP studies, analyzing scalp potential distribution, suggested that responses with longer latencies (40-70 msec) were probably generated primarily at the "secondary-sensory" cortical areas (Regan, 1972; Celesia, 1976; Spekreijse et al., 1977; Wood and Wolpaw, 1982).

CEPs at Theta MF region had latencies of 200-240 msec and delays of 50-60 msec. Other CEP and TEP studies suggested that such late-responses primarily originated from multiple cortical sources, overlapping the initial earlier responses of the "primary and secondary sensory" cortical areas (Spekreijse et al., 1977; Goff et al., 1978; Wood and Wolpaw, 1982).

Auditory CEPs at "40 Hz" MF region had latencies of 20-30 msec and delays of 10 msec. Latencies of the initial compound-potentials originating from the "primary-sensory" auditory cortical areas were found to be 10-25 msec (Celesia, 1976). The degree to which subcortical neural structures (from the receptor level to the Geniculate Body of the Thalamus) contributed to the recorded compound CEPs is believed to be negligible. Each of the "primary sensory" cortical areas (Brodmann 17, 42) contains at least two-orders more excitable neurons than any subcortical afferent nucleus, with the exception of the relatively remote retina structures (Jung, 1973; Kay, 1982).

The results of the following experiments further characterize the Theta and Beta MF region CEPs (in terms of response stability and linearity, intensity and attention effects) and describe the auditory-visual bisensory CEP interaction.

Chapter 5

Continuous Evoked Potentials at Beta and Theta Modulation Frequency Regions

The previous chapter described the general features of the Continuous Evoked Potential (CEP) Modulation Transfer Functions (MTFs) and characterized the most responded-to Modulation Frequency (MF) regions. The experiments described in this chapter have investigated CEPs in response to selected Beta and Theta MF region stimuli, have confirmed previous results (MTF experiment) and have provided new response characteristics and controls for the following Auditory-Visual Interaction (AxV) experiment. Beta and Theta MF stimuli were selected for the following reasons: they induce optimal CEP responses in both modalities (highest magnitudes, best Signal/Noise Ratios, SNRs, low variability); the CEPs were associated with meaningful delays and latencies (suggesting the cortical level as the AxV site).

In all the following experiments, the raw magnitude data was expressed and manipulated in dB units instead of absolute RMS microvolt units. This is not an arbitrary choice, but rather an implementation of the conceptualized model of the data. The in-

dependent variables tested in this chapter (stimulus order, stimulus intensity level, and attention) and in the following chapter (attention, cross-modality stimulus intensity and MF) were regarded as control inputs, modifying some parameters (gain, filter sharpness, etc.) of the linear elements producing the CEP fundamental responses. Neither this model nor the alternative model (stimulus and independent variables as multiple input) could be proven here, but the parametric control model is more feasible physiologically and easier to work with.

5.1 DISC experiment: CEP harmonics and trends

5.1.1 Introduction

5.1.1.1 Short-term CEP trends

Intra-subject CEP magnitude instability has been attributed to many factors. Some of them were seemingly controllable (variations of recording conditions, myogenic artifacts, subject state and orientation, etc.) and some were not (noise, "trends"). "Trend effect" implied a monotonic (non-random) CEP parameter variation, which was not (or could not be) related to any of the investigated Independent Variables (IVs). Long-term trends (durations of minutes and hours), showed mostly a continuous decrease of CEP magnitudes (Perry and Childers, 1966; Moise, 1980), referred to as "habituation". In another study (Yolton et al., 1983), mixed trend effects (increasing or decreasing magnitudes) and noise effect accounted for 25% and 50% of the total intra-subject CEP magnitude variability, respectively.

Since long stimulus durations were used in the AxV experiment (90-100 sec), controls of short-term CEP trends had to be established first. The DISC ("DISCRETE") experiment provided parameter trends of CEPs recorded under maintained attention level during the first 90-100 sec past stimulus initiation.

5.1.1.2 1st and 2nd harmonics of CEPs

Latencies and delays were estimated in the previous chapter from the phase MTFs, assuming a linear minimum-phase system plus a fixed delay. The validity of the linearity assumption is tested in this experiment where the CEPs 1st and 2nd harmonic components are evaluated.

5.1.2 Methodology

The four consecutive, most responded-to frequency values in each of the Beta and Theta MF regions (magnitude peak frequencies) were tested for every subject, a total of 16 audio and visual discrete MFs (4 "mini" MTFs). Within the audio or visual series, MFs were alternatively sequenced between Beta and Theta MF regions. Each run consisted of a twice-repeated pattern of three repetitive, single MF stimuli. Average durations of stimulus-on, Inter Stimulus Interval (ISI) and Inter Pattern Interval (IPI) were 32.5, 1.4 and 32.5 sec, respectively. CEPs were recorded under the same attentiveness (Reaction Time test, RT) and stimulus intensity ("0" dB) conditions utilized in the previous MTF experiment. The DISC experiment recording session, audio first and visual second, lasted three hours, including rest breaks. For more details, refer to TABLE I 3.3.

The DISC experiment data set was processed with a Lock-In Amplifier (LIA) output Time-Constant (TC) of 10 sec. CEP magnitudes and phases of sequentially corresponding stimuli were cross-pattern averaged for each run. Since trend effects within a time-frame of 90-100 sec were the focal point of this investigation, the inter-pattern variability was regarded as noise. Relative magnitude (dB) and phase (degrees) values (relative to the the run's averaged values) were used. The resultant 1st, 2nd and 3rd CEP vectors (ORDIER classes) were tested for response stability.

In order to extract the CEP 2nd harmonic vectors, the DISC data set was off-line re-demodulated with a reference signal having twice the stimulus MF. For this analysis, the fundamental and 2nd harmonic component vectors were obtained by cross-stimulus averaging of magnitude and phase values in each run (run average values). For each group of MF (Beta, Theta) x signal (audio, visual) x subject, the most responded-to MF

was identified (peak magnitude and frequency). The latency and its reliability level of the CEPs recorded for that MF, were estimated from regression and correlation coefficients, respectively (computed on a 3 or 4 phase-point-wide window).

5.1.3 Results

5.1.3.1 *Raw data example*

An example of LIA output of a complete run is presented in FIGURE II 5.1. The 1st harmonic vector was obtained with LIA output TCs of 1 and 10 sec, and the 2nd harmonic vector with an LIA output TC of 10 sec. Note the different magnitude scales and the relatively "noisier" 2nd harmonic response. It is also evident that the TC of the neural response was much smaller than the 10 sec LIA output TC.

5.1.3.2 *CEP stability*

CEP variations over time are presented in FIGURE II 5.2 and tested for significance in TABLE II 5.1. In light of the large inter-subject variability, the average trends in each plot are supplemented with the individual data for comparison. In general, a significant trend was detected only for the magnitudes ($P > F$ of 0.006). CEP magnitudes tended to increase with time (an average increment of 15% over a time period of 90-100 sec), significantly at audio Beta and visual Theta MF regions ($P > F$ of 0.03). CEP phases showed only non-significant mixed trends at audio Theta (increase) and visual Beta (decrease) MF regions.

CEP HARMONICS EXAMPLE

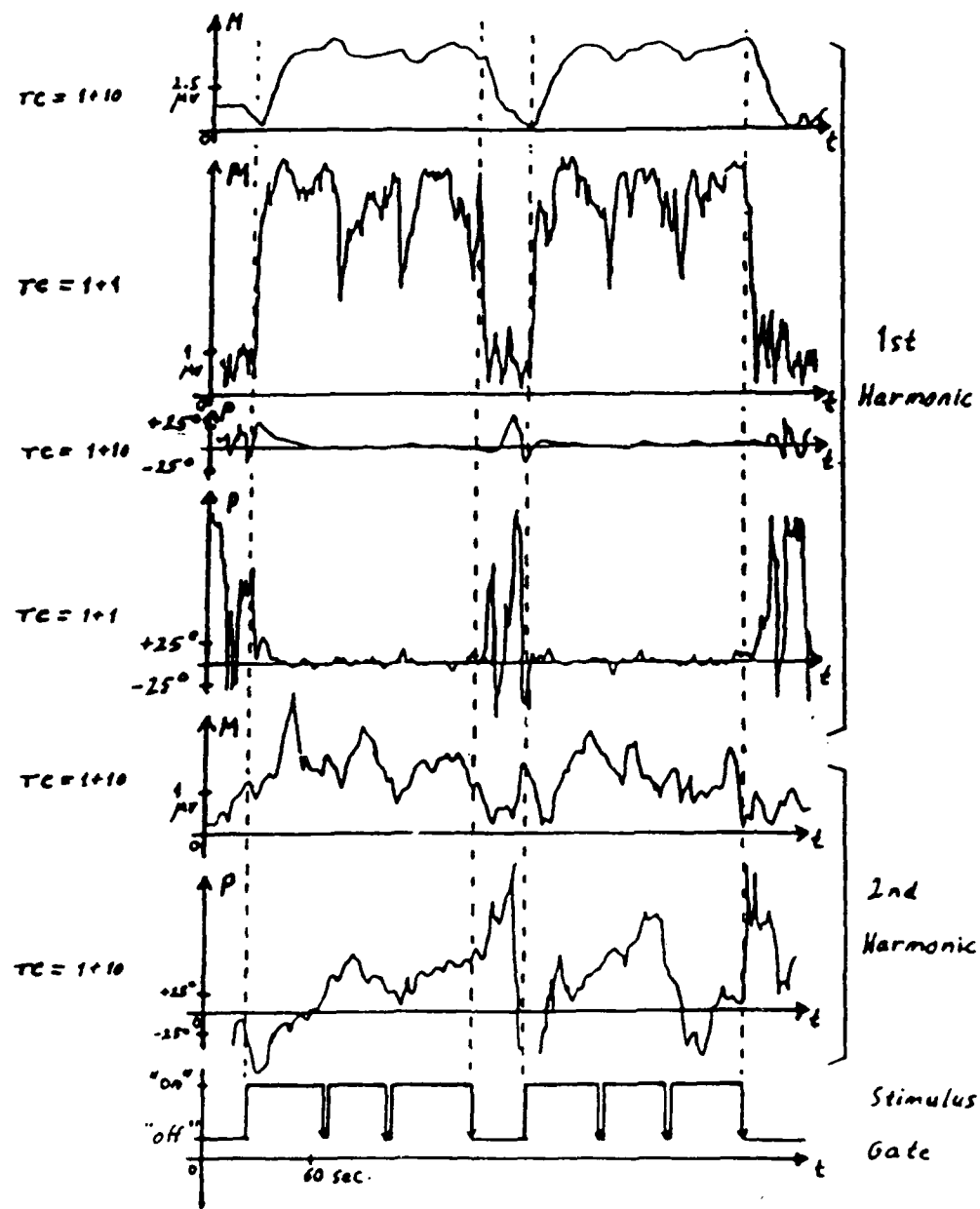


FIGURE II 5.1 : VISUAL CEP, SUBJECT MR, 35 SECONDS AVERAGED STIMULUS-ON DURATION, 5.5 Hz MODULATION FREQUENCY. M: CEP MAGNITUDE, P: CEP PHASE, TCs: LOCK-IN AMPLIFIER PRE- AND OUTPUT AMPLIFIER TIME-CONSTANTS, STIMULUS-OFF TRANSITION: REACTION-TIME CLUE.

AUDITORY AND VISUAL CEP TRENDS

TABLE II 5.1 : Trend significance between ORDER groups. MEAN : Average across N observations, ORDER : 1st, 2nd and 3rd sequential CEPs reduced by the run's mean value, NS : Not Significant, P > F of > 0.2, MF : Modulation Frequency.

PARAMETERS	AUDITORY MFs		VISUAL MFs		ALL	
	BETA	THETA	BETA	THETA		
CEP MAGNITUDES						
Number of Observations	8	8	7	7	30	
ORDER MEANS : (in dB)	1st	-1.49	-0.48	-0.25	-0.34	-0.66
	2nd	0.86	-0.23	0.27	-0.64	0.08
	3rd	0.62	0.71	-0.02	0.98	0.58
F-test between ORDER groups : (PR > F values)	All	0.029	NS	NS	0.028	0.006
	1st-2nd	0.015	NS	NS	NS	0.052
	1st-3rd	0.028	0.12	NS	0.036	0.001
	2nd-3rd	NS	NS	NS	0.012	0.19
CEP PHASES						
Number of Observations	9	9	8	8	34	
ORDER MEANS : (in degrees)	1st	0.37	-5.00	3.33	-1.04	-0.69
	2nd	-3.52	-1.67	0.83	1.46	-0.83
	3rd	3.15	6.67	-4.17	-0.42	1.52
F-test between ORDER groups : (PR > F values)	All	NS	0.094	0.195	NS	NS
	1st-2nd	NS	NS	NS	NS	NS
	1st-3rd	NS	0.036	0.079	NS	NS
	2nd-3rd	NS	0.13	NS	NS	NS

5.1.3.3 CEP harmonics

Ist and 2nd harmonic comparison of CEP peak absolute magnitudes and latencies is presented in TABLE II 5.2. The 2nd harmonic magnitudes were significantly smaller than the fundamental magnitudes (approximately 43% of the fundamental magnitudes).

STABILITY OF CEP MAGNITUDES AND PHASES

SIG=AUDIO FREQ=BETA

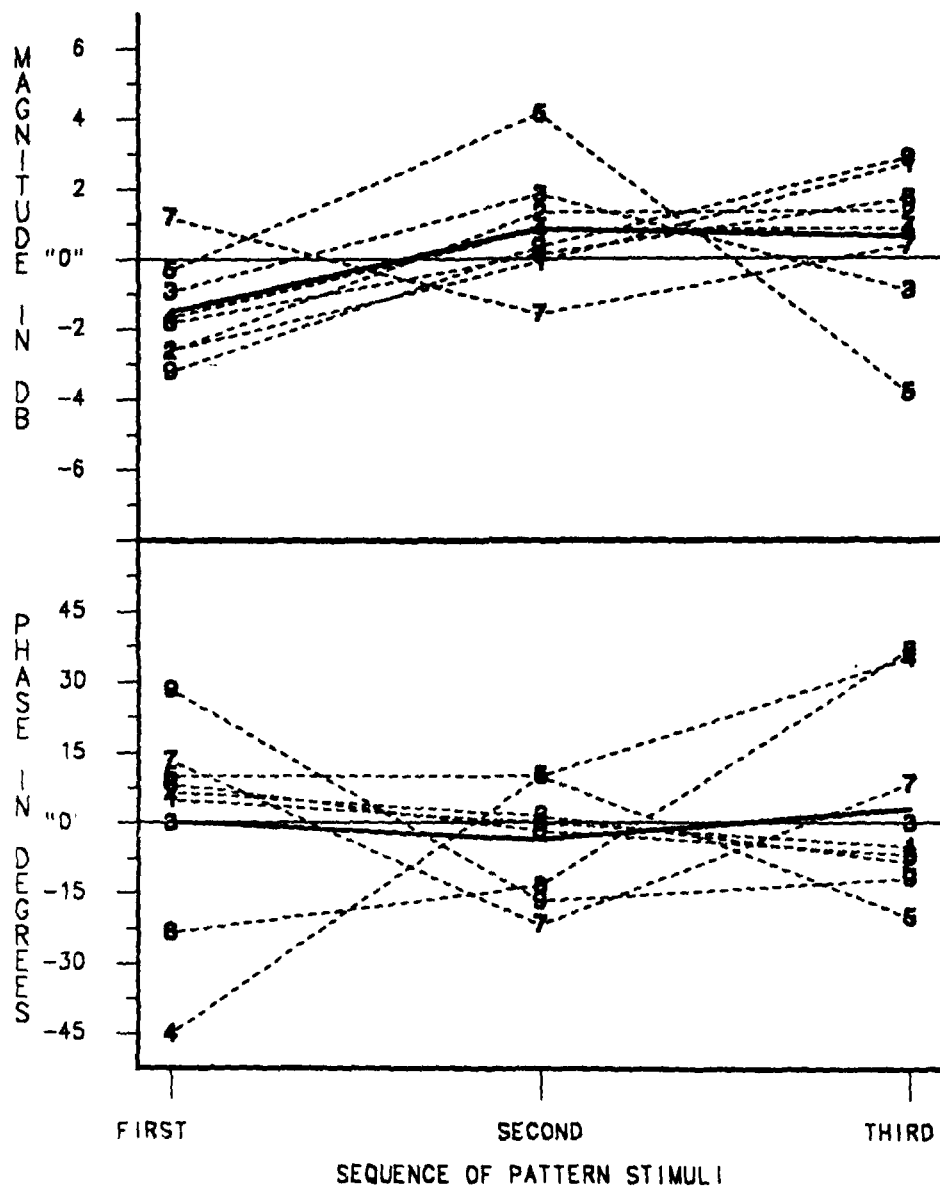


FIGURE II 5.2 : MAGNITUDE GAIN (DB) AND PHASE SHIFT (DEGREES) RELATIVE TO THE VALUES OF THE AVERAGED 1ST, 2ND AND 3RD SEQUENTIAL STIMULI.
NUMBERS: INDIVIDUAL SUBJECTS, THICK LINE: MEAN OF 9 SUBJECTS.

STABILITY OF CEP MAGNITUDES AND PHASES

SIG=AUDIO FREQ=THETA

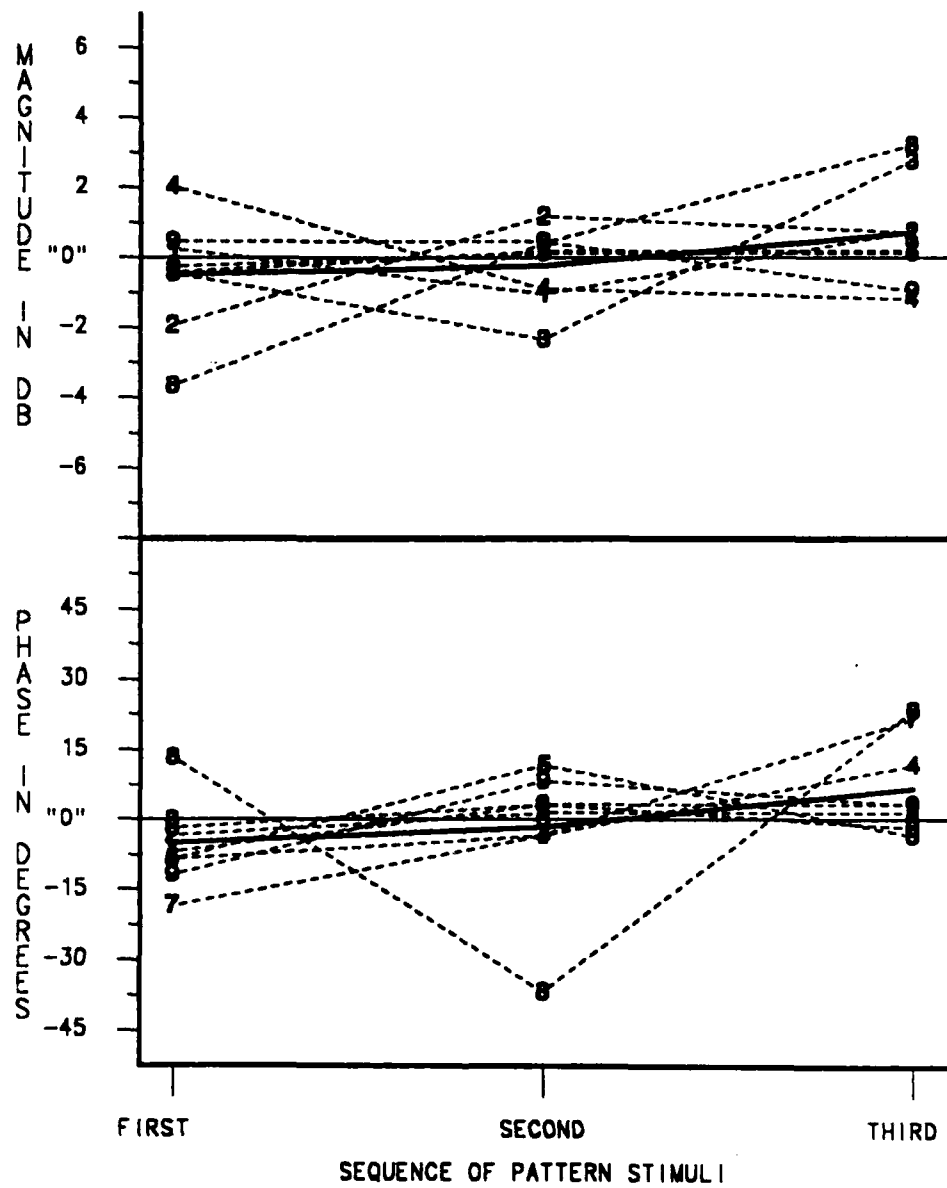


FIGURE II 6.2 : MAGNITUDE GAIN (DB) AND PHASE SHIFT (DEGREES) RELATIVE TO THE VALUES OF THE AVERAGED 1ST, 2ND AND 3RD SEQUENTIAL STIMULI.
NUMBERS: INDIVIDUAL SUBJECTS, THICK LINE: MEAN OF 9 SUBJECTS.

STABILITY OF CEP MAGNITUDES AND PHASES

SIG=VISUAL FREQ=BETA

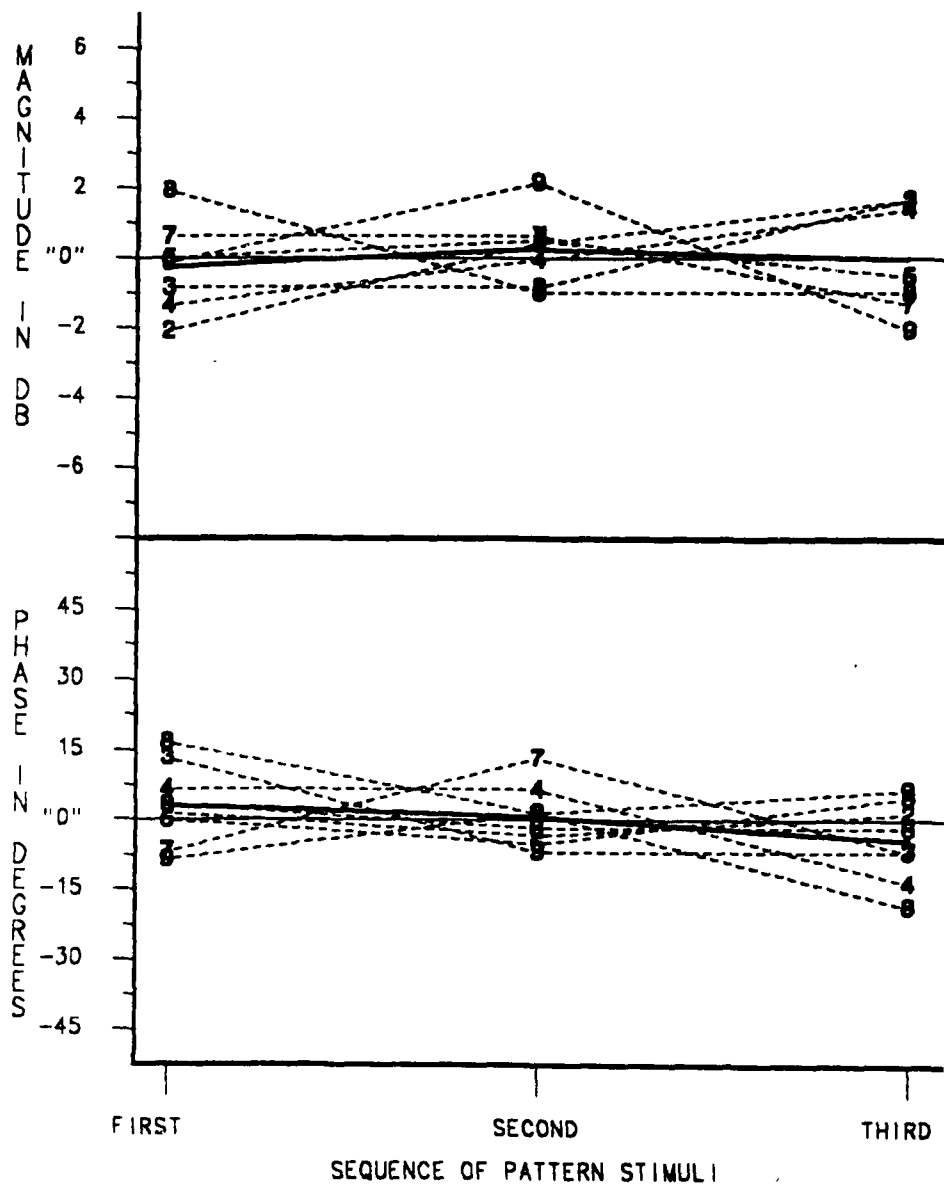


FIGURE II 5.2 : MAGNITUDE GAIN (DB) AND PHASE SHIFT (DEGREES) RELATIVE TO THE VALUES OF THE AVERAGED 1ST, 2ND AND 3RD SEQUENTIAL STIMULI.
NUMBERS: INDIVIDUAL SUBJECTS, THICK LINE: MEAN OF 9 SUBJECTS.

STABILITY OF CEP MAGNITUDES AND PHASES

SIG=VISUAL FREQ=THETA

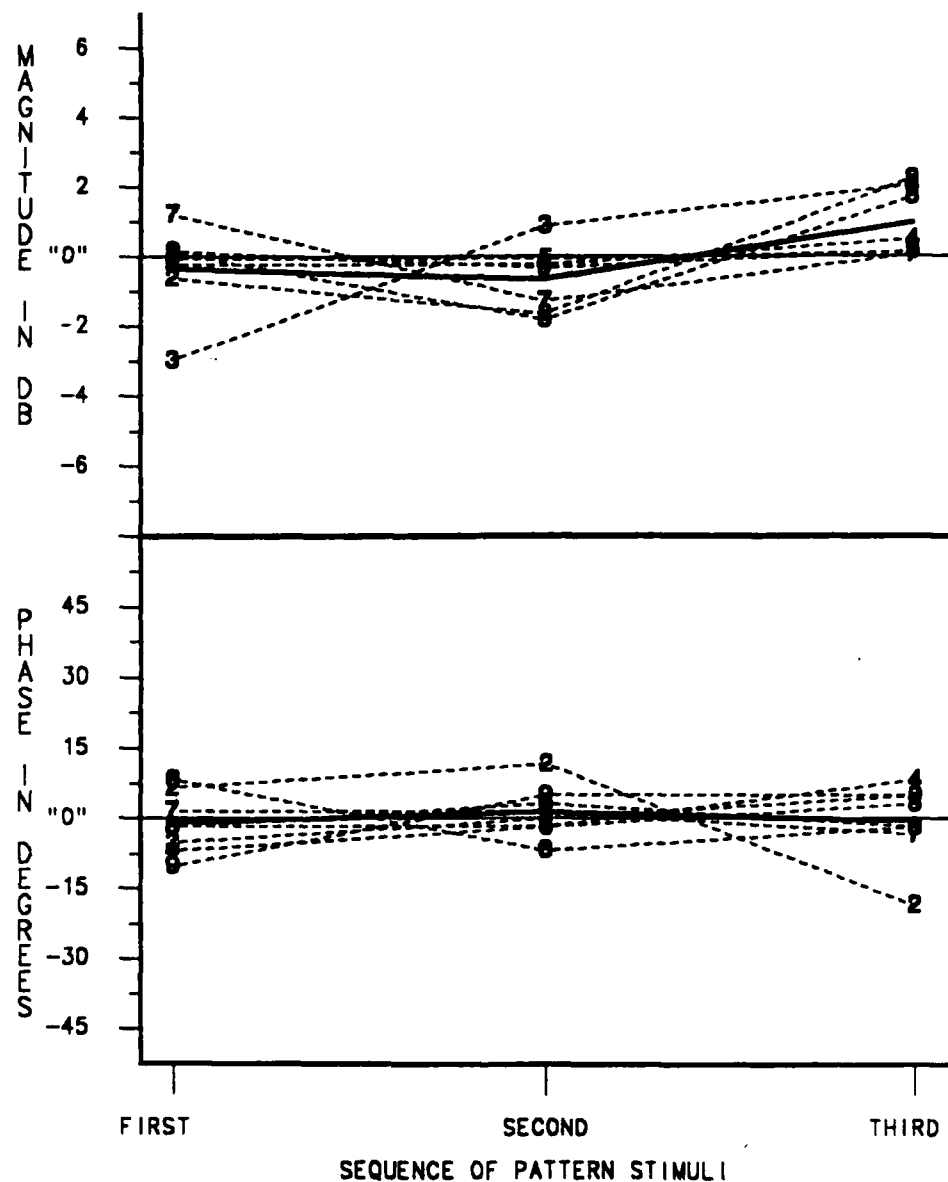


FIGURE II 5.2 : MAGNITUDE GAIN (DB) AND PHASE SHIFT (DEGREES) RELATIVE TO THE VALUES OF THE AVERAGED 1ST, 2ND AND 3RD SEQUENTIAL STIMULI.
NUMBERS: INDIVIDUAL SUBJECTS, THICK LINE: MEAN OF 9 SUBJECTS.

The latencies of the CEP harmonics did not significantly differ, although a trend of shorter auditory CEP 2nd harmonic latencies was observed (predominantly at Beta MF region).

CEP FUNDAMENTAL AND 2ND HARMONIC COMPARISON

TABLE II 5.2 : t-test of CEP harmonic components. MEAN : averaged value over N observations, SD : Standard Deviation, R : correlation coefficient of the estimated latency, BETA and THETA : modulation frequency regions, NS : Not Significant, $P > |t|$ of > 0.2 .

PARAMETER	FUNDAMENTAL			2nd HARMONIC			t-TEST
	N	MEAN±SD		N	MEAN±SD		
Magnitudes in microvolt RMS							
Auditory BETA	9	0.62±0.35		9	0.26±0.13		0.015
Auditory THETA	9	1.69±0.49		9	0.68±0.37		0.0002
-----	-----	-----	-----	-----	-----	-----	-----
Visual BETA	8	0.84±0.57		8	0.34±0.14		0.04
Visual THETA	8	1.49±1.28		8	0.72±0.48		0.14
Latencies in msec	N	MEAN±SD	R	N	MEAN±SD	R	P > t
Auditory BETA	9	93±102	0.94	6	36±16	0.90	0.14
Auditory THETA	9	181±73	0.95	6	166±108	0.95	NS
-----	-----	-----	-----	-----	-----	-----	-----
Visual BETA	9	88±20	0.97	8	83±16	0.98	NS
Visual THETA	9	191±57	0.98	8	192±53	0.97	NS

5.1.4 Discussion

5.1.4.1 CEP trends

The general trend of a 15% average increase in magnitude was evenly distributed over the 90-100 sec trial duration. It was not accompanied by any equivalent phase trend nor was it significantly associated with a particular MF region or modality. With an output TC of 10 sec, (single pole LPF), the LIA magnitude response to a step-function input

was higher than 90%, 99% and 99.9% of the full-scale magnitude after 30, 60 and 90 sec, respectively, a total of 11% increase, most of it obtained after only 60 sec. Since the observed experimental magnitude trend was variable and different from the expected LIA response (to a step-function input), it is believed to be a predominantly physiological phenomenon.

Short-term magnitude trends (within the first 90 sec of the recorded data) were investigated in only a few studies (Perry and Childers, 1966; Regan, 1966; Yolton et al., 1983). Visual CEP magnitude trends were obtained from time periods of 30-240 sec (Perry and Childers, 1966) and 30-70 sec (Yolton et al., 1983) after stimulus initiation, avoiding initial high magnitude transient responses. Perry and Childers used 1500 lux, 2.2 degree visual angle, 4 Hz flash stimuli. Regan used 9000 troland, 14 degree stimulus field, spotlight stimuli modulated at 15.5 Hz. Yolton et al. used 102.8/15.4 cd/m² (bright/dark checks), checkerboard pattern stimuli with an alternation reversal rate of 15 Hz. All these studies found that the CEP magnitudes recorded approximately 30 sec after stimulus initiation were constant and stable over the trial duration. Subject attentiveness, uncontrolled in any of the above cited studies, might explain the apparent contradiction regarding the significant trend observed in this current study. While performing the RT test, the subjects could gradually "tune in" to the stimulus duration (although it was partially randomized), improving their scores and possibly increasing their CEP magnitudes in the process.

Regan (1966) described an initial transient CEP magnitude increase that occurred in some subjects during the first 20 sec of the response. Although it may have occurred in some of the runs, the general CEP magnitude trend in this present study did not reveal such an initial transient response. The first 30 sec of the CEPs were characterized by the smallest magnitudes (LIA TC-independent).

The CEP temporal trends observed in this experiment could not be predicted from the simple model of delay-line followed by a linear tuned filter (assumed in this, and many other studies). Practically, it implies that the so-called "steady-state" response could be assumed only if it is referred-to within a defined time-frame past the stimulus onset.

5.1.4.2 CEP harmonics

Auditory and visual CEP magnitudes obtained at Beta and Theta MF regions were predominantly composed of fundamental components. Rodenburg et al. (1972) and Rees (1981) demonstrated similar auditory CEP results at Theta MF region (4 Hz), using stimuli of Amplitude Modulated (AM) noise and AM 1 KHz tone stimuli, respectively. Comparable analysis of the auditory Beta MF region was not available.

In the visual system, Spekreijse et al. (1977) characterized the Beta MF region CEPs as highly linear and relatively distortionless responses. On the other hand (and contrary to the findings of this current study), their Theta MF region CEPs were highly non-linear, comprised predominantly of the 2nd harmonic component (see section II 4.1.1.2). These differences were addressed in section II 4.4.4.

In conclusion, the CEPs recorded in this study, in response to sinusoidally amplitude-modulated signals, were predominantly composed of fundamental components (averaged fundamental/2nd harmonic magnitude ratio of 0.43). However inaccurate (due to temporal trends, and fundamental magnitude saturation discussed in the next experiment), the CEP was predominantly linear. More research is needed to determine the type and location of the non-linear elements.

5.2 INT experiment: stimulus intensity level effect

5.2.1 Introduction

The gain of a linear system is independent of the input signal magnitude. In general, this is not the case in the auditory and visual systems where Evoked Potential (EP) magnitude-gains and latencies were found to be stimulus intensity-level dependent. Since the intensity variable was regarded in this study as a control input (i.e. the AxV experiment), its effect had to be determined.

In a pilot study, auditory and visual CEPs were obtained for the highest stimulus intensity, tolerated (audio) or producible (visual, with the available instrumentation), in order to maximize their magnitudes and SNRs. These "0" dB levels were 108 dB SPL and equivalent source illumination of 44 lux for the audio and visual stimuli, respectively. The INT experiment characterized the response vector in the "0" to -24 dB stimulus intensity range.

5.2.2 Methodology

The most responded-to MFs, a total of 4 audio and visual discrete Beta and Theta MFs were tested for each subject. Intensity level was increased from -24 dB to "0" dB in 6 dB increments, maintaining a 100% modulation depth and constant background level. Each run was comprised of a series of 15 stimuli, with a repetition of 3 stimuli per intensity level. Average Stimulus duration (S) and ISI were 32.5 and 1.4 sec, respectively. CEPs were recorded under attentiveness conditions (RT test, similar to the MTF experiment), and the entire INT recording session, audio first and visual second, lasted one hour, including rest breaks. For more details, refer to TABLE I 3.3.

5.2.3 Results

Compensated CEP magnitude (dB) and phase values (relative to the run's mean value) were plotted against stimulus intensity levels in FIGURE II 5.3. In light of the large inter-subject variability, each trend (average values' regression-line) was supplemented by the individual data for comparison. Statistical significance of the trends is presented in TABLE II 5.3, where CEP vectors obtained at Low (-24, -18 dB) and High (-6, "0" dB) stimulus intensity levels were compared.

In general, an increase in stimulus intensity was significantly associated with visual CEP magnitude increase and visual CEP Beta MF region phase lead. The dynamic range of the visual Beta MF region CEP magnitudes (from noise level to maximal magnitude level) was fully exposed by the stimulus intensity range, while the Theta MF region dynamic range was not. In both MF regions the "0" and -12 dB intensity levels evoked significantly different magnitudes.

Common significant trends were not observed in the auditory CEPs. The cross-subject average magnitude and phase were generally unaffected by the stimulus intensity level, although within subject, mixed trends were observed.

CEP MAGNITUDE AND PHASE VERSUS STIMULUS INTENSITY
SIG=AUDIO FREQ=BETA

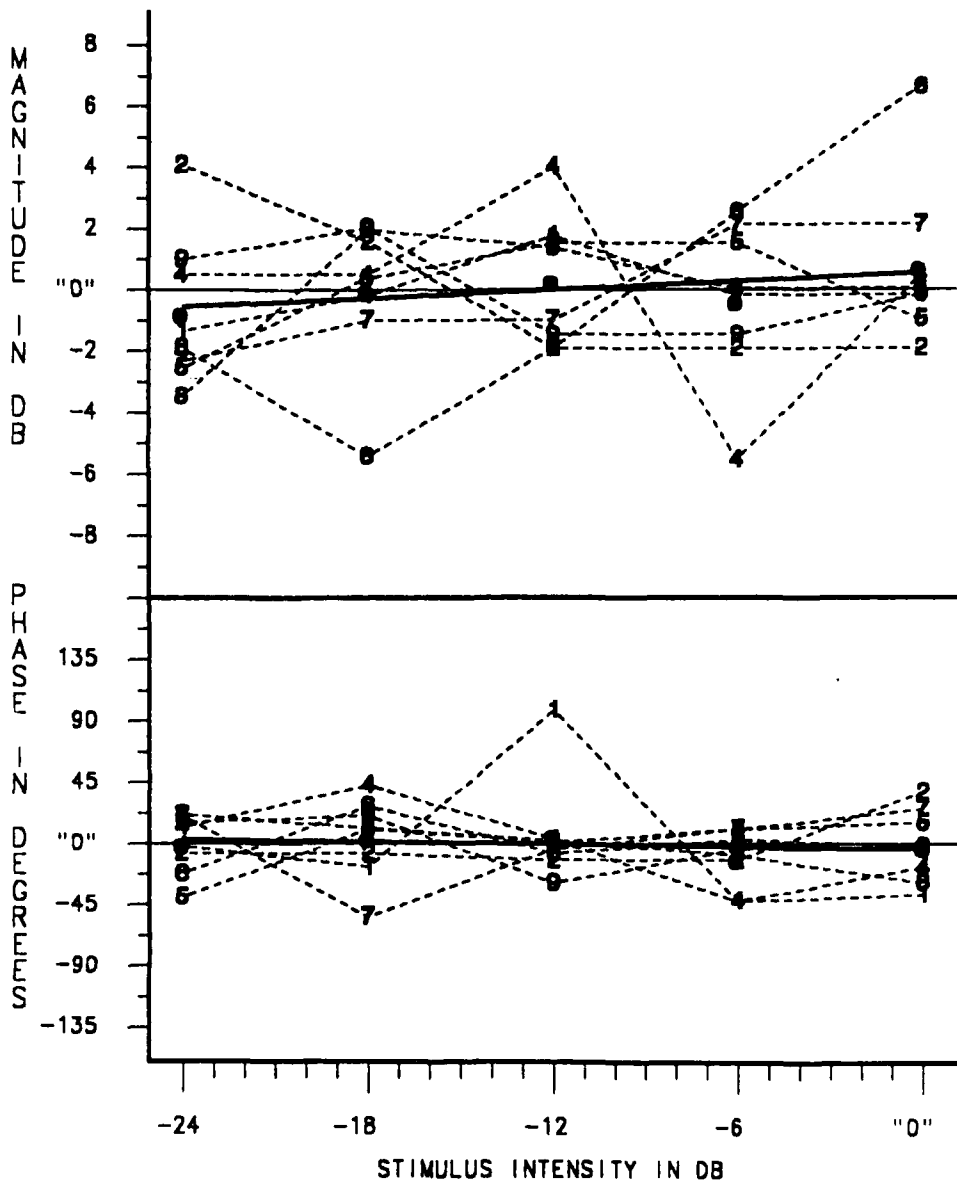
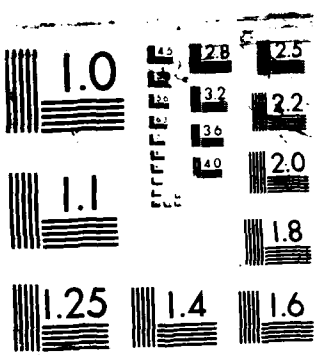


FIGURE II 5.3 : MAGNITUDE GAIN (DB) AND PHASE SHIFT (DEGREES) RELATIVE TO THE CROSS-INTENSITY AVERAGED VALUES. NUMBERS: INDIVIDUAL SUBJECTS, DOTS: AVERAGES OF 8 SUBJECTS, SOLID LINE: LINEAR REGRESSION LINE FITTED TO THE AVERAGES.

AD-A198 845 HUMAN AUDITORY AND VISUAL UNIMODAL AND BIMODAL 2/2
CONTINUOUS-EVOKED POTENTIALS(U) CONNECTICUT UNIV STORMS
BIOMEDICAL ENGINEERING LAB 22 GOLDMAN MAR 88
UNCLASSIFIED RAMRL-TR-88-016 F33615-81-K-0510 F/G 6/4 ML

END
DATE
TIME
17 88



CEP MAGNITUDE AND PHASE VERSUS STIMULUS INTENSITY
SIG=AUDIO FREQ=THETA

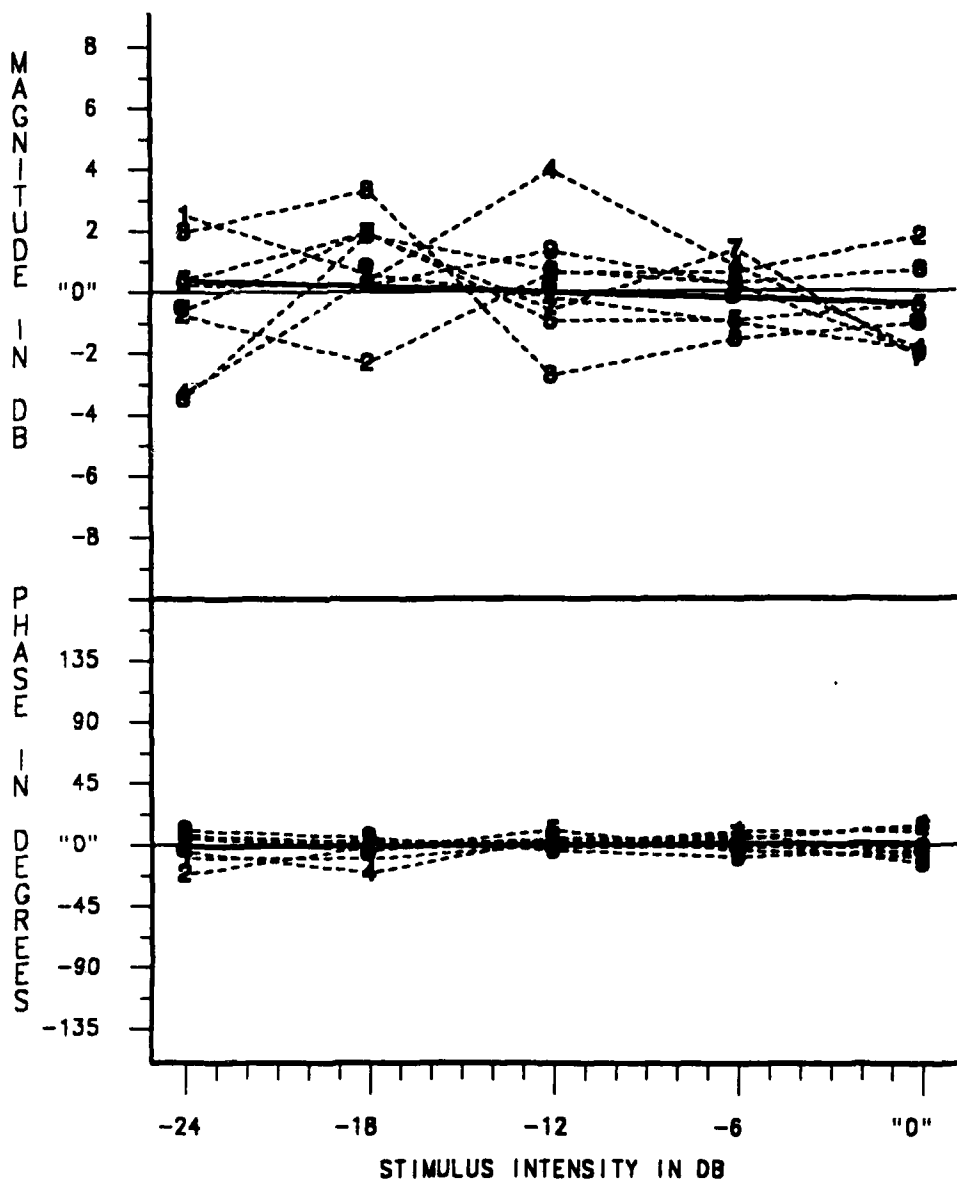


FIGURE II 5.3 : MAGNITUDE GAIN (DB) AND PHASE SHIFT (DEGREES) RELATIVE TO THE CROSS-INTENSITY AVERAGED VALUES. NUMBERS: INDIVIDUAL SUBJECTS, DOTS: AVERAGES OF 8 SUBJECTS, SOLID LINE: LINEAR REGRESSION LINE FITTED TO THE AVERAGES.

CEP MAGNITUDE AND PHASE VERSUS STIMULUS INTENSITY
 SIG=VISUAL FREQ=BETA

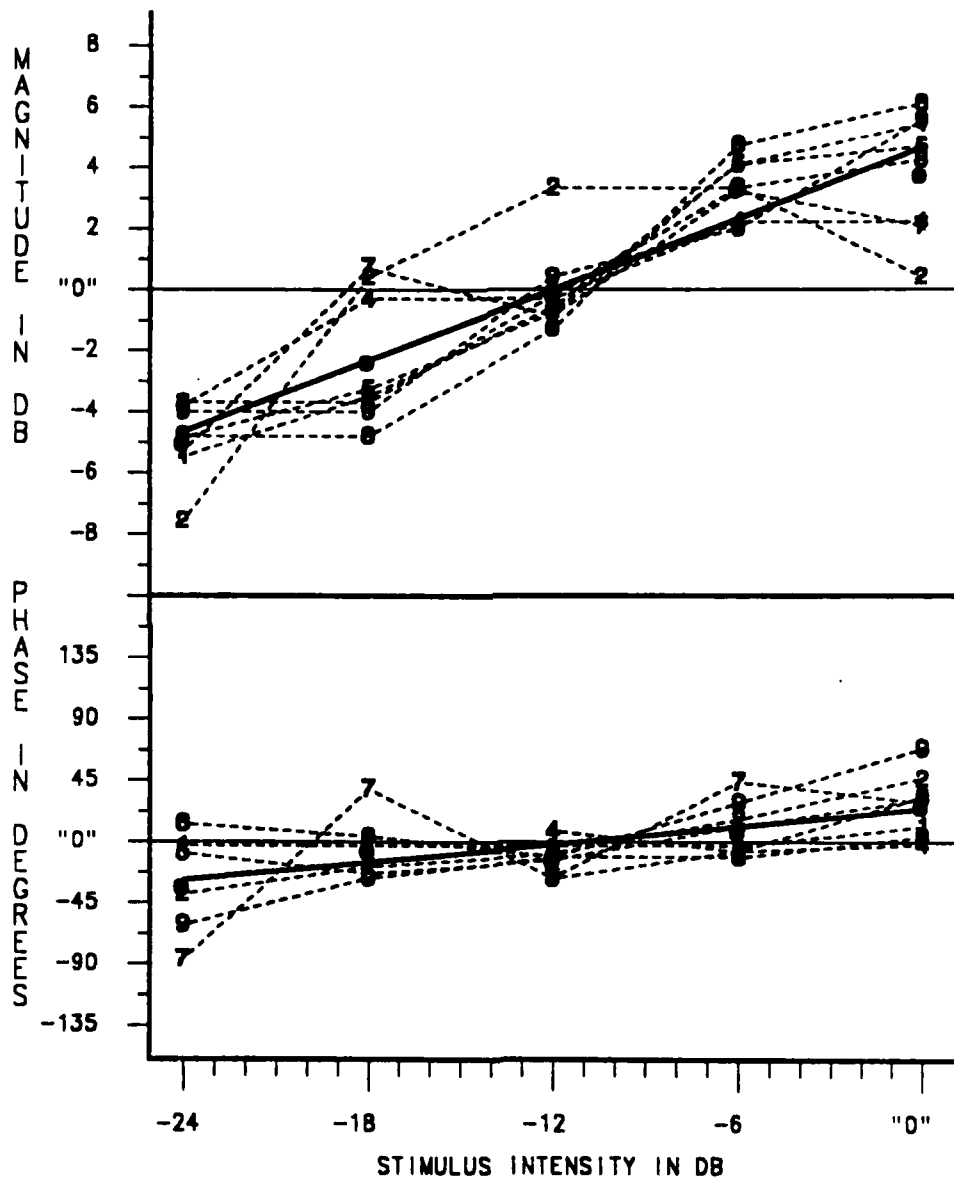


FIGURE II 5.3 : MAGNITUDE GAIN (DB) AND PHASE SHIFT (DEGREES) RELATIVE TO THE CROSS-INTENSITY AVERAGED VALUES. NUMBERS: INDIVIDUAL SUBJECTS, DOTS: AVERAGES OF 8 SUBJECTS, SOLID LINE: LINEAR REGRESSION LINE FITTED TO THE AVERAGES.

CEP MAGNITUDE AND PHASE VERSUS STIMULUS INTENSITY
 SIG=VISUAL FREQ=THETA

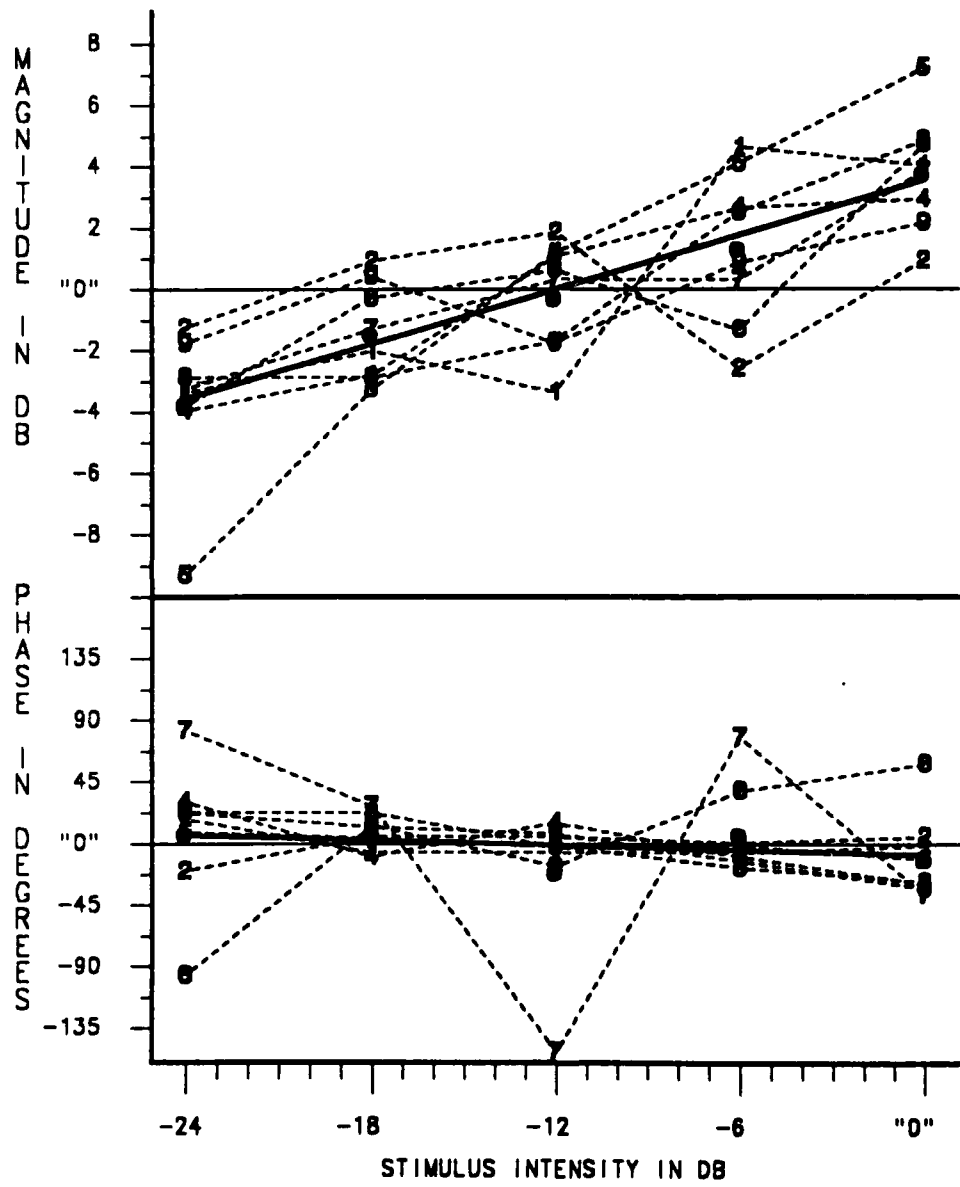


FIGURE II 5.3 : MAGNITUDE GAIN (DB) AND PHASE SHIFT (DEGREES) RELATIVE TO THE CROSS-INTENSITY AVERAGED VALUES. NUMBERS: INDIVIDUAL SUBJECTS, DOTS: AVERAGES OF 8 SUBJECTS, SOLID LINE: LINEAR REGRESSION LINE FITTED TO THE AVERAGES.

INTENSITY EFFECT ON AUDITORY AND VISUAL CEPs

TABLE II 5.3 : t-test between "High" and "Low" CEP groups. "High" : ("0", -6 dB) INTensity levels, "Low" : (-18, -24 dB) INTensity levels, MEAN : average across N observations reduced by the run's mean value, SD : Standard Deviation, MF : Modulation Frequency, NS : Not Significant, P > F of > 0.2.

PARAMETERS	AUDITORY CEP		VISUAL CEP	
	BETA MF	THETA MF	BETA MF	THETA MF
MAGNITUDES (in dB)				
INT groups				
MEAN±SD :				
"High"	0.21±2.61	-0.45±1.29	3.62±1.55	2.63±2.50
"Low"	-0.37±2.40	0.31±2.00	-3.61±2.20	-2.52±2.33
INT groups				
t-test:				
N (group)	16	16	16	16
P > t	NS	NS	0.0001	0.0001
PHASES (in degrees)				.
INT groups				
MEAN±SD :				
"High"	-5.7±23.6	1.1±8.7	18.7±23.0	0.1±32.4
"Low"	2.4±25.7	-2.0±9.5	-17.4±33.4	9.1±36.0
INT groups				
t-test:				
N (group)	16	16	16	16
P > t	NS	NS	0.005	NS

5.2.4 Discussion

With the current hardware setup, only the fundamental and the 2nd harmonic CEP components could be investigated. In the DISC experiment, high average fundamental/2nd harmonic magnitude ratios (of 2.4, TABLE II 5.2) were obtained even

at the highest stimulus intensity level ("0" dB). The INT experiment was designed to explore only the fundamental CEP component.

Due to the small CEP magnitudes and poor SNRs obtained in the pilot study (under "0" dB stimulus level), a stimulus intensity range of "0" to -24 dB was thought to be adequate to fully expose the CEP magnitude dynamic range. This intensity range was adequate for the visual CEPs, but insufficient for the auditory CEPs. The cross-subject-averaged CEP magnitude seemed to be stimulus intensity-independent. This phenomenon, the flattening of the fundamental CEP magnitude component (plotted versus intensity), is referred to here, and in the following cited studies, as "saturation". The nature of this saturation ("hard" or "soft") could not be determined here due to the insufficient intensity scale resolution (6 dB decrements).

When the audio stimulus intensity range of 84-108 dB SPL was tested, the auditory CEP magnitude averages of both MF regions were flat, probably completely saturated (FIGURE II 5.3). Rees (1981) recorded CEPs in response to 1 KHz tone, 100% AM by 4 Hz MF stimuli (Theta MF region), administered binaurally at 0-80 dB SL. He demonstrated magnitude saturation (in two subjects) at stimulus intensity levels exceeding 50 dB SL. Rickards and Clark (1984) recorded CEPs in response to 500 Hz tone, 94% AM by 24 Hz MF stimuli (Beta MF region), ipsilaterally administered at 0-100 dB SPL. They obtained a magnitude increase of 20 dB and a phase-lead of 60 degrees over the 50-100 dB SPL stimulus intensity range.

Results difference between Rickards and Clark (1984) study and this study might be attributed to the different carrier frequencies utilized. The saturation phenomenon observed in this study might be attributed to the high modulation depth utilized (100%), instead of to the stimulus averaged intensity. Other studies showed that CEP magnitude

saturation occurred at modulation depths exceeding 10-50% (Spekreijse, 1966; Regan, 1972; Rodenburg et al., 1972).

To summarize, at "0" dB, both auditory and visual CEP magnitudes were saturated, the auditory more profoundly. Apparently related to this fact, only the visual CEPs showed significant differences between "0" and -12 dB stimulus intensity levels. Since these two intensity levels were utilized in the AxV experiment, no inter-modality intensity effect should be detected there for the auditory CEPs.

5.3 ATT experiment: subject attentiveness effect

5.3.1 Introduction

The effect of subject attentiveness on Transient Evoked Potentials (TEPs) has been extensively investigated. In general, attended-to stimuli evoked higher EP magnitudes (Squires et al., 1977; Hillyard et al., 1978). Many models were constructed to define attentive behavior and suggest the underlying mental processes. An early stage of "signal recognition" was related to variations of 50-75 msec latency, TEP magnitude components. This process required a simple physical cue and high stimulus rate, and was enhanced by low intensity level stimulation (Hillyard et al., 1978). Attention allocation could be controlled by more discriminable, inter-modality cues (Donchin and Cohen, 1967; Hartley, 1970; Ford et al., 1973; Schechter and Buchsbaum, 1973). The behavioral parameters actually being measured in these cited studies were debatable. It can be argued that the TEP stimulation procedure (requiring low frequency clicks or flashes) and the necessity to "mix" the relevant stimuli (reacted-upon cues) with other "inert" stimuli, the so-called "attended-to" TEPs mostly reflected the recognition process of the transient target clue.

The purpose of the ATT experiment in this current study was to investigate the CEP vector recorded in response to attended-to versus non-attended-to continuous stimuli. Attention allocation was controlled by inter-modality simple cues with an a-priori known sequence. In this experiment, the recognition process of the transient cues could not interfere with the attention allocation effect.

5.3.2 Methodology

In this experiment, each run consisted of simultaneously presented and only mar-

ginally overlapping, audio and visual series, each consisting of 4 repetitive stimuli. Average Stimulus duration (S), ISI and inter-modality Audio-Visual Delay (AVD), all were 32.5 sec. Since the stimulus durations were randomized (10% and 25% of Beta and Theta MF region stimulus duration, respectively), the inter-modality sequence of stimulus gate transitions (during the short time when both audio and visual stimuli were overlapping) appeared to be random too. Each run utilized a single MF region and Low (-12 dB) or High ("0" dB) stimulus intensity levels. Beta and Theta MFs were similar to the optimal frequencies previously determined in the DISC experiment; only one frequency bin differentiated between the audio and visual MFs within the same MF region (average frequency difference of 9%). Therefore both sensory channels were stimulated by similar and nearly optimal MFs. Attention was controlled by instructing and training the subjects to respond to the following clues (RT test): stimulus "on" and "off" transitions were reacted upon in the first and last two stimuli in each series, respectively. The auditory series always led and its third stimulus required both "on" and "off" responses. Consequently, CEPs were recorded in response to unattended-to and attended-to stimuli under cross-modality and intra-modality attention allocation conditions, respectively. The entire ATT recording session lasted one hour, including training and rest breaks. For more details, refer to TABLE I 3.3.

5.3.3 Results

The results of magnitude ratios (in dB) and phase differences (of CEPs in response to attended-to versus unattended-to stimuli) were plotted against stimulus categories (signal-MF region-intensity) in FIGURE II 5.4. In light of the large inter-subject variability, the trends (average values) were supplemented with the individual data for comparison. Statistical significance of the attention effect was tested on the visual CEP magnitude (in dB) and phase (in degrees) compensated data (relative to the run's mean values, TABLE II 5.4).

Significant trends of higher magnitudes recorded in response to attended-to stimuli were observed only for the visual CEPs. The attention effect on visual CEPs was associated with unequal average magnitude-gains of 4.70 and 2.76 dB for the High and Low stimulus intensity levels, respectively. A significant visual CEP phase-lead was recorded in response to Beta MF region, low intensity level (-12 dB), attended-to stimuli. The auditory CEPs did not reveal any significant trends.

5.3.4 Discussion

Attention effect was found only in visual CEPs where attended-to stimuli elicited higher magnitudes. -Fagan et al. (1984), recording CEPs in response to a 15.6 Hz phase reversal rate checkerboard stimulus, found a similar, statistically non-significant trend. They obtained higher average visual CEP magnitudes under hypnotically-induced attention condition. Their ill-defined control session, during which subjects' attention was not directed or verified, could have prevented them from obtaining more conclusive results.

In this study, similar attention-related magnitude gains were detected independently in early (Beta, 75-85 msec latency) and late (Theta, 165-210 msec) visual CEP responses (TABLE II 4.2). Inter-MF region correlation of the attention-related magnitude gains did not reveal any dependency (non-significant correlation coefficients of $R < 0.1$). This observation may suggest that attention allocation effects are independently induced at various levels of the visual system.

ATTENTION EFFECTS ON CEP MAGNITUDES

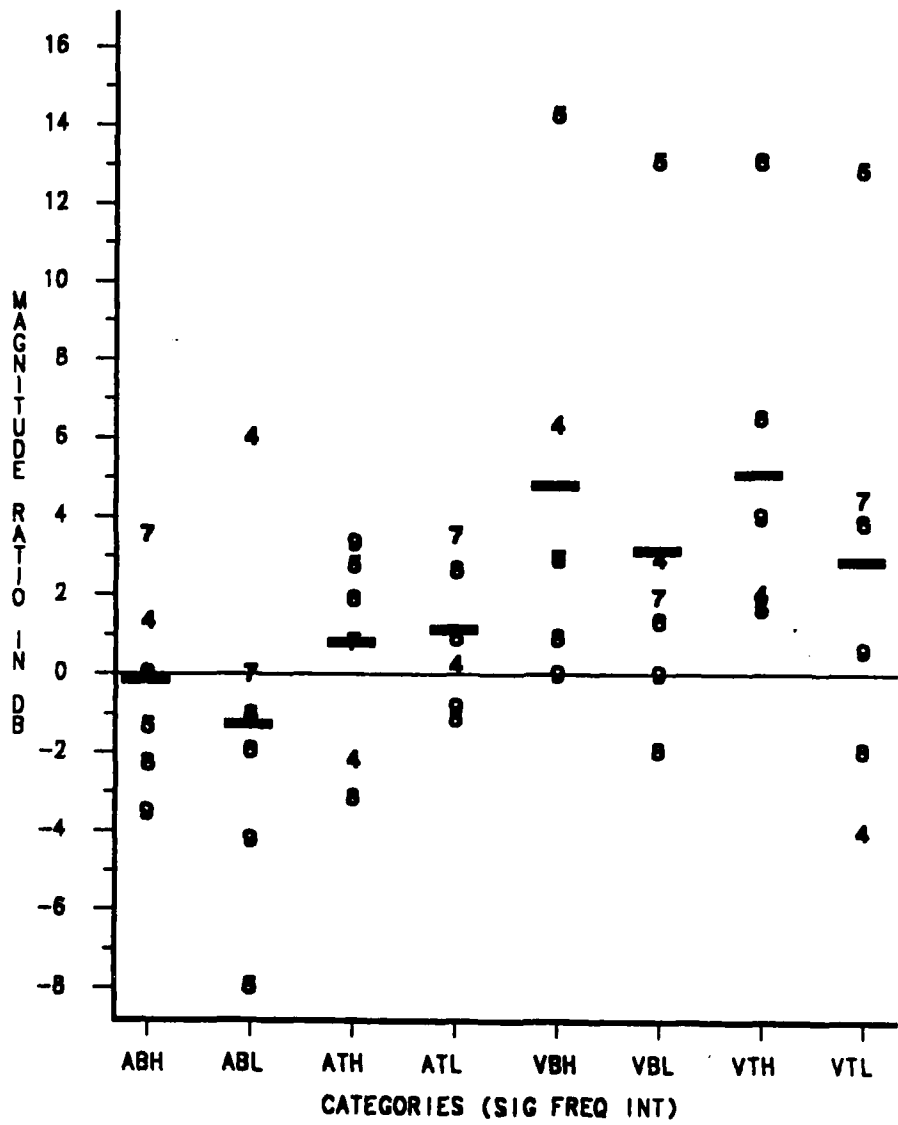


FIGURE II 5.4A : MAGNITUDE RATIOS IN DB (ATTENDED / NOT ATTENDED).
NUMBERS: INDIVIDUAL SUBJECTS, BARS: AVERAGES OF 6 SUBJECTS.
CODES: AUDITORY (A) AND VISUAL (V) CEP'S, BETA (B) AND THETA (T)
MODULATION FREQUENCIES, HIGH (H) AND LOW (L) INTENSITY LEVELS.

ATTENTION EFFECTS ON CEP PHASES

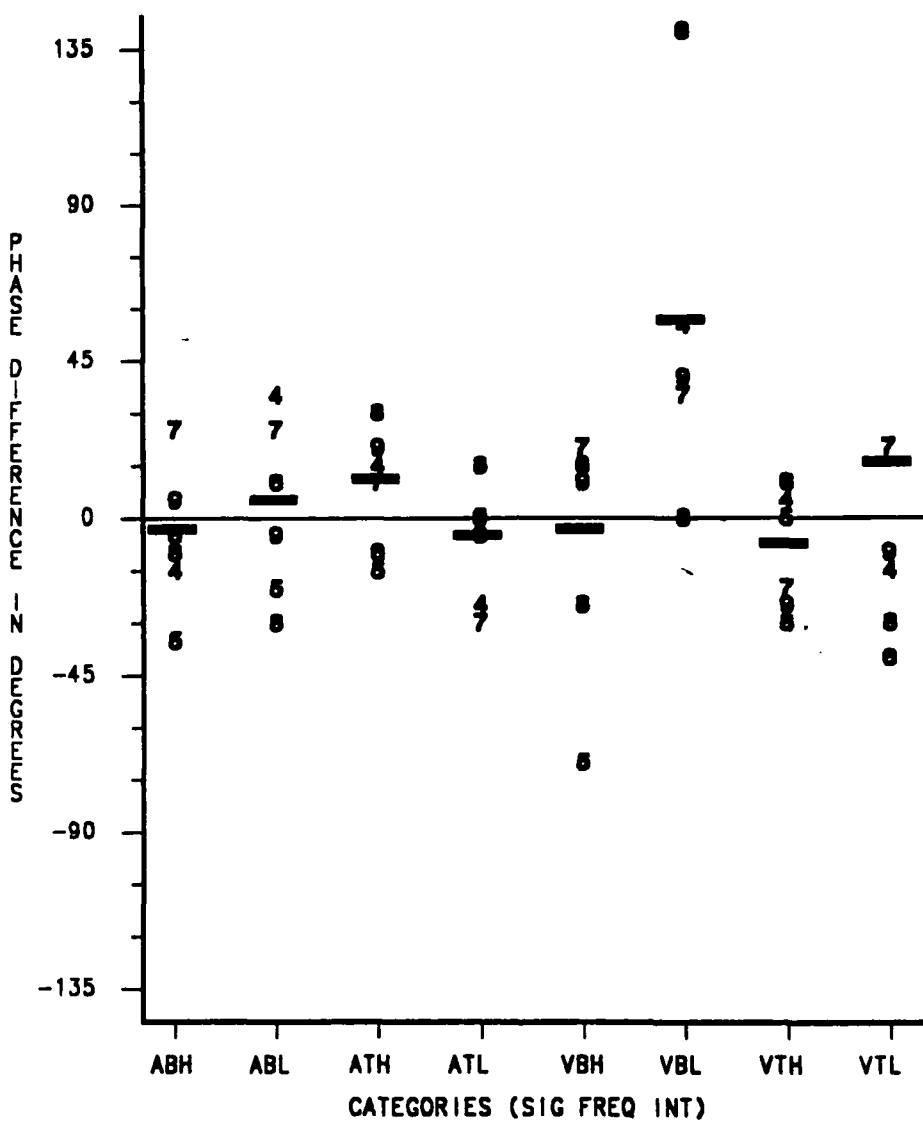


FIGURE II 6.4B : PHASE DIFFERENCES IN DEGREES (ATTENDED - NOT ATTENDED).
NUMBERS: INDIVIDUAL SUBJECTS, BARS: AVERAGES OF 6 SUBJECTS.
CODES: AUDITORY (A) AND VISUAL (V) CEP'S, BETA (B) AND THETA (T)
MODULATION FREQUENCIES, HIGH (H) AND LOW (L) INTENSITY LEVELS.

ATTENTION EFFECT ON VISUAL CEPs

TABLE II 5.4 : t-test between ATT and NAT CEP groups. MEAN : average ATT-NAT difference across N observations, SD : Standard Deviation, HIGH/LOW : "0"/-24 dB intensity levels, ATT/NAT : ATTended-to/Not-ATTended-to CEPs, NS : Not Significant, $P > |t|$ of > 0.2 .

	INTENSITY-> ALL	HIGH : LOW	HIGH : LOW	HIGH : LOW
	FREQUENCY-> ALL	ALL : ALL	BETA : THETA	BETA : THETA
ATT & NAT MAGNITUDES (in dB)		:	:	:
diff. MEAN (ATT-NAT)	3.72	4.70 : 2.76	4.56 : 4.84	2.88 : 2.62
SD/group (ATT,NAT)	2.50	2.31 : 2.68	2.61 : 2.22	2.63 : 2.98
N/group (ATT,NAT)	24	12 : 12	6 : 6	6 : 6
P > t (ATT--NAT)	0.0001	0.0001 : 0.019	0.012 : 0.003	0.085 : 0.160
ATT & NAT PHASES (in degrees)		:	:	:
diff. MEAN (ATT-NAT)	11.1	- 7.9 : 31.1	- 4.8 : -10.0	54.0 : 13.4
SD/group (ATT,NAT)	25.8	13.3 : 32.2	17.7 : 8.5	26.1 : 36.0
N/group (ATT,NAT)	23	12 : 11	6 : 6	5 : 6
P > t (ATT--NAT)	0.15	0.16 : 0.031	NS : 0.07	0.011 : NS

The visual CEPs also displayed an interesting interaction between intensity and attention IVs. The lower visual attention-related gains (obtained for low stimulus intensity level) could not be explained by the limiting noise level boundary. Mean (and SD) values of noise level magnitudes were 0.2 (0.1) and 0.45 (0.2) microvolt RMS at Beta and Theta MF regions, respectively. The corresponding values of absolute CEP magnitudes recorded in response to unattended-to, low intensity level stimuli (conditions under which the lowest magnitudes were obtained), were higher, 0.23 (0.04) and 0.50 (0.27) microvolt RMS, respectively (MEAN (SD) values). Thus, more attention-related gain was "afforded" for the low intensity level visual CEP magnitudes.

Auditory CEPs did not display any significant attention effect in this current study, although a trend of higher magnitudes in response to attended-to stimuli was observed at Theta MF region. The inconclusiveness of the auditory results may be attributed to the well-saturated auditory CEP magnitudes, even at a -12 dB stimulus intensity level (see INT experiment).

Part III: Bisensory Continuous Evoked Potentials

Chapter 6

Introduction for The Bisensory Continuous Evoked Potentials Experiment

6.1 Terminology and approach comparison

Sensory interaction has been inferred, when response variations of one sensory channel could be related to parameter changes of an additional stimulus, simultaneously presented to another sensory channel. This introduction reviews Evoked Potential (EP) studies in which the Auditory-Visual Interaction (AxV) has been investigated in humans, and presents some of the terminology used. Most of the following literature review is based on Transient Evoked Potential (TEP) studies in which averaged EP waveforms were recorded for unimodal or bimodal transient stimuli (Walter, 1964; Ciganek, 1966; Davis et al., 1972; Andreassi and Greco, 1975; Walsh, 1979; Lewis and Froning, 1981). An AxV process was proclaimed whenever the algebraic summation of the unisensory EP waveforms (recorded for unimodal stimuli) significantly deviated from the bisensory EP waveform (recorded for bimodal stimuli). This deduction did not take into account

the inherent non-linearities of each sensory channel response. Also, since an isolated sensory response to a bimodal stimulus could not be directly and independently recorded, the summed EP results could be misinterpreted. Auditory, visual or both sensory channel responses might have been modified by the bimodal stimulus. Consequently, both independent sensory channels (with linearly summed responses) or inter-related sensory channels (with inversely related responses) could generate a similar bisensory response.

Increment and decrement of the bisensory EP magnitude response (relative to the algebraically-summed, unisensory EP responses) were often termed "facilitation" and "inhibition", respectively. Traditionally, these terms were used to describe changes of normal baseline activity of a defined source. The use of these terms in AxV TEP studies was therefore ambiguous; Variations of scalp recorded EPs could not be attributed to a single sensory channel, and the choice of the unisensory response as the sensory channel "normal" baseline activity was questionable. These terms are used, however, in the following review in order to simplify comparisons between studies.

The present study investigated the AxV phenomenon, utilizing a phase-lock technique in recording Continuous Evoked Potentials (CEPs) under unimodal and bimodal stimulus conditions. A similar technique was used by Regan and Spekreijse (1977), investigating the AxV process in conjunction to the perception of auditory and visual spaces. Substantial differences exist between the phase-lock (recording of CEPs) and ensemble averaging (recording of TEPs) approaches. Bimodal TEPs are affected by the stimulus Inter Modality Interval (IMI), and reflect non-sensory-channel specific, AxV transient processes. In contrast, the bimodal CEPs are IMI-irrelevant responses, reflecting sensory channel specific, AxV sustained processes. The lock-in approach is

therefore preferable in situations where a sensory channel response is monitored under unpredictable, cross-modal stimulus conditions.

Results entailed in the following literature review reflect the AxV process but could not be confirmed against the current study results. Differences in recording sites and techniques (ensemble averaging versus phase-lock) would make any such comparison invalid. Sorting out the AxV-related results of the following TEP studies revealed varying and conflicting trends. The major experimental parameters governing the results are assumed to be the following: relative unimodal stimuli intensities, bimodal stimulus IMI, subject's allocated attention and EP recording sites.

6.2 Auditory-visual interaction in evoked potentials

In comparison to visual stimuli, audio stimuli generally generate shorter latency TEP components and are reacted upon with faster Reaction Times (RTs) (Squires et al., 1977). This might be the reason why an experiment paradigm, in which the audio stimulus lagged the cross-modal visual stimulus (IMI of 0-500 msec), was chosen in most of the bisensory TEP studies.

Walter (1964) investigated convergence and interaction of audio-visual information in the human non-specific cortex, utilizing both intracranial and scalp recording techniques (TEPs were recorded between Cz-Oz referring to a grounded right mastoid). IMIs of 30-270 msec between flash and click (lagging) bimodal stimuli did not disclose any AxV effect. Walter concluded that the sensory projections into the non-specific cortex (frontal, temporal and occipital lobes) were "idiodromic" (private independent sensory tracks), and that any bisensory interaction occurred at the "superficial" cortical

level. Statistical tests of the actual difference between the bisensory and the summed unisensory TEPs were not conducted.

An IMI-dependent AxV effect was described by Morrell (1968). TEPs were recorded from C3-Cz and Cz-C4 (referring to a grounded forehead) in response to attended-to flash and click bimodal stimuli. IMIs of 20-120 msec (click lag) were applied, and 140-240 msec post-flash epochs were analyzed. Short IMI (less than 70 msec and only at C3-Cz recording site) and long IMI (longer than 70 msec and recording-site-independent) were associated with "facilitated" or "inhibited" bisensory TEP magnitudes, respectively.

Different results were obtained by Andreassi and Greco (1975). TEPs were recorded from O2,Cz-left mastoid in response to attended-to, flash and noise burst bimodal, stimuli. A fixed IMI of approximately 30 msec (noise burst lag) was used and 65-225 msec post-flash magnitude components were evaluated. Their data showed that the response to the bimodal stimuli was consistently smaller than the algebraically summed unimodal responses. In comparison, Morrell's results (1968), obtained under similar IMI and epoch range, showed bisensory "facilitation" and "inhibition" for magnitude responses recorded from C3-Cz and Cz-C4, respectively. This discrepancy could be related to the different recording sites. A multi-origin AxV process would generate a recording-site-dependent potential distribution.

Bisensory "inhibition" of medium-long latency magnitude components at long IMIs (longer than 100 msec) was commonly detected. Davis et al. (1972) demonstrated that this "inhibition" persisted even for magnitude components generated 600-700 msec after presentation of the leading bimodal stimulus-component. It was presumed that the isolated sensory channel response at latencies greater than 600 msec was indistinguish-

able from the noise level. TEPs were recorded from Cz-M1 (referring to a grounded forehead) in response to equal subjective-magnitude, flash and tone burst, bimodal or unimodal stimulus pairs. IMIs of 0.5 and 5 sec were employed and 100-200 msec epochs of the magnitude response to the lagging stimulus were analyzed. Relative magnitudes (of the short IMI/long IMI) computed for inter- and cross-modality stimulus pair conditions were: $\Delta|a = 0.25$, $\Delta|v = 0.59$, $V|v = 0.51$ and $V|a = 0.71$ (where X|y should be read as the relative magnitude of the X-modality response, given that a y-modality stimulus preceded; Δ or a : audio; V or v : visual). These results indicated that the auditory TEPs were more susceptible to inhibition and that the inhibitory effect of intra-modality stimulus was more profound (in both sensory channels).

Walsh (1979) and Lewis and Froning (1981) utilized a simultaneously-presented (zero IMI) audio-visual bimodal stimulus and obtained conflicting results regarding the AxV process. Walsh (1979) recorded TEPs from Cz-Oz (referring to a grounded forehead) in response to equal sensation level magnitude tone burst and flash bimodal stimuli. Walsh concluded that magnitude components within the 100-150 msec latency epoch did not exhibit any AxV phenomenon. Lewis and Froning (1981) recorded TEPs from F3,F4,T3,T4,P3,P4,O1,O2-nose (referring to a grounded Pz) in response to click and checkerboard pattern bimodal stimuli. They found a recording-site-independent bisensory "inhibition" in 250-500 msec magnitude components. Shorter latency magnitude components showed recording-site-dependent, mixed AxV trends. A bisensory "facilitation" of 150 msec magnitude components could be detected in TEPs recorded from frontal recording sites ($F3,4 > T3,4 > P3,4$).

The effects of cross-modal audio stimulation on visual EPs were investigated by Ciganek (1966) and Regan and Spekreijse (1977). Ciganek (1966) recorded TEPs from Oz-Pz in response to click and flash bimodal stimuli. IMIs of 40-250 msec were em-

ployed (flash lag), and the visual unimodal TEP was compared to the visual TEP component within the bimodal response. Although significant AxV effects were not reported by Ciganek, analysis of his raw data revealed some consistent trends. Short (40-100 msec) and long (150-250 msec) IMIs were associated with a visual TEP "inhibition" beginning at magnitude components with latencies of 120-130 and 70-80 msec, respectively.

Regan and Spekreijse (1977) applied a phase-lock technique in monitoring the effect of cross-modal audio stimulation on visual CEP. The visual stimulus consisted of a fixed Modulation Frequency (MF of 12, 13.7, 16 or 18 Hz), 60% modulation depth, Amplitude Modulated (AM), Maxwellian view of xenon light source. The audio stimuli consisted of variable-MF, 100% modulation depth, AM sounds (tone bursts or clicks). The audio MF was linearly varied (triangularly frequency modulated) across the centered, fixed visual MF. Therefore, if the perception of "visual flicker rate driven by the audio flutter rate" had an EP basis, it could be reflected in the visual CEP magnitude response. Visual CEP magnitude variations were expected whenever the audio and visual stimuli MFs were similar, twice within the audio MF sweep period. No such periodic AM visual CEP magnitude response was found, possibly due to the following reasons: (1) The visual CEP magnitude could have been affected evenly during the entire range (relatively small) of the audio MF sweep range. (2) The triangular waveform duration was 20 sec, thus similar audio and visual MFs existed for only a short time (5-10 sec). With a minimal Lock-In Amplifier (LIA) output Time Constant (TC) of 3-10 sec, magnitude variations due to an AxV process would be indistinguishable from noise-related variations.

Chapter 7

Methodology for The Bisensory Continuous Evoked Potentials Experiment

7.1 Experiment paradigm and variables

Each run in this experiment consisted of simultaneously presented, partially overlapping audio and visual stimulus series. The audio series always led. Each series consisted of three repetitive stimuli (see TABLE I 3.3 and FIGURE III 8.1). Average stimulus duration (S), Inter Stimulus-Interval (ISI) and Audio-Visual stimulus Delay (AVD) were 106.5, 35.5 and 71 seconds, respectively. Stimulus durations were randomized within the range of -5% to + 5% of the mean value. Four audio-visual Modulation Frequency (MF) combinations were tested (Beta-Beta, Theta-Beta, Beta-Theta, Theta-Theta, presented in this order), each at four audio-visual intensity combinations (Low-Low, Low-High, High-Low, High-High, presented in this order). The High and Low terms were attributed to the "0" and -12 dB intensity levels, respectively. Each run, one of the 16 MF x intensity combinations lasted for an average of 7 minutes, 50 seconds. The

entire Auditory-Visual Interaction (AxV) recording session, including trial runs and test breaks, required an average of three hours.

The subjects were instructed to attend to the bimodal stimuli and to quickly respond to a stimulus turning-off clue (Reaction Time test, RT). After recording each of the MF combinations and before disclosing their actual RT scores, the subjects were asked to evaluate their performance. They had to describe their attention, concentration and quickness levels and the degree of difficulty encountered in maintaining that level (a five point scale for each qualifier). In addition, at the end of the AxV recording session, the subjects were asked to assess their inter-sensory channel attention allocation strategies. All of the subjects confirmed that during the bimodal stimulus sections, they attended to the modality whose stimuli were expected to be turned off.

Audio and visual stimulus gates (A GATE, V GATE) and the investigated within-run Independent Variables (IVs) are presented in FIGURE III 8.1. The analyzed run section consisted of two repetitions of the four basic bimodal combinations (avoiding the runs' "on" and "off" transitions). Statistical analysis was conducted on the cross-pattern averaged data. Continuous Evoked Potential (CEP) magnitudes and phases were defined by the levels of the following IVs: SIG, SF, CF, SI, CI, ORDER, MOD, and ATT. A summary of all the AxV experiment variables is provided in TABLE III 8.1A. NL magnitudes were recorded for stimulus-off condition while the Lock-In Amplifier (LIA) was still locked-on the stimulus MF. Except for NAME (subjects' codes), all the other IVs were treated as fixed effects in the tested ANOVA models.

AxV EXPERIMENT PARADIGM AND INDEPENDENT VARIABLES

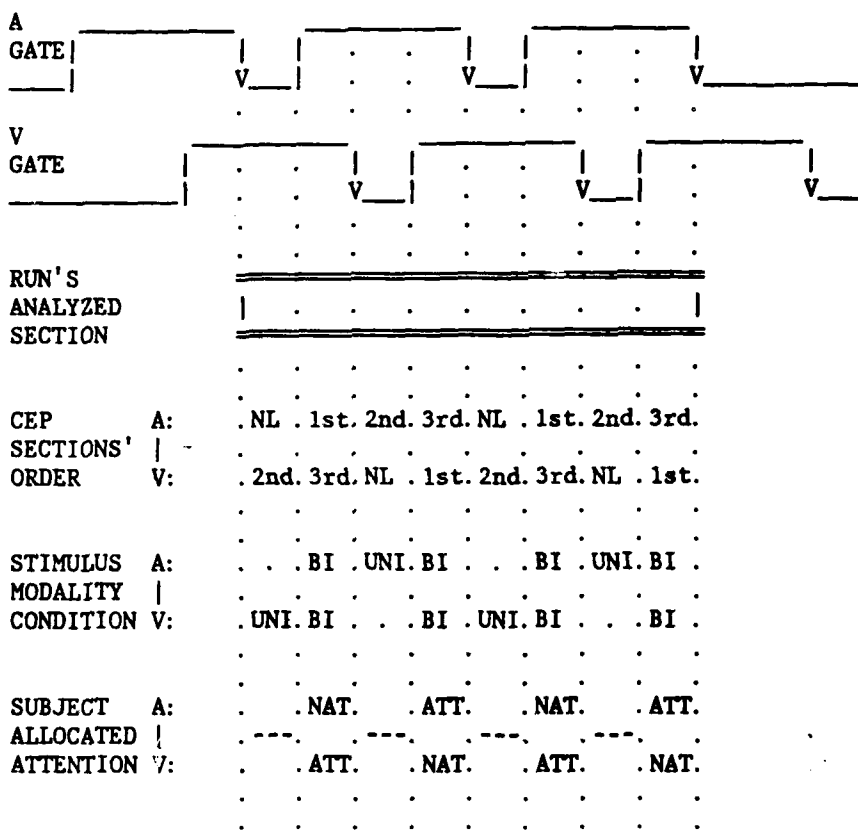


FIGURE III 8.1 : AUDITORY (A) AND VISUAL (V) STIMULUS GATES (GATE) AND THE WITHIN-RUN INDEPENDENT VARIABLES. AVERAGED STIMULUS ON DURATION (GATE HIGH) WAS 106.5 SECONDS. STIMULUS-OFF TRANSIENT: REACTION-TIME CLUE, ATT/NAT: ATTENDED-/NOT-ATTENDED-TO STIMULUS, BI/UNI: BIMODAL/UNIMODAL STIMULUS, NL: NOISE LEVEL RESPONSE (STIMULUS-OFF CONDITION).

AxV EXPERIMENT INDEPENDENT VARIABLE DEFINITIONS

TABLE III 8.1A : Definitions of the independent variables.

INDEPENDENT CLASS VARIABLES	ACROSS- WITHIN- RUNS	LEVELS (CLASSES)	DEFINITION
NAME	ACROSS	AM, CR, EW, KC, MR, PM, RT, SC, TN	subjects' codes
SIGnal	ACROSS	Auditory, Visual	stimulus modality & the recorded-from sensory channel
SFrequency	ACROSS	Beta, Theta	modulation frequency region of the SIGnal stimulus
CFrequency	ACROSS	Beta, Theta	modulation frequency region of the cross-SIGnal stimulus
SIntensity	ACROSS	High, Low	intensity level of the SIGnal stimulus
CIntensity	ACROSS	High, Low	intensity level of the cross-SIGnal stimulus
ORDER	WITHIN	1st, 2nd, 3rd, NL	SIGnal's response sections 1st--3rd: evoked potentials, NL: noise level response
Modalities	WITHIN	BImodal, UNImodal	SIGnal's stimulus modalities (BI and UNI classes are the 1st & 3rd and 2nd ORDER sections, respectively)
ATTention	WITHIN	ATTended, Not-ATT-ended-to	SIGnal's stimulus attention allocation (ATT and NAT classes are the 3rd & 1st ORDER sections, respectively)

7.2 Auditory-visual interaction assessment

The AxV was characterized by the promoting stimulus conditions (the IVs) and the resultant trend directions (inhibited or facilitated magnitudes, leading or lagging phases). Consequently, two orthogonal analyses were performed to answer the following two questions:

- ~Which IVs and IV interactions induced any significant AxV trend?~
- ~Which IVs were significant in promoting the AxV trend peaks?~

The first question was investigated by a simple ANOVA where the mean sum of squares of each effect was tested for significance. The second question, regarding the parameter-space origin of the AxV trend, was investigated by a "Trend Analysis". This analysis was an iterative process in which IVs associated with the highest F-ratio (the highest significance level of the difference between the IVs levels) were successively selected. Chosen IV levels (enhancing the investigated trend) successively reduced the data-base of the following iteration (a nested structure). This analysis always converged to the trend peak value. It provided an entering priority list and levels of the IVs enhancing that trend. The contribution of a lower priority IV (late to enter and therefore deduced from a smaller sample size) was regarded as less reliable.

Three data-base versions: "absolute", "compensated" and "relative" were employed. The absolute data set was comprised of the raw data magnitudes (in dB, relative to 1 microvolt RMS) and phases (in degrees). It was used in testing the NL magnitude dependency on the IVs. The relative data set was comprised of the within run magnitude-gains (in dB) and phase-shifts (in degrees) of the bimodal CEPs relative to the

unimodal CEPs (within NAME x SIG x SF x SI x CF x CI groups). It was used to assess the factors contributing to the AxV phenomenon. The compensated data set contained mean-reduced absolute data (absolute value - group mean difference, within NAME x SIG x SF x SI groups). This data set was used to expose contributions of inter- or cross-modality IVs (the data was compensated for the intra-modality SF and SI effects). The dependent variables and the data set definitions are summarized in TABLE III 8.1B.

AxV EXPERIMENT DEPENDENT VARIABLE DEFINITIONS

TABLE III 8.1B : Definitions of the dependent variables and the data-bases.

DATA-BASE ATTRIBUTES	DEFINITIONS : Magnitude & Phase VARIABLES
ABSOLUTE	absolute magnitude (dB relative to 1 microvolt RMS) and phase (degrees) values
COMPENSATED	group-mean-reduced absolute data (within groups of NAME x SIG x SF x SI)
RELATIVE	magnitude-gains and phase-shifts between MOD classes (BImodal-UNImodal CEP difference)

Exposing the AxV phenomenon within the auditory and visual CEPs utilized primarily the relative data set. The following linear model describes the AxV contributing factors. In this model, BI represents the 1st and 3rd run components, UNI represents the 2nd run component (a component can be magnitude or phase), and a,b,c,d,e,a',b' are weighting coefficients (partial regression coefficients). The "*" symbol stands here for multiplication.

$$\begin{aligned} BI &= a * SF + b * SI + c * CF + d * CI + e * ATT + \text{error}, \\ UNI &= a' * SF + b' * SI + \text{error}' \end{aligned}$$

$$\begin{aligned} "AxV" : BI-UNI &= (a-a') * SF + (b-b') * SI && \text{"Internal Effects"} \\ &+ c * CF + d * CI + e * ATT && \text{"External Effects"} \\ &+ (\text{error} - \text{error}') && \text{"Error Effects"} \end{aligned}$$

To summarize, using the relative data set, both "Internal" (due to SF and SI) and "External" (due to CF, CI and ATT) IVs might have contributed to the AxV phenomenon.

No restrictions were imposed on the data-bases, since only less than 3% of the run data could definitely be regarded as noise. A run was "noisy" if: the average CEP magnitude (of 1st, 2nd and 3rd ORDER sections) was lower than the value of the group's average NL + 1 Standard Deviation (SD) magnitude, and concurrently, the CEP phase SD exceeded the group SD (tested in SIG x SF groups).

The distribution of the relative data-base appeared symmetrical ($|\text{skewness}| < 1$), and normality could be assumed for the magnitude data. After verifying the similarity between parametric and non-parametric tests (due to the data distribution symmetry), parametric statistics were invoked for both magnitude and phase data. ANOVA and MANOVA of balanced-cells, repeated measure design saturated models were tested. Since IV contributions could not have been a-priori hypothesized, and due to the small sample size of the study, care must be exercised in interpreting the AxV results. Therefore, only highly significant or integrable results were considered and discussed. Overall, a rather conservative approach was employed.

Chapter 8

Results of The Bisensory Continuous Evoked Potentials Experiment

8.1 Raw data and results outline

Auditory and visual Continuous Evoked Potentials (CEPs), recorded in a typical run, are demonstrated in FIGURE III 8.2 . Noise Level (NL) sections showed the lowest magnitudes and unstable, random-like phases. Absolute NL magnitudes were checked for stimulus-independent artifacts, biological (EEG contribution) and instrumental ("cross-talk" between similar Modulation Frequencies, MFs, due to a lack of adequate Lock-In Amplifier, LIA, frequency resolution). Relative CEP data were tested for stimulus-dependent, physiological Auditory-Visual Interaction (AxV) effect. The ANOVA results consist of tabulated statistical summaries and figures highlighting significant or important AxV effects. The trend analysis provided schematics of the effective Independent Variables (IVs) inducing the peak AxV trends. These schematics model the data structure, but not necessarily the invoking sensory system structures.

In the following text, and whenever it was possible, the analyzed IVs were explicitly named. However, IV abbreviations and statistical notations had to be employed to facilitate comprehension of complex dependencies (effect interactions). The IVs included in an ANOVA model are termed "effects" (SIG, SF, CF, SI, CI and ATT class variables). Effects can be "main effects" (i.e. SF CF) and "interactions" (i.e. SF * CF), describing first-order and higher-order dependencies, respectively. The bar notation, where X|Y is short for X, X * Y and Y effects, was frequently used to describe the tested ANOVA models.

8.2 Data description of the runs

The general trends of the compensated runs' magnitudes and phases are disclosed in FIGUREs III 8.3, 8.4. Magnitude-wise, the auditory CEPs revealed a smaller inter-subject variability and MF-dependent MOD effect trends. That is, bimodal and unimodal stimuli were associated with different CEP magnitudes (FIGURE III 8.3). The visual CEP average magnitude was clearly influenced by two subjects (Subjects 1 and 6), whose responses to the audio-attended, bimodal stimuli (the 1st ORDER magnitude, see FIGURE III 8.1) were completely suppressed. In general, the visual response was associated with larger absolute CEP magnitudes and lower absolute NL magnitudes. Phase-wise, both modalities were associated with high inter-subject variability and displayed MF-dependent, opposing trends of progressing phase-shifts (primarily for the visual CEPs, FIGURE III 8.4).

Compensated magnitudes of the runs were further characterized by these three sets of categorizing IVs: SF--CF, SI--CI and CF--CI (FIGUREs III 8.5-8.7). The IV definitions are provided in TABLE III 8.1A. These figures were also referred to when NL and relative magnitudes were analyzed.

**RUN EXAMPLE OF THE AUDITORY-VISUAL INTERACTION
EXPERIMENT**

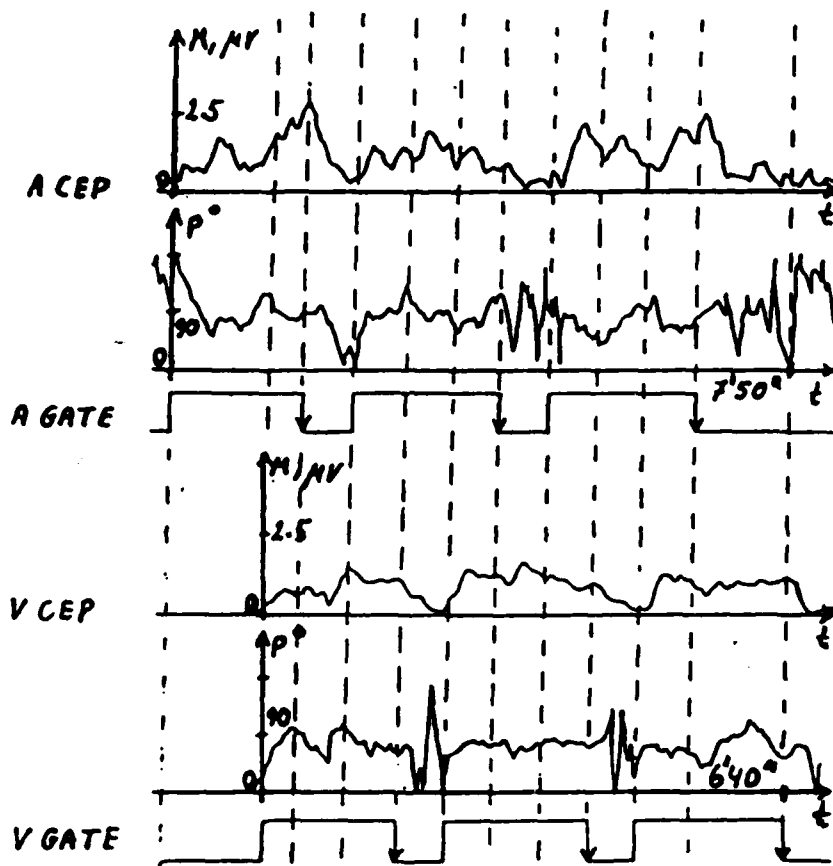


FIGURE III 8.2 : LOCK-IN AMPLIFIER (LIA) VECTOR OUTPUT OF AUDITORY (A) AND VISUAL (V) CEPs AND STIMULUS GATES (GATE). LIA OUTPUT TIME-CONSTANT: 10 SEC. OBTAINED FROM SUBJECT PM UNDER THETA--THETA MODULATION FREQUENCY REGIONS AND HIGH--HIGH INTENSITIES A--V CONDITIONS. STIMULUS-OFF TRANSITION: REACTION-TIME CLUE.

AXV CEP MAGNITUDES

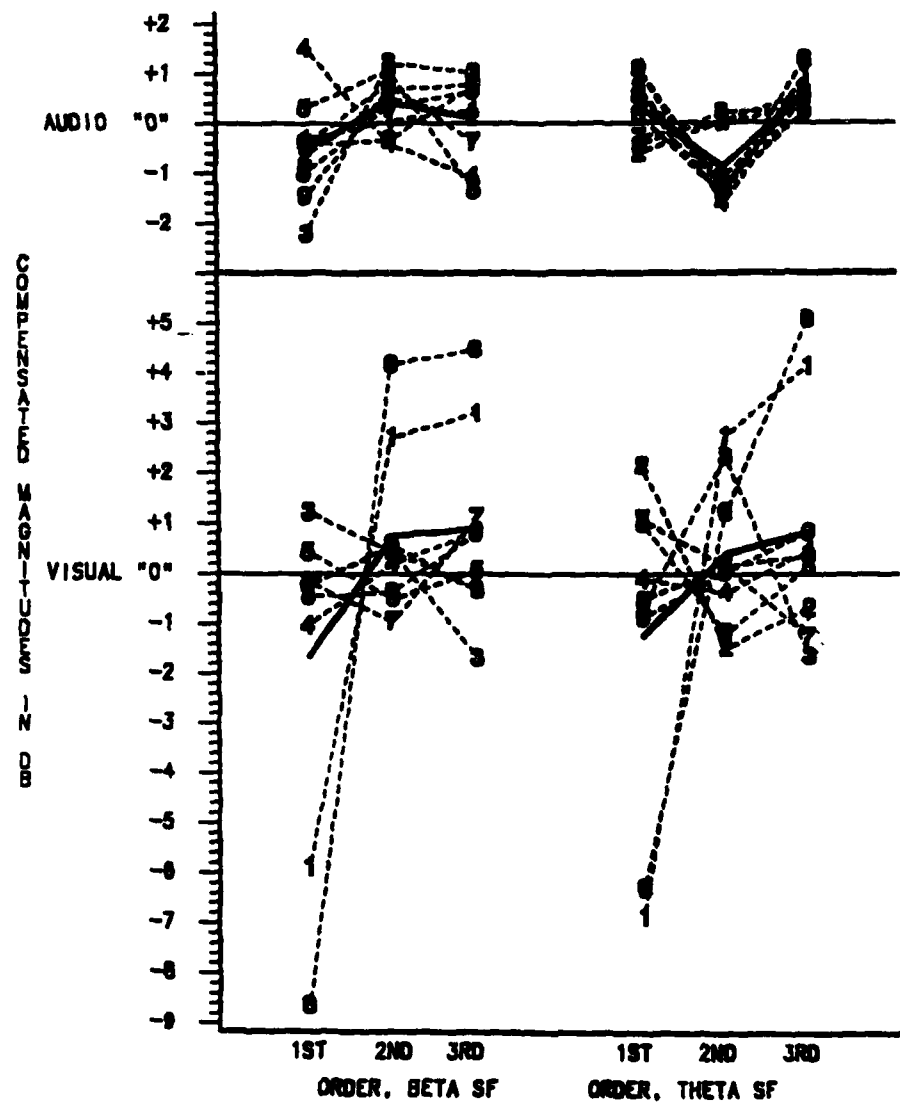


FIGURE III B.3 : MEANS AND INDIVIDUAL COMPENSATED MAGNITUDES OF 9 SUBJECTS.
 SOLID/INTERRUPTED LINE: AVERAGED/INDIVIDUALS DATA. SF: STIMULUS
 MODULATION FREQUENCY (MF) REGION. CEP/NOISE LEVEL ABSOLUTE
 MAGNITUDES IN DB (A/V: AUDITORY/VISUAL, B/T: BETA/THETA MF):
 AB: -6.4/-14.6, AT: -0.7/-6.5, VB: -7.5/-15.8, VT: -0.8/-10.3.

AXV CEP PHASES

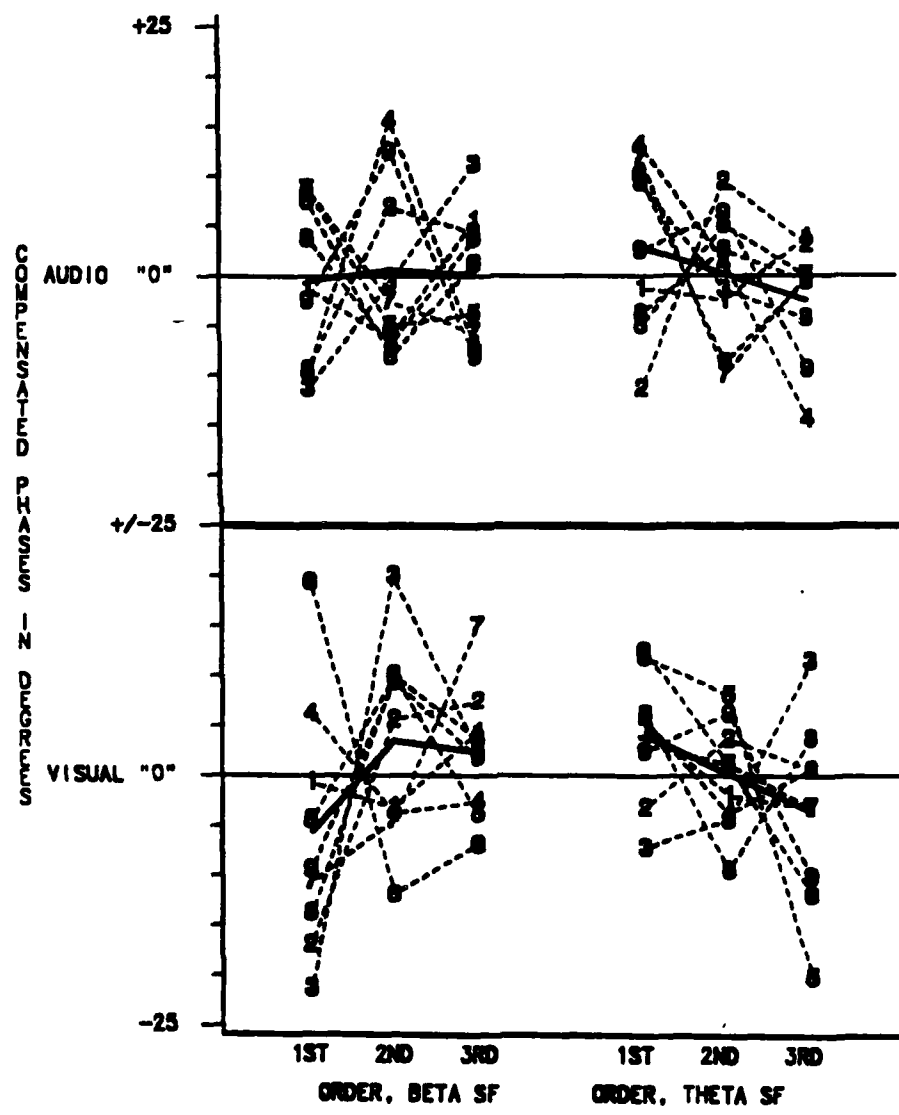


FIGURE III 8.4 : MEANS AND INDIVIDUAL COMPENSATED MAGNITUDES OF 9 SUBJECTS.
 SOLID/INTERUPTED LINE: AVERAGED/INDIVIDUALS DATA,
 SF: THE STIMULUS MODULATION FREQUENCY REGION (BETA OR THETA).

MAGNITUDE SF * CF EFFECT

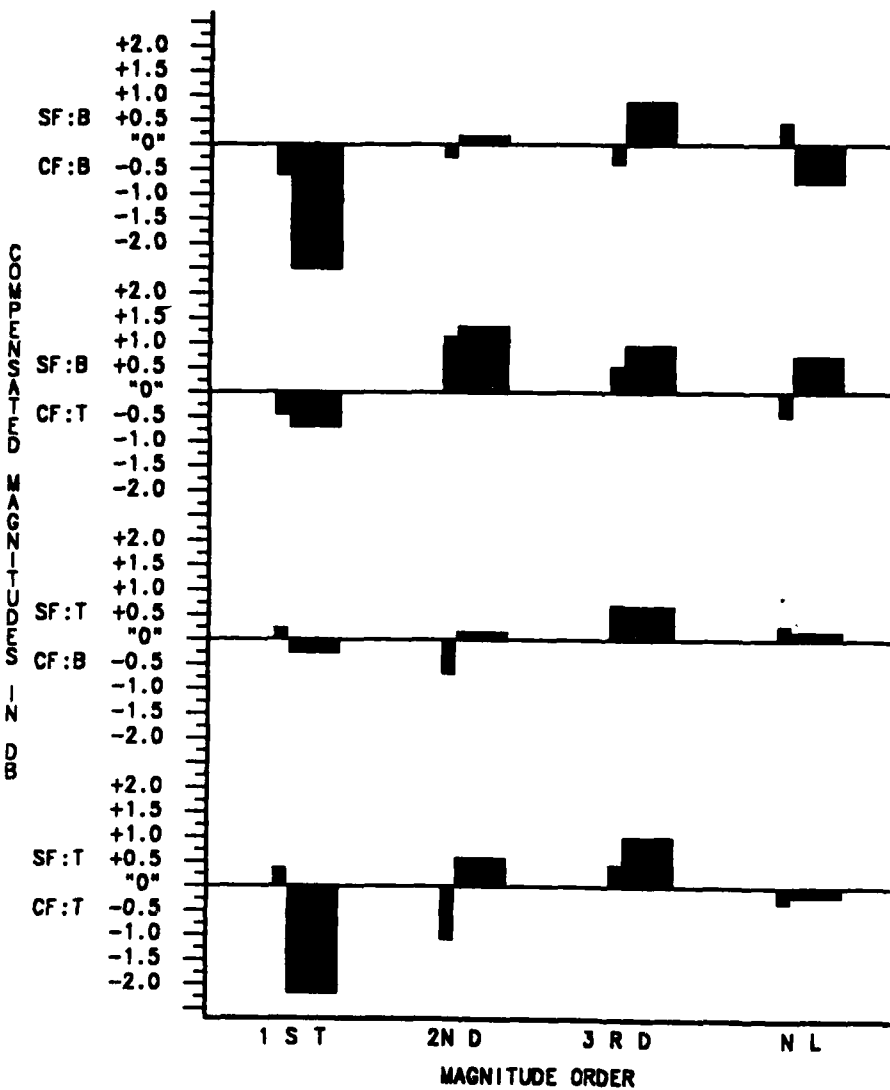


FIGURE III 8.5 : MEAN COMPENSATED MAGNITUDES IN SF X CF X ORDER GROUPS. SF/CF: STIMULUS/CROSS-MODULATION FREQUENCY (MF). B/T: BETA/THETA MF. THIN/THICK BAR: AUDITORY/VISUAL DATA. NL: NOISE LEVEL.

MAGNITUDE SI * CI EFFECT

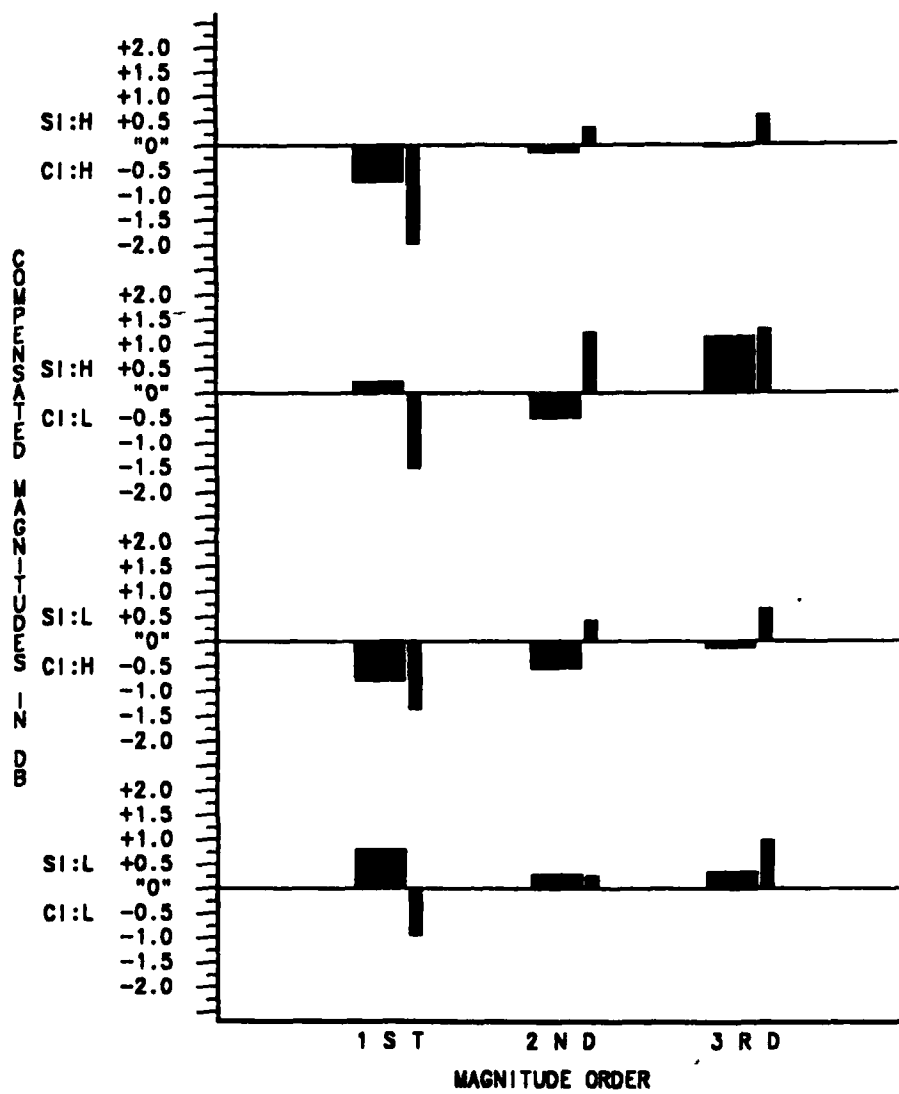


FIGURE III 8.6 : MEAN COMPENSATED MAGNITUDES IN SI X CI X ORDER GROUPS. SI/CI: STIMULUS/CROSS-MODALITY STIMULUS INTENSITY, H/L: "0"/-12 DB INTENSITY LEVEL, THICK/THIN BAR: AUDITORY/VISUAL DATA.

MAGNITUDE CF * CI EFFECT

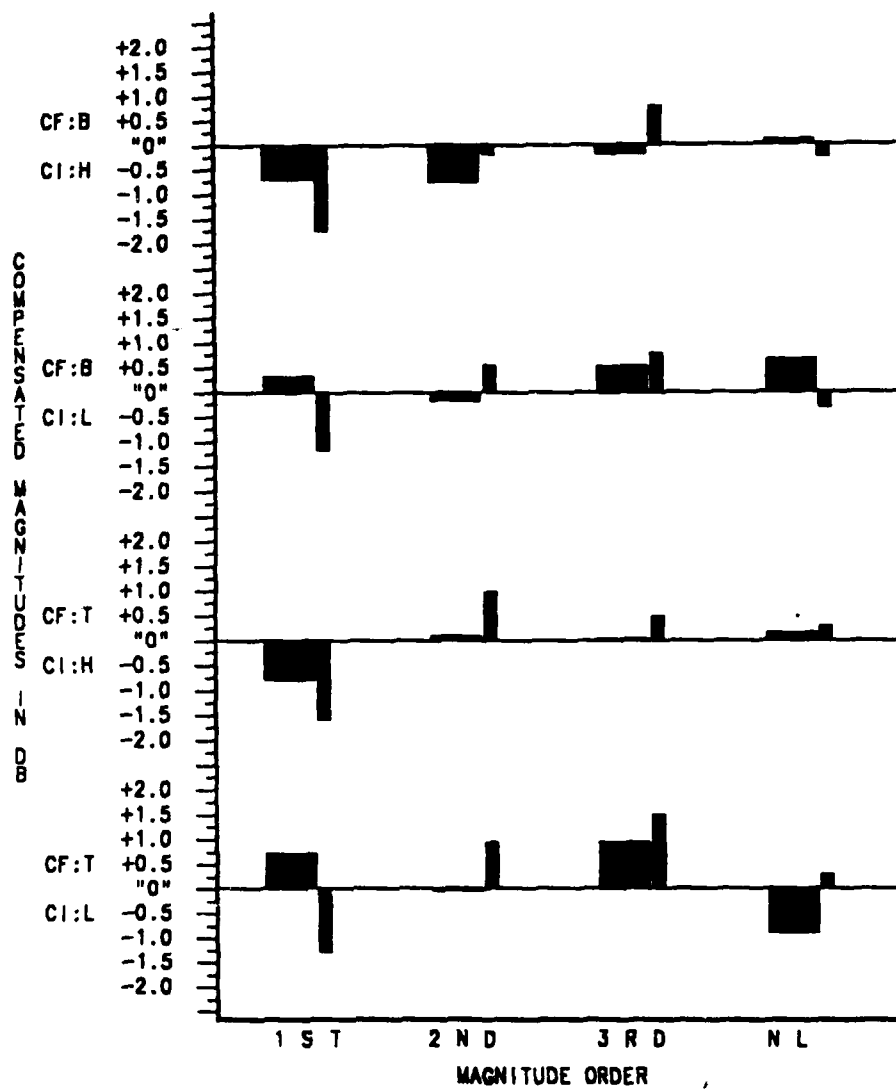


FIGURE III 8.7 : MEAN COMPENSATED MAGNITUDES IN CF X CI X ORDER GROUPS. CF/CI: CROSS-MODALITY STIMULUS MODULATION FREQUENCY (MF)/INTENSITY, B/T: BETA/THETA MF, H/L: "0"/-18 DB INTENSITY LEVEL,
THICK/THIN BAR: AUDITORY/VISUAL DATA, NL: NOISE LEVEL.

8.3 Noise level absolute magnitudes

The results of the ANOVA of auditory, visual and both combined NL absolute magnitudes (in dB) are presented in TABLE III 8.2. Since the NL magnitudes were recorded under no intra-modality stimulus condition (see FIGURE III 8.1), some of the investigated IVs were attached different meanings. SIG and SF were interpreted as the effects of the recording site and noise frequency-band, respectively, and SI effect (the intra-modality stimulus intensity) became irrelevant. The SI IV was, however, separately tested in order to discard the possibility of magnitude response aliasing due to too-long LIA TCs; if the NL magnitudes were predominantly composed of the preceding response tails, they would exhibit an SI effect. Since no such stimulus intensity-NL magnitude dependency could be demonstrated, the exclusion of the SI IV from the NL magnitude model was justified (upper part of TABLE III 8.2).

NL magnitudes significantly differed between noise frequency-bands (SF effect, $|\text{Beta}| < |\text{Theta}|$) and recording sites (SIG effect, $|\text{auditory}| > |\text{visual}|$). The notation of |IV class| symbolizes the averaged CEP magnitude at that IV class. The actual CEP/NL magnitude ratio values at each of the SIG x SF groups are provided in the legend of FIGURE III 8.3. In addition to the SF, SF * SIG and SIG effects (* means interaction), two other effects were considered. The significant CF * CI effect and the non-significant SF * CF effect (TABLE III 8.2).

The SF * CF effect demonstrated the LIA fine frequency resolution. The overall trend (predominantly of the visual CEP recording site) was of smaller NL magnitudes associated with "same" inter-modality SF attributes. Beta--Beta and Theta--Theta MF region combinations (similar SF and CF MF attributes) produced the smallest magnitudes (FIGURE III 8.5). This observation proved that no instrumental "cross-

"talk" artifacts had occurred. This conclusion is important, since an SF * CF * ATT significant effect was detected for the visual relative magnitudes (see TABLE III 8.5 in the next section).

The CF * CI effect exclusively resided within NL magnitudes obtained from the auditory CEP recording site (TABLE III 8.2, FIGURE III 8.7). This effect could be interpreted as a CI-dependent CF effect, where higher "auditory" NL magnitudes (recorded from Cz-A1/nose sites) were associated with visual Beta MF stimuli (FIGURE III 8.7). This effect was free of any intra-modality stimulus parameter influence (no significant SF * CF * CI, SI * CF * CI or SF * SI * CF * CI effects).

8.4 Bimodal - unimodal relative auditory CEPs

8.4.1 Analysis of variance

The results of the ANOVA of relative CEP magnitudes and phases, and the MANOVA of both together are presented in TABLE III 8.3. These relative values (the bimodal - unimodal CEP magnitudes and phases differences) reflect the AxV phenomenon (as defined in section III 7.2). Cross-subject averages of relative magnitudes and phases were computed for the 32 possible SF x SI x CF x CI x ATT combinations (five, two-levels IVs), and their univariate tests are provided in TABLE III 8.4. Relative magnitudes and phases were clearly unrelated. None of the model's tested effects exhibited an increase of the MANOVA significance level score over that of the ANOVA scores (TABLE III 8.3). Therefore, relative magnitudes and phases were separately analyzed.

AxV NOISE LEVEL MAGNITUDES

TABLE III 8.2 : ANOVA and MANOVA of repeated-measure models. M: absolute noise level Magnitudes (in dB). Notation: X|Y is equivalent to X X*Y Y, MS: Mean Square (using Type III sum of squares), DF: Degrees of Freedom (num/den), PR>F significance level codes: . > 0.1, a < 0.1, b < 0.05, c < 0.01, d < 0.005, e < 0.001, f < 0.0005, g <= 0.0001.

----EFFECTS----		ANOVA OF NOISE LEVEL MAGNITUDES-----					
		F-tests, 1/8 DF					
Tested against							
NAME*effects	error terms	AUDITORY (A)	VISUAL (V)	A & V			
		MS F, PR>F	MS F, PR>F	MS F, PR>F			
NAME		837	1024	1658			
SF		2355 91.1 g	1101 132 g	3339 184 g			
CF		19.3 4.6 a	11.7 2.6 .	0.5 0.1 .			
SF*CF		0.9 0.1 .	29.8 1.8 .	10.1 1.4 .			
CI		1.9 0.2 .	0.0 0.0 .	1.2 0.4 .			
SF*CI		6.0 1.6 .	0.2 0.0 .	4.1 0.3 .			
CF*CI		23.5 8.5 b	0.1 0.0 .	10.5 1.1 .			
SF*CF*CI		0.4 0.1 .	2.2 0.3 .	0.4 0.0 .			
SIG	- - - - -	- - - - -	- - - - -	442 17.5 d			
SIG*S傅	- - - - -	- - - - -	- - - - -	118 7.3 b			
SIG*CF	- - - - -	- - - - -	- - - - -	30.5 6.2 b			
SIG*SF*CF	- - - - -	- - - - -	- - - - -	20.6 1.3 .			
SIG*CI	- - - - -	- - - - -	- - - - -	0.8 0.0 .			
SIG*SF*CI	- - - - -	- - - - -	- - - - -	2.1 0.2 .			
SIG*CF*CI	- - - - -	- - - - -	- - - - -	13.1 1.0 .			
SIG*SF*CF*CI	- - - - -	- - - - -	- - - - -	2.3 0.4 .			
<hr/>							
MODEL: M= SF CF CI NAME, for A and V separate data sets							
MODEL: M= SIG SF CF CI NAME, for A & V combined data set							
<hr/>							
SI		0.1 0.0 .	0.4 0.0 .	0.4 0.0 .			
SF*SI		6.6 1.4 .	7.3 0.7 .	0.0 0.0 .			
SIG*SI	- - - - -	- - - - -	- - - - -	0.0 0.0 .			
SIG*SF*SI	- - - - -	- - - - -	- - - - -	13.9 2.5 .			
<hr/>							
MODEL: M= SF SI NAME, for A and V separate data sets							
MODEL: M= SIG SF SI NAME, for A & V combined data set							
<hr/>							

8.4.1.1 Auditory relative magnitudes

Auditory relative magnitudes were primarily affected by the audio stimulus MF (SF effect) and the inter-modality intensity attributes (SI * CI effect). Regarding the SF effect, Beta and Theta auditory MF regions were associated with decrease (bisensory "inhibition") and increase (bisensory "facilitation") of CEP relative magnitudes, respectively (FIGURE III 8.3, TABLE III 8.4). This effect was independent of the visual stimulus MF, inter-modality intensities and attention.

Facilitated relative magnitudes ($|BI| > |UNI|$) were also associated with "different" inter-modality intensity attributes . Larger relative magnitudes were associated with High--Low and Low--High Audio--Visual stimulus intensity conditions, further resolved by attention (SI * CI and SI * CI * ATT effects, TABLE III 8.3 and FIGURE III 8.8). This SI * CI effect could be interpreted as an audio stimulus intensity-dependent, visual stimulus intensity effect (CI effect of $|Low| > |High|$ at SI = High, FIGURE III 8.8).

8.4.1.2 Auditory relative phases

Auditory relative phases were primarily affected by the SI * CF * ATT interaction (TABLE III 8.3, FIGURE III 8.9). FIGURE III 8.9 reveals that the SI * CF effect within the "NAT" attention level was the source of that phenomenon. The combinations of Beta visual stimulus MF--High audio stimulus intensity and Theta visual stimulus MF--Low audio stimulus intensity were associated with leading relative phases ($BI > UNI$ at Beta CF--High SI and Theta CF--Low SI combinations, FIGURE III 8.9).

RELATIVE (BIMODAL-UNIMODAL) AUDITORY CEP VECTORS

TABLE III 8.3 : ANOVA and MANOVA of repeated-measure models, M: relative CEP Magnitudes (in dB), P: relative CEP Phases (in degrees). Notation: X|Y is equivalent to $X \times Y$, Y, MS: Mean Square (using Type III sum of squares), DF: Degrees of Freedom (num/den), PR>F significance level codes: . > 0.1, a < 0.1, b < 0.05, c < 0.01, d < 0.005.

-----EFFECTS-----		ANOVA-----				-MANOVA-		
Tested against		F-tests, DF: 1/8		DF: 2/7		M	P	
NAME*effects		MAGNITUDES (M)	PHASES (P)					
error terms		MS	F, PR>F	MS	F, PR>F	F, PR>F		
NAME		164.2		1049				
SF	277.4	26.7	e	84	0.1	.	11.7	c
SI	5.5	0.6	.	852	0.9	.	1.1	.
SF*SI	11.9	1.5	.	1878	1.4	.	1.1	.
CF	4.7	0.4	.	32	0.0	.	0.3	.
SF*CF	24.1	1.2	.	11	0.0	.	0.6	.
SI*CF	10.1	1.2	.	6569	2.4	.	1.8	.
SF*SI*CF	11.1	0.6	.	4	0.0	.	0.3	.
CI	46.4	2.3	.	8618	2.5	.	4.0	a
SF*CI	20.0	1.1	.	243	0.1	.	0.7	.
SI*CI	26.0	16.4	d	4	0.0	.	10.6	c
SF*SI*CI	0.5	0.0	.	2308	0.7	.	0.3	.
CF*CI	20.9	1.3	.	175	0.0	.	0.6	.
SF*CF*CI	3.5	0.2	.	9287	3.0	.	1.3	.
SI*CF*CI	0.4	0.0	.	263	0.1	.	0.0	.
SF*SI*CF*CI	13.3	0.4	.	3169	1.1	.	0.5	.
ATT	14.0	1.7	.	489	0.6	.	2.2	.
SF*ATT	2.0	0.3	.	461	1.0	.	0.4	.
SI*ATT	8.5	3.4	.	4	0.0	.	1.8	.
SF*SI*ATT	1.0	0.2	.	1071	2.1	.	1.1	.
CF*ATT	0.5	0.1	.	83	0.1	.	0.2	.
SF*CF*ATT	6.0	1.2	.	1269	1.6	.	1.0	.
SI*CF*ATT	2.4	1.0	.	3934	15.3	d	6.9	b
SF*SI*CF*ATT	0.6	0.1	.	7	0.0	.	0.0	.
CI*ATT	3.7	0.8	.	54	0.0	.	0.4	.
SF*CI*ATT	4.6	0.5	.	7	0.0	.	0.3	.
SI*CI*ATT	7.9	5.2	a	346	0.4	.	2.3	.
SF*SI*CI*ATT	2.5	0.6	.	1	0.0	.	0.5	.
CF*CI*ATT	0.4	0.1	.	303	0.5	.	0.3	.
SF*CF*CI*ATT	0.3	0.2	.	20	0.0	.	0.1	.
SI*CF*CI*ATT	1.5	0.4	.	3038	2.5	.	1.9	.
SF*SI*CF*CI*ATT	6.0	1.4	.	626	1.5	.	1.0	.

MODEL: M or P or M P = SF|SI|CF|CI|ATT|NAME

AUDITORY AxV UNIVARIATE STATISTICS

TABLE III 8.4 : ANOVA of the intercept (null hypothesis of M or P = 0) for CEP relative Magnitudes (M) and Phases (P). "H"/"L": "0"/-12 dB intensity level, PR > F significance level codes: . > 0.1, a < 0.1, b < 0.05, c < 0.01.

SF	SI	CF	CI	ATT	INDEPENDENT VARIABLE LEVELS		CEP MEANS		F-tests	
							M dB	P deg.	PR>F M	P
BETA	"H"	BETA	"H"	ATT	-0.78	7.2
BETA	"H"	BETA	"H"	NAT	-1.87	12.2	a	.	.	.
BETA	"H"	BETA	"L"	ATT	0.90	7.2
BETA	"H"	BETA	"L"	NAT	0.51	3.3
BETA	"H"	THETA	"H"	ATT	-1.33	2.8
BETA	"H"	THETA	"H"	NAT	-2.59	-3.3	a	.	.	.
BETA	"H"	THETA	"L"	ATT	0.00	3.3
BETA	"H"	THETA	"L"	NAT	-0.60	-7.8
BETA	"L"	BETA	"H"	ATT	-0.12	12.8
BETA	"L"	BETA	"H"	NAT	-0.20	-1.1
BETA	"L"	BETA	"L"	ATT	-0.48	-27.8
BETA	"L"	BETA	"L"	NAT	0.14	-27.2
BETA	"L"	THETA	"H"	ATT	-0.87	-11.7
BETA	"L"	THETA	"H"	NAT	-2.80	8.3	a	.	.	.
BETA	"L"	THETA	"L"	ATT	-0.14	-3.3
BETA	"L"	THETA	"L"	NAT	-0.26	6.7
THETA	"H"	BETA	"H"	ATT	1.97	-7.2	a	.	.	.
THETA	"H"	BETA	"H"	NAT	1.93	24.4	a	b	.	.
THETA	"H"	BETA	"L"	ATT	2.80	-6.7	c	.	.	.
THETA	"H"	BETA	"L"	NAT	0.78	3.9
THETA	"H"	THETA	"H"	ATT	0.55	12.2
THETA	"H"	THETA	"H"	NAT	0.22	3.3
THETA	"H"	THETA	"L"	ATT	2.73	-19.4	b	.	.	.
THETA	"H"	THETA	"L"	NAT	2.19	-17.8	a	.	.	.
THETA	"L"	BETA	"H"	ATT	1.25	-2.8
THETA	"L"	BETA	"H"	NAT	0.40	-15.6
THETA	"L"	BETA	"L"	ATT	-0.47	-5.0
THETA	"L"	BETA	"L"	NAT	0.50	7.2
THETA	"L"	THETA	"H"	ATT	1.40	11.7
THETA	"L"	THETA	"H"	NAT	1.63	24.4
THETA	"L"	THETA	"L"	ATT	1.32	-3.9
THETA	"L"	THETA	"L"	NAT	1.69	-10.0	b	.	.	.

MODEL: M or P = intercept
(at each SF x SI x CF x CI x ATT group)

MAGNITUDE SI * CI * ATT EFFECT

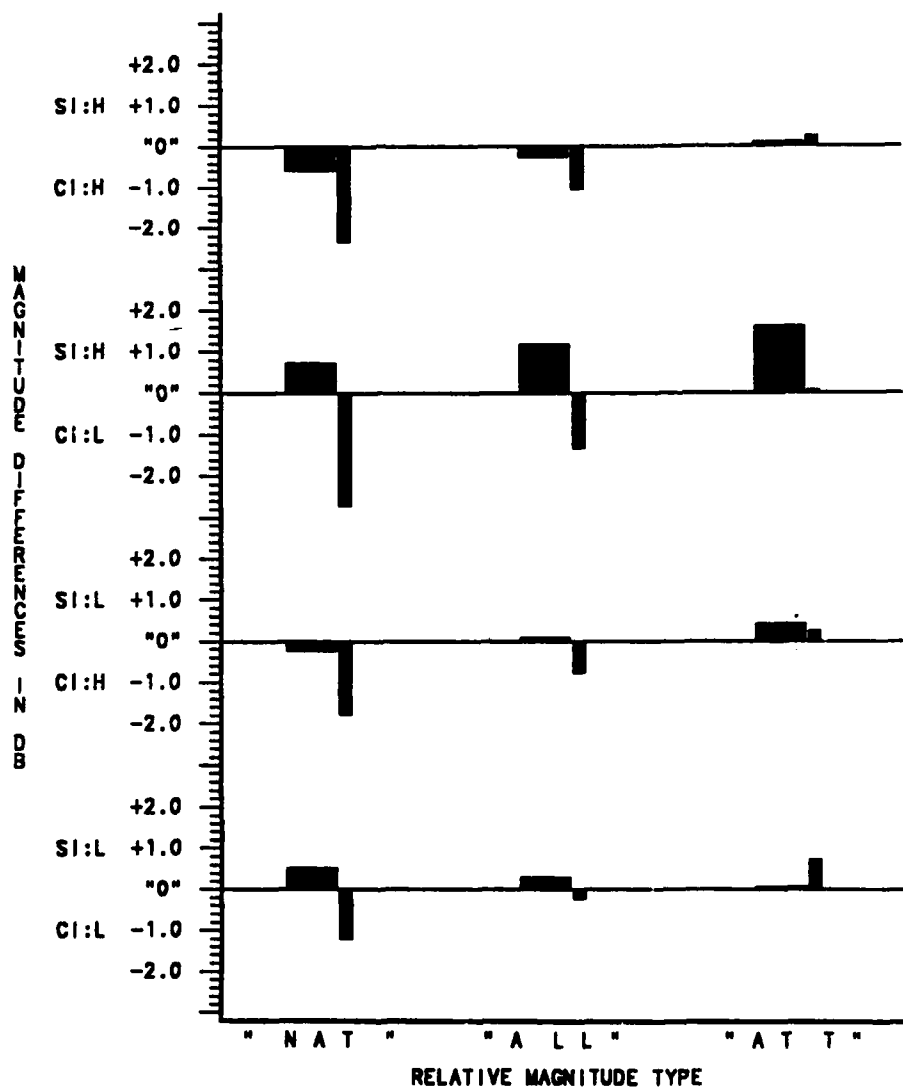


FIGURE III 6.8 : MEAN RELATIVE MAGNITUDES (BIMODAL-UNIMODAL DIFFERENCE IN DB).
 SI/CL: STIMULUS/CROSS-MODALITY STIMULUS INTENSITY, H/L.
 "0"/-12 DB INTENSITY LEVEL, THICK/THIN BAR: AUDITORY/VISUAL
 DATA, ATT/NAT/ALL: ATTENDED/NON-ATTENDED/BOTH-AVERAGED DATA.

PHASE SI * CF * ATT EFFECT

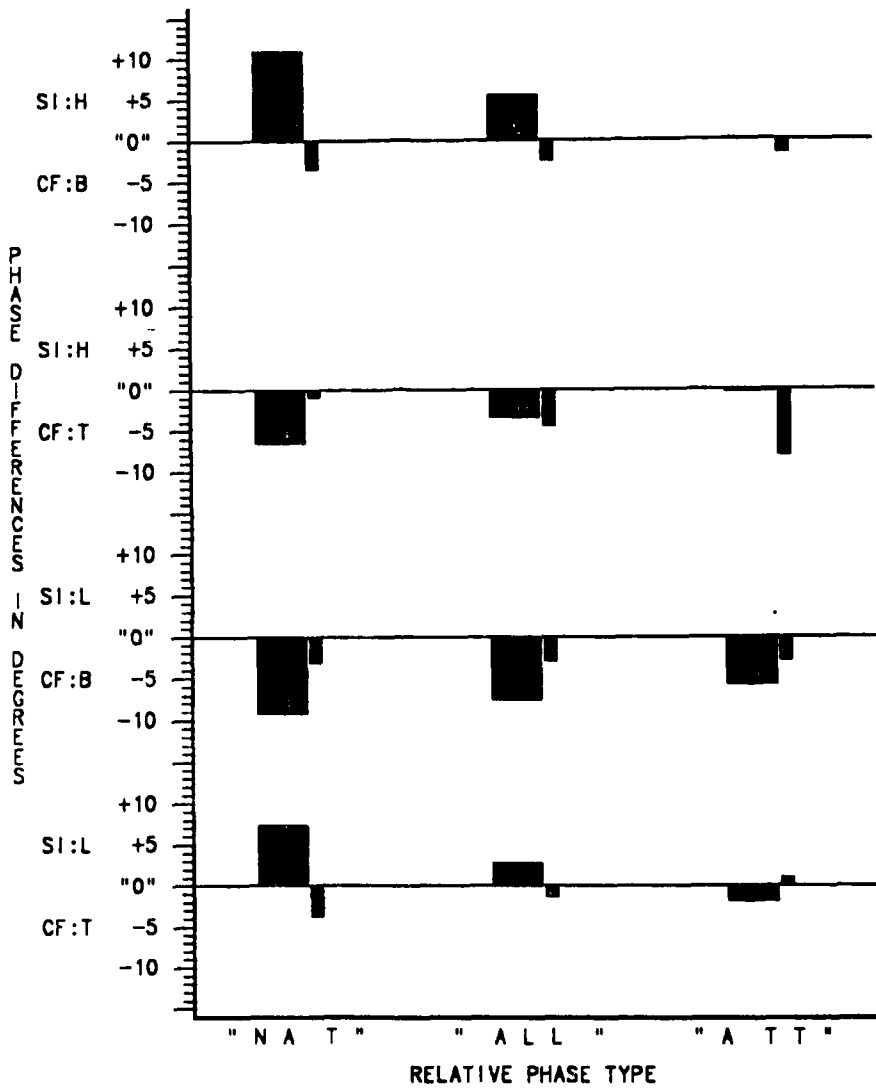


FIGURE III 8.9 : MEAN RELATIVE PHASES (BIMODAL-UNIMODAL DIFFERENCE IN DEGREES). SI/CF: STIMULUS INTENSITY/CROSS-MODALITY STIMULUS MODULATION FREQUENCY (MF), H/L: "0"/-12 DB INTENSITY LEVEL, B/T: BETA/THETA MF, THICK THIN BAR: AUDITORY/VISUAL DATA, ATT/NAT/ALL: ATTENDED/NON-ATTENDED/BOTH-AVERAGED DATA.

8.4.2 Trend analysis

Parameter-space origins of the positive ("+" and negative ("-) relative (BI-UNI) Magnitudes (in dB) and Phases (in degrees) were disclosed, and the resultant trend paths are described in FIGURE III 8.10. The investigated trend in each path (+ M, -M, + P, and -P) was defined by a primary (1st priority) stimulus parameter, an IV (one of the MFs, INTensities and ATTention IVs) associated with the highest significance level in exhibiting that trend. The other parameter levels were successively selected to enhance that trend. Each parameter was selected from the formerly-defined parameter-space. The values of the 4th priority parameter levels (averaged across the levels of the lowest priority parameter) made up the final trend peak values. When checked against the univariate means of TABLE III 8.4, it was evident that this iterative procedure converged to (or conversely was influenced by) the peak values.

Overall, magnitude trend paths were resolved with higher parameter significance levels. Thus, within the same five-dimensional parameter-space, inhibition and facilitation trends of relative magnitudes were significantly more confined (and consequently more susceptible to "noisy" data influence). In comparison, the leading and lagging trends of relative phases were more general (broader) and less significant.

Magnitude and phase trends appeared inverted between the audio MF regions. Positive and negative trends were primarily associated with the Theta (late CEPs) and Beta (early CEPs), respectively. Peak trends of relative magnitudes and phases were defined by different primary parameters and generally characterized by different priority and parameter level lists. Therefore magnitude and phase trends were separately assessed in the following paragraphs.

8.4.2.1 Auditory magnitude trends

The parameter lists of negative (" -M ", bisensory "inhibition") and positive (" + M ", bisensory "facilitation") relative magnitude trends complemented each other. That is, all the parameters' levels deferred between the trends. Primarily determined by the Audio stimulus MF parameter, inhibition and facilitation trends were associated with the Beta and Theta MF regions, respectively. Within these MF regions, inhibition and facilitation were further enhanced by High, Audio and Visual stimulus INTensities, respectively (2nd priority parameter).

Investigation of the 5th priority parameters revealed that inhibition and facilitation enhanced trends were independent of the Audio INTensity and the Visual MF, respectively. It is interesting to note that although ATT effect was generally not significant (see previous ANOVA of relative magnitudes, TABLE III 8.3), ATTending to the Audio stimulus increased the relative magnitude facilitory trend and vice versa. :

8.4.2.2 Auditory phase trends

Overall, the two phase trend paths were non-complementary and differed structurally. Positive relative phase trend (" + P ", "leading") was primarily defined by the Visual stimulus parameters (V INTensity, V MF) and enhanced by the Audio stimulus parameters (A MF, A INTensity). Negative relative phase trend (" -P ", "lagging") was primarily defined by the INTensity parameters (V INTensity, A INTensity) and enhanced by the MF parameters (V MF, A MF).

STIMULUS PARAMETERS INDUCING THE AUDITORY PEAK AxV TRENDS

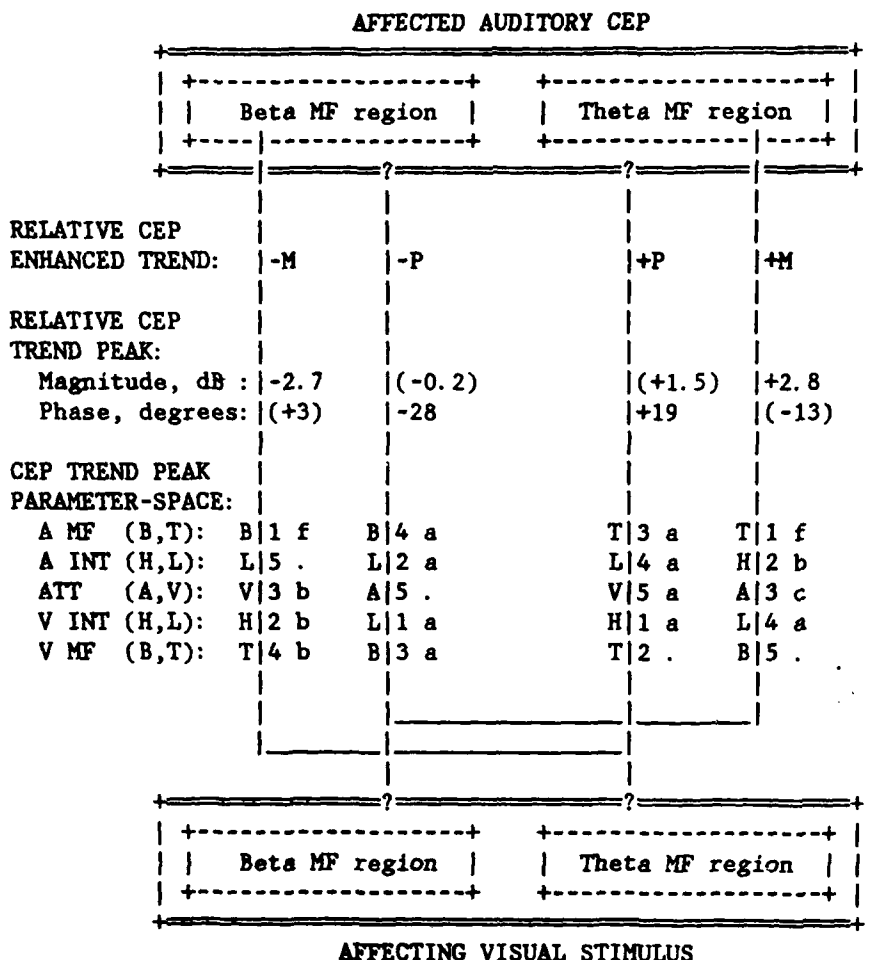


FIGURE III 8.10 : TREND ANALYSIS OF RELATIVE (BISENSORY-UNISENSORY) CEP MAGNITUDES (M) AND PHASES (P). EACH TREND-ENHANCING PATH WAS AFFECTED BY FIVE STIMULUS PARAMETERS AND DEFINED BY (LEFT TO RIGHT): PARAMETER LEVELS, PRIORITIES AND SIGNIFICANCES. KEY-CHARACTERS: AUDIO (A), VISUAL (V), MODULATION FREQUENCY (MF), INTENSITY (INT), BETA (B), THETA (T), HIGH (H), LOW (L), ATTENTION (ATT), "+"/-": POSITIVE/NEGATIVE BISENSORY-UNISENSORY TREND. PR>F SIGNIFICANCE LEVEL CODES: . > 0.5, a < 0.5, b < 0.1, c < 0.05, d < 0.01, e < 0.005, f < 0.001.

Primarily determined by the Visual stimulus INTensity parameter, leading and lagging relative phase trends were associated with High and Low INTensity levels, respectively. Note that both phase trends were ATTention-independent and a clear-cut association between Auditory and Visual MFs was not established.

8.5 Bimodal - unimodal relative visual CEPs

8.5.1 Analysis of variance

The results of the ANOVA of relative CEP magnitudes and phases, and the MANOVA of both, are presented in TABLE III 8.5. Univariate means and tests of relative magnitudes and phases are provided in TABLE III 8.6. Similar to the auditory relative CEPs, the visual relative magnitude and phase data were found to be unrelated and thus were analyzed separately.

8.5.1.1 Visual relative magnitudes

Visual relative magnitudes were primarily affected by the SF * CF * ATT and SF * SI * CF * CI interactions. The SF * CF * ATT significant interaction could be interpreted as an attention-dependent, inter-modality stimulus MF attributes effect (ATT/NAT-dependent SF * CF effect, FIGURE III 8.11). Overlooking the within-run average trend of lower 1st magnitude (ORDER's 1st, see section 8.2), larger and smaller relative magnitudes were associated with ATT--"same" inter-modality MF attributes and NAT--"same" inter-modality MF attributes stimulus conditions, respectively. Attentiveness conditions are referred to the visual stimulus.

RELATIVE (BIMODAL-UNIMODAL) VISUAL CEP VECTORS

TABLE III 8.5 : ANOVA and MANOVA of repeated-measure models, M: relative CEP Magnitudes (in dB), P: relative CEP Phases (in degrees). Notation: X|Y is equivalent to $X \times Y$, MS: Mean Square (using Type III sum of squares), DF: Degrees of Freedom (num/den), PR>F significance level codes: . > 0.1, a < 0.1, b < 0.05, c < 0.01, d < 0.005.

----EFFECTS----		-----ANOVA-----				-MANOVA-	
Tested against		F-tests, DF: 1/8				DF: 2/7	
NAME*effects		MAGNITUDES (M)	PHASES (P)	M	P		
error terms		MS	F, PR>F	MS	F, PR>F	F, PR>F	
NAME	1049		19116				
SF	23.2	0.6	.	2278	1.0	.	2.0
SI	33.2	3.2	.	127	0.1	.	1.4
SF*SI	13.4	1.1	.	354	0.3	.	0.8
CF	32.4	1.0	.	1	0.0	.	0.4
SF*CF	21.0	1.0	.	292	0.1	.	0.6
SI*CF	16.2	0.9	.	219	0.1	.	0.4
SF*SI*CF	10.8	0.4	.	871	0.5	.	0.3
CI	1.2	0.1	.	3206	4.1	a	1.9
SF*CI	8.0	0.2	.	5967	2.7	.	1.9
SI*CI	11.9	0.4	.	59	0.0	.	0.3
SF*SI*CI	25.9	0.6	.	6805	1.6	.	0.8
CF*CI	23.2	1.0	.	1508	0.2	.	0.4
SF*CF*CI	0.9	0.0	.	526	0.1	.	0.1
SI*CF*CI	11.1	0.5	.	528	0.3	.	0.3
SF*SI*CF*CI	153.2	5.6	b	2112	0.4	.	4.7
ATT	386.8	1.8	.	0	0.0	.	1.3
SF*ATT	4.6	0.5	.	4391	13.3	c	5.9
SI*ATT	8.6	0.6	.	464	0.7	.	0.7
SF*SI*ATT	39.7	5.0	a	208	0.1	.	2.8
CF*ATT	0.7	0.0	.	95	0.0	.	0.0
SF*CF*ATT	75.6	11.1	b	20	1.0	.	5.2
SI*CF*ATT	0.4	0.1	.	818	0.6	.	1.3
SF*SI*CF*ATT	6.3	2.4	.	2717	1.2	.	2.4
CI*ATT	0.1	0.0	.	1823	2.6	.	1.1
SF*CI*ATT	0.0	0.0	.	859	1.2	.	0.5
SI*CI*ATT	0.5	0.0	.	461	0.4	.	0.2
SF*SI*CI*ATT	4.3	0.5	.	656	0.9	.	0.5
CF*CI*ATT	7.3	1.6	.	0	0.0	.	0.7
SF*CF*CI*ATT	7.2	0.7	.	283	0.3	.	0.4
SI*CF*CI*ATT	0.0	0.0	.	25	0.0	.	0.0
SF*SI*CF*CI*ATT	12.4	1.1	.	147	0.2	.	0.7
<hr/>							
MODEL: M or P or M P = SF SI CF CI ATT NAME							

VISUAL AxV UNIVARIATE STATISTICS

TABLE III 8.6 : ANOVA of the intercept (null hypothesis of M or P = 0) for CEP relative Magnitudes (M) and Phases (P). "H"/"L": "0"/-12 dB intensity level, PR > F significance level codes: . > 0.1, a < 0.1, b < 0.05, c < 0.01.

SF	SI	CF	CI	ATT	CEP MEANS		F-tests	
					M dB	P deg.	M	P
BETA	"H"	BETA	"H"	ATT	0.54	12.8	.	.
BETA	"H"	BETA	"H"	NAT	-5.01	16.7	.	.
BETA	"H"	BETA	"L"	ATT	-0.27	-13.9	.	.
BETA	"H"	BETA	"L"	NAT	-3.44	-29.4	b	a
BETA	"H"	THETA	"H"	ATT	-0.08	3.3	.	.
BETA	"H"	THETA	"H"	NAT	-2.15	-0.6	.	.
BETA	"H"	THETA	"L"	ATT	0.41	-8.9	.	.
BETA	"H"	THETA	"L"	NAT	-3.44	-21.1	a	.
BETA	"L"	BETA	"H"	ATT	2.34	3.3	b	.
BETA	"L"	BETA	"H"	NAT	-0.34	-12.8	.	.
BETA	"L"	BETA	"L"	ATT	0.15	-9.4	.	.
BETA	"L"	BETA	"L"	NAT	-2.44	-19.4	a	.
BETA	"L"	THETA	"H"	ATT	-1.77	2.5	.	.
BETA	"L"	THETA	"H"	NAT	-1.70	-6.9	.	.
BETA	"L"	THETA	"L"	ATT	-0.03	-3.3	.	.
BETA	"L"	THETA	"L"	NAT	-0.75	-2.2	.	.
THETA	"H"	BETA	"H"	ATT	1.37	-13.3	.	a
THETA	"H"	BETA	"H"	NAT	1.25	-7.2	.	.
THETA	"H"	BETA	"L"	ATT	-0.69	8.3	.	.
THETA	"H"	BETA	"L"	NAT	-2.39	6.1	.	.
THETA	"H"	THETA	"H"	ATT	-0.89	-21.7	.	.
THETA	"H"	THETA	"H"	NAT	-3.36	12.8	.	.
THETA	"H"	THETA	"L"	ATT	0.83	-4.4	.	.
THETA	"H"	THETA	"L"	NAT	-1.55	5.6	.	.
THETA	"L"	BETA	"H"	ATT	-0.38	1.1	.	.
THETA	"L"	BETA	"H"	NAT	-2.05	22.8	b	b
THETA	"L"	BETA	"L"	ATT	1.79	-6.1	.	.
THETA	"L"	BETA	"L"	NAT	1.51	-2.8	.	.
THETA	"L"	THETA	"H"	ATT	0.79	-3.9	.	.
THETA	"L"	THETA	"H"	NAT	-3.03	0.0	.	.
THETA	"L"	THETA	"L"	ATT	1.00	8.9	.	.
THETA	"L"	THETA	"L"	NAT	-3.09	-5.6	.	.

 MODEL: M or P = intercept
 (at each SF x SI x CF x CI x ATT group)

MAGNITUDE SF * CF * ATT EFFECT

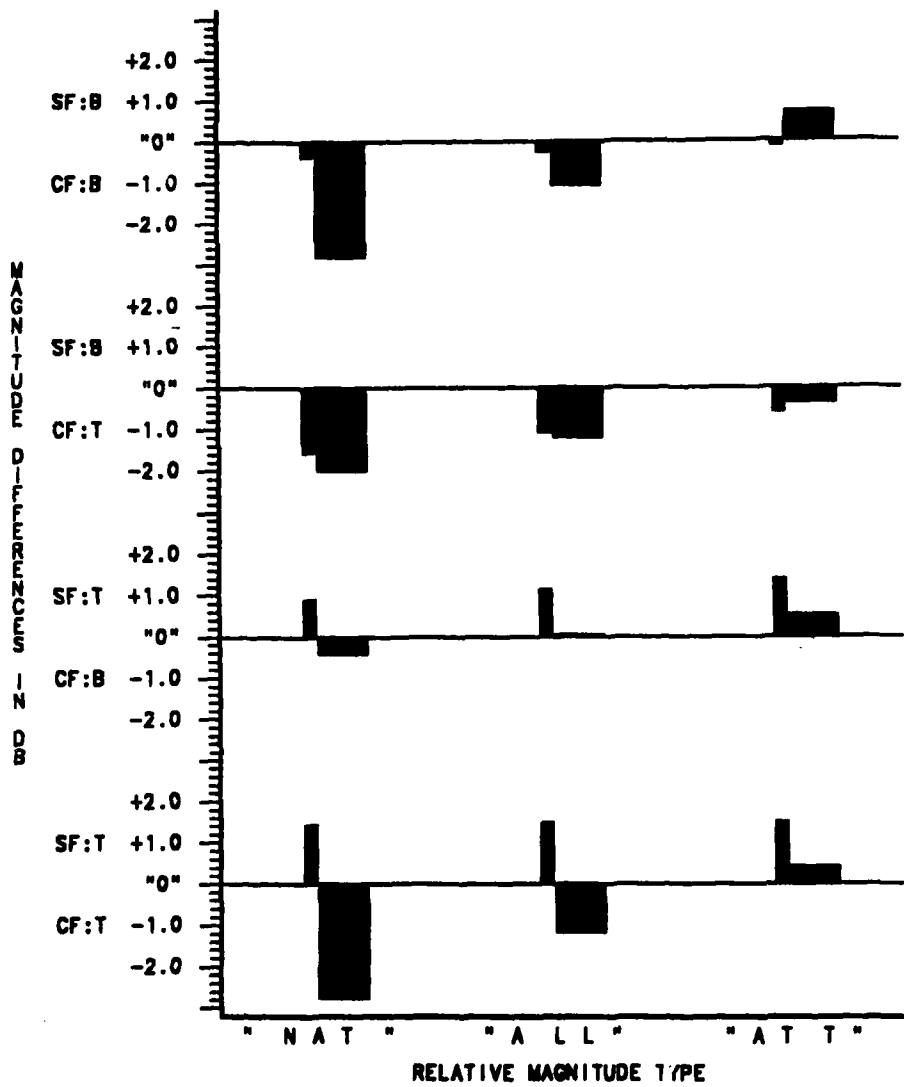


FIGURE III 8.11 : MEAN RELATIVE MAGNITUDES (BIMODAL-UNIMODAL DIFFERENCE IN DB).
 SF/CF: STIMULUS/CROSS-MODALITY STIMULUS MODULATION FREQUENCY
 (MF), B/T: BETA/THETA MF, THIN/THICK BAR: AUDITORY/VISUAL
 DATA, ATT/NAT/ALL: ATTENDED/NON-ATTENDED/BOTH-AVERAGED DATA.

The significant SF * SI * CF * CI interaction was interpreted as an SI * CI-dependent SF * CF effect. The following relative magnitude means were calculated for the "same MF" and "different MF" SF * CF combinations under the "same INT" and "different INT" SI * CI conditions. "Same MF--"same INT", "same MF--"different INT", "different MF--"same INT" and "different MF--"different INT" combination values were -1.6, -0.6, 0.4 and -1.5, respectively. These means support the above interpretation; "Same INT" condition enhanced the "same MF" - "different MF" difference.

8.5.1.2 Visual relative phases

Visual relative phases were significantly affected by the SF * ATT effect (TABLE III 8.5, FIGURE III 8.4). FIGURE III 8.4 shows that non-attended Beta and Theta MF visual stimuli were associated with lagging ($BI < UNI$) and leading ($BI > UNI$) phases, respectively. Attentiveness influenced only the Theta MF visual responses.

8.5.2 Trend analysis

Visual trend analysis, similar to the one conducted for the auditory CEPs is presented in FIGURE III 8.12. The converged-upon final trend values matched the peak values of the univariate means of TABLE III 8.6. The visual trend analysis was carried out on the entire sample size, including Subjects 1 and 6. Since the F-test (which determines the parameter selection priorities) is less susceptible to "outliers" than the means, the overriding magnitude contribution of Subjects 1 and 6 (FIGURE III 8.3) was moderated. And indeed, the parameter priority lists of the relative magnitude trends (FIGURE III 8.12) incorporated the ATTention parameter, only as the 3rd parameter on the priority list. Nevertheless, the magnitude trend paths were regarded as less reliable than the phase trend paths.

Overall, the visual trend analysis picture was not as sharp as that of the auditory. Specific auditory <--> visual paths (MF region association) could not be established. Contrary to the auditory paths, all the visual trends were associated with only one cross-modality MF, the Auditory Beta MF region.

Magnitude and phase trend paths were resolved with similar parameter significance levels. They were, however, defined by different primary parameters, and generally characterized by different priority and parameter level lists. The following trend assessment was therefore conducted separately for the magnitude and phase data.

8.5.2.1 Visual magnitude trends

Both magnitude trends ("+ M", "-M") were associated with Beta Auditory <--> Beta Visual MF regions path. Confirming the relative magnitude trend previously displayed in FIGURE III 8.3, inhibitory trends were more prominent than the facilitory trends (FIGURE III 8.12). Primarily determined by the Visual stimulus INTensity, inhibition and facilitation magnitude trends were associated with High and Low INTensity levels, respectively. Both trend peaks were independent of the Audio stimulus INTensity level.

8.5.2.2 Visual phase trends

Primarily determined by the Audio stimulus INTensity, lagging and leading phase trends were associated with Low and High INTensity levels, respectively. Within these INTensity levels, the trends were further enhanced by Beta and Theta Visual stimulus MFs, respectively. Both trend peaks were independent of the Audio stimulus MF.

STIMULUS PARAMETERS INDUCING THE VISUAL PEAK AxV TRENDS

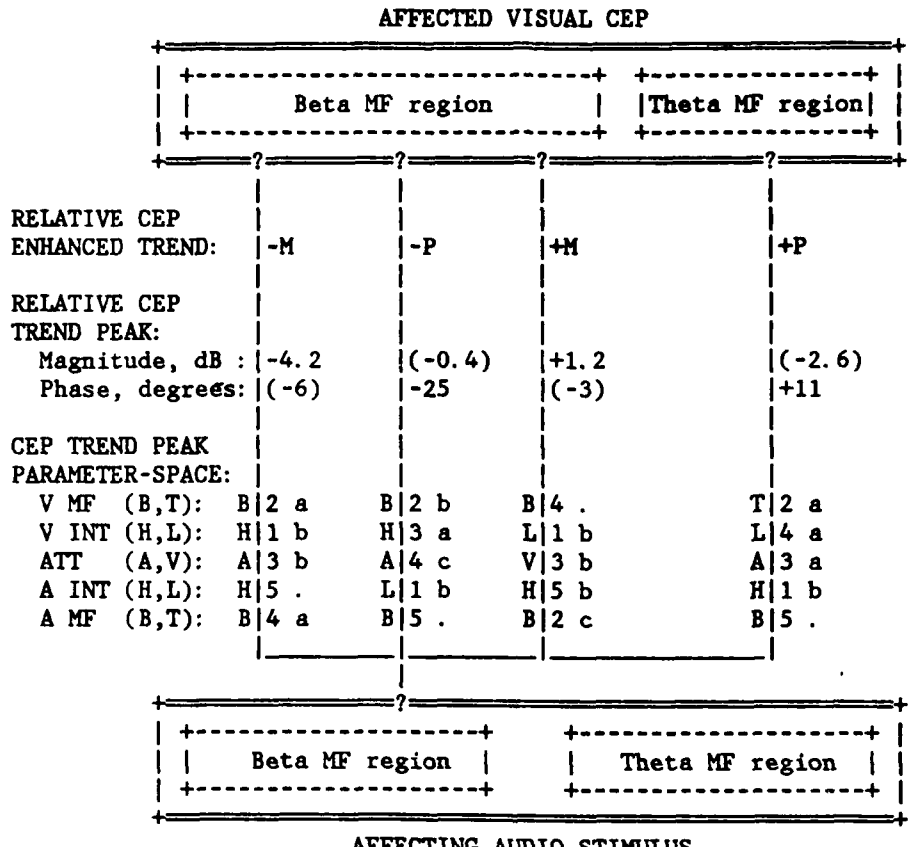


FIGURE III 8.12 : TREND ANALYSIS OF RELATIVE (BISENSORY-UNISENSORY) CEP MAGNITUDES (M) AND PHASES (P). EACH TREND-ENHANCING PATH WAS AFFECTED BY FIVE STIMULUS PARAMETERS AND DEFINED BY (LEFT TO RIGHT): PARAMETER LEVELS, PRIORITIES AND SIGNIFICANCES. KEY-CHARACTERS: AUDIO (A), VISUAL (V), MODULATION FREQUENCY (MF), INTENSITY (INT), BETA (B), THETA (T), HIGH (H), LOW (L), ATTENTION (ATT), "+"/-": POSITIVE/NEGATIVE BISENSORY-UNISENSORY TREND. PR>F SIGNIFICANCE LEVEL CODES: . > 0.5, a < 0.5, b < 0.1, c < 0.05, d < 0.01, e < 0.005, f < 0.001.

Chapter 9

Discussion of The Bisensory Evoked Potentials

Experiment

9.1 Data validity and reliability

The basic experimental unit of the Auditory-Visual Interaction (AxV) experiment was an absolute response vector (magnitude and phase of response obtained from the auditory or visual recording sites) of a single ORDER section (1st, 2nd, 3rd or NL sections, defined in TABLE III 8.1A). For the AxV data to be valid, the experimental units had to be "instrumentation-independent", intra-modality (between sequential ORDER sections) and inter-modality (between temporally-corresponding ORDER sections). The Lock-In Amplifier (LIA, PAR EG&G MOD: 5204) used in this study satisfied both requirements. With an averaged ORDER section duration of 35.6 sec and output Time-Constant (TC) of 10 sec, the LIA provided adequate temporal resolution and excellent frequency specificity. As indicated by the Noise Level (NL) magnitude results, the Continuous Evoked Potentials (CEPs) recorded in one modality were not

"instrumentationally" affected by intra- or inter-modality stimulus parameters (no significant SI * SIG, SI * SF, SI * SIG * SF and SF * CF effects TABLE III 8.2).

In analyzing the AxV results, it was assumed that the within-run CEP variations were exclusively invoked by the bimodal-unimodal-bimodal stimulation paradigm. This reasonable assumption could not be directly confirmed or refuted in this study. In a previously conducted pilot study, long records of unimodal auditory CEPs (longer than 90 sec) never revealed consistent magnitude trends, such as those described in FIGURE III 8.3. In any event, such a mysterious, unimodal significant trend, would have been much harder to explain without resorting to the AxV phenomenon.

9.2 Auditory and visual bisensory responses

9.2.1 Trend interpretation

Testing the effects of a two-level Independent Variable (IV, X and Y levels), it was impossible to determine whether, for example, X induced a positive trend, or Y (or the absence of X) induced a negative trend, or both. Without having a baseline reference, the ANOVA and trend analysis model the data and not necessarily the true underlying invoking system. For example, consider the auditory relative magnitude trends (FIGURE III 8.10) and their associated MF region latencies and delays (TABLE II 4.2). An "inverting" sensory stage between the two auditory MF regions' loci could have accounted for the observed, MF-dependent, sign inversion of the relative magnitude trends.

In any case, the ranges between the values of the positive and negative trend peaks indicated a solid AxV phenomenon. Within the investigated parameter-space, average ranges of 5.5 dB (relative magnitudes) and 40 degrees (relative phases) were obtained.

9.2.2 Trend detectability

Trend detectability in both ANOVA and trend analysis paradigms was a function of CEP Signal/Noise Ratio (SNR) and inter- and intra-subject variabilities. In comparison to the auditory, the visual response was characterized by higher CEP and lower NL absolute magnitudes (FIGURE III 8.3, legend), higher inter-subject variability (compensated and relative magnitudes and phases , FIGUREs III 8.3, 8.4, TABLEs III 8.3, 8.5, NAME effect) and lower intra-subject magnitude variability (DISC experiment, FIGURE II 5.2). The findings of this experiment, regarding the CEP SNR and inter-subject variability, matched those of the MTF experiment (section 4.4.2 and TABLE II 4.1).

All the above "features" should have, retrospectively, made the visual CEP a "preferred" vehicle for the AxV phenomenon. Instead, mixed relative magnitude and phase trends were obtained (FIGUREs III 8.10, 8.12). Phase-wise, visual paths were slightly more significant, but magnitude-wise, the auditory paths were much more significant and reliable. These results may indicate that the auditory magnitudes were more susceptible to cross-modal influence, and/or, the auditory recording site was closer to, or better oriented towards the AxV loci.

Some previous evidence has indicated that the AxV process was indeed best recorded from frontal and parietal, non-specific cortical areas (Walter, 1964; Lewis and Froning, 1981). Walter (1964) investigated the convergence of auditory, visual and tactile responses in the human non-specific cortex, recorded both from implanted microelectrodes and surface scalp electrodes. He found that signals in all studied modalities converged at the frontal cortex and were widely dispersed therein. Lewis and Froning (1981) recorded TEPs from F3,F4,T3,T4,P3,P4,O1,O2-nose/Pz in response to click and checkerboard pattern bimodal stimuli. They found a recording-site-dependent bisensory

"facilitation" in 150 msec latency magnitude components, maximized in TEPs recorded from more frontal recording sites ($F3,4 > T3,4 > P3,4$).

9.2.3 Magnitude and phase data comparison

The results of the ANOVA and trend analysis of both auditory and visual relative CEP data revealed that magnitude and phase information did not constructively complement each other (TABLE III 8.3, 8.5, FIGUREs III 8.10, 8.12). Within the investigated parameter-space, magnitude and phase trends differed in their origins. Furthermore, they were primarily defined by a different type ("Internal", "External") of effective IVs. Relative Phase trends were primarily defined by an "External" IV (CI effect in both auditory and visual trends). Relative magnitude trends were primarily defined by "Internal" IVs (SF and SI effects for the auditory and visual trends, respectively). These observations led to the following implications.

9.2.4 Modeling of the auditory-visual interaction process

Cross-modality averaged delay/latency estimations of Beta and Theta MF region CEPs were found to be 35/65 msec and 55/230 msec, respectively, suggesting different cortical sources of these potentials. Since phase variations induced by the cross-modality stimulus were unaffected by the MF region of the intra-modality stimulus and were uncoupled from the magnitude variations, a serially-connected, "Beta"- "Theta" cortical afferent system model could be deduced. In this model, the magnitude variation dependency on intra-modality parameters (i.e. the audio MF region) could imply the existence of selective, inter-sensory inhibitory pathways (negative feedbacks).

In this study, such an AxV-related CEP magnitude inhibition was associated with the shorter-latency, Beta MF region (FIGUREs III 8.10, 8.12). It is interesting to speculate on the source of this cross-sensory inhibition. Ciganek (1966) recorded TEPs in response

to click and flash bimodal stimuli with inter-modality intervals of 40-250 msec (flash lag). A consistent trend of reduced visual TEP magnitude components at 70-80 msec latency was associated with long (150-250 msec) inter-modality intervals. Morrell (1968) recorded TEPs in response to attended-to flash and click bimodal stimuli with inter-modality intervals of 20-120 msec (click lag). Reduced bisensory TEP magnitudes at 45-130 msec latency were associated with long inter-modality intervals (longer than 70-120 msec). These results may suggest that inhibition of "early" latency magnitude components was prompted by the cross-sensory, "late" evoked response region. If CEP and TEP studies are comparable, these "early" and "late" latencies could correspond to the estimated cross-modality averaged latencies of Beta (60-70 msec) and Theta (200-240 msec) MF regions, respectively. Consequently, the inhibitory effect on Beta MF magnitudes observed in this study might have originated from the cross-modality, late latency, Theta MF region neural system.

Part IV: Summary and Conclusions

Chapter 10

Summary and Conclusions

This chapter summarizes the major findings and conclusions obtained in pursuing the following research objectives: developing a Continuous Evoked Potential (CEP) research system utilizing the phase-lock technique, characterizing the auditory and visual unisensory responses and demonstrating an Auditory-Visual Interaction process (AxV) on a selective stimulus parameter-space. The specific AxV aspect investigated here was the dependency of single sensory channel CEP variations on cross- or inter-modality stimulus parameters.

1. Detectable stimulus-exclusive CEPs were obtained under the following experiment conditions: 68-108 dB SPL monaurally administered audio stimuli, 4-44 lux binocularly viewed visual stimuli, controlled subject attention, Cz-A1 (auditory) and Oz-A1 (visual) recording sites and 1-10 second Lock-In Amplifier (LIA) Time-Constant (TC) (section I 3.4). The CEP Signal/Noise Ratio (SNR) must be further enhanced to allow detection of CEPs, evoked by more tolerable and applicable stimuli level, within a similar 1-10 second acquisition time.

2. Within the 5-61 Hz Modulation Frequency (MF) range, magnitude peaks (magnitude range of 0.3-3 microvolt RMS, visual higher than auditory) were found at the following MF regions: 5-6 Hz ("Theta", most prominent peak in both modalities), 10.5 Hz ("Alpha", auditory CEP only), 16-25 Hz ("Beta", both modalities) and 50 Hz ("40 Hz", auditory CEP only) (FIGURE II 4.4). The visual CEP magnitude data of Alpha and Theta MF regions contradicted the results of other investigators. The differences were attributed to the effects of controlled subject attention and the driven-reference CEP recording method utilized in this study (section II 4.4.4).
3. Except for the Theta frequency region, similar EEG background activity (0.5-2 microvolt RMS, predominantly Alpha) was obtained from both auditory and visual recording sites. The higher auditory Theta EEG level was attributed to myogenic and other sources (FIGURE II 4.2). The dissimilarity between the EEG spectrums and the CEP Modulation Transfer Functions (MTFs) suggested the origin or source dissociation of these two phenomena.
4. Theta and Beta MF regions were further investigated in the DISC, INT and ATT experiments and employed in the AxV experiment. CEPs recorded from these MF regions were characterized by the following: consistent responses (magnitude peaks were detected in 75-85% of the Modulation Transfer Function (MTF) records, FIGURE II 4.11); evoked responses (CEP sources could not be modeled by the EEG equivalent filters, FIGUREs II 4.2, 4.4); modality compatible (similar magnitude and latency MF regions were identified in both modalities, FIGURE II 4.4, 4.9); response repeatability (a similar Beta/Theta CEP magnitude ratio was obtained in all the experiments); physiologically interpretable (meaningful CEP delay and latency estimations were obtained).

5. CEPs recorded in response to 100% modulation depth, sinusoidally amplitude-modulated signals were predominantly composed of the fundamental components (average 2nd/fundamental harmonic ratio of 0.43) (TABLE II 5.2). This harmonic ratio was obtained at the highest stimulus intensity ("0" dB) where the CEP fundamental magnitudes were saturated (FIGURE II 5.3). Based on these findings, it was concluded that the Beta and Theta MF region responses were predominantly linear.
6. Linear models of the Theta, Alpha, Beta and "40 Hz" MF regions (quadratic BPF or LPF models) were fitted to the CEP magnitude data. CEP delays and latencies were estimated from the phase plots of the models and CEP data in the vicinity of the transfer function peak frequencies. These models served to validate the physiological origins of the CEPs. In general, the higher magnitude visual CEPs were characterized by lower "Q" factor models, and longer and more reliable estimated delays (FIGURE II 4.10, TABLE II 4.2).
7. Delay and latency estimations of Beta MF region CEPs were 30-40 msec and 60-70 msec, respectively, suggesting the "secondary-sensory" cortical areas as the origin of these potentials. Theta MF region delay and latency estimations were 50-60 msec and 200-240 msec, respectively, suggesting multiple, secondary cortical area sources (section II 4.4.6). These results, indicating the cortical level as the plausible origins of the CEPs, generally agrees with previously published results. Since the sensory integration phenomena is more likely to be discovered at late evoked potentials (50-500 msec latency range), the CEPs recorded in this study might possibly reflect an AxV process.
8. Attention allocation significantly affected only the visual CEPs. Attended-to stimuli induced higher magnitude CEPs (FIGURE II 5.4, TABLE II 5.4). The inconclusiveness of the auditory results may be attributed to the well-saturated

- auditory CEP magnitudes, even at a -12 dB stimulus intensity level (see FIGURE II 5.3).
9. Regarding the intra-modality CEP variability, the visual response was characterized by higher CEP absolute magnitude and lower NL absolute magnitude (FIGURES II 4.4, III 8.3), higher SNR (section II 4.4.2 and FIGURE III 8.3, legend), higher inter-subject variability (TABLE II 4.1, SD measure; TABLES III 8.3, 8.5 NAME effect; FIGURES III 8.3, 8.5) and lower intra-subject magnitude variability (FIGURE II 5.2). All the above "features" should have, retrospectively, made the visual CEP a "preferred" vehicle for the AxV phenomenon. Nevertheless, both sensory channels exhibited an AxV process (difference between unimodal and bimodal responses).
10. Variations of CEPs recorded in one modality could reliably and physiologically be attributed to the cross-modal sensory channel activity (section III 9.1), validating the AxV experiment ad-hoc assumptions (section I 3.2). Within the investigated parameter-space, maximal bimodal-unimodal CEP differences of 5.5 dB magnitude-gain and 40 degrees phase-shift were attributed to the AxV phenomena (section III 9.2.1, FIGURES III 8.10, 8.12).
11. CEP magnitude inhibition and phase lag, attributed to the AxV process, were generally associated with, and induced by the short-latency, Beta MF regions. These inter-sensory mutual decrements were not, however, associated with a common parameter-space origin (the enhanced "-" trend in FIGURES III 8.10, 8.12). This phenomena could be interpreted as a "lateral inhibition" between sensory primary cortical areas.

12. In general, trend peaks of relative magnitude and phase data (bimodal-unimodal CEP response difference) were not concurrently induced or constructively complemented (TABLEs III 8.3, 8.4; FIGUREs III 8.10, 8.12; Section III 9.2.3). Magnitude data was primarily influenced by "Internal" parameters (intra-modality Stimulus Intensity or MF) and phase data by "External" parameters (Cross-modality stimulus Intensity). Surprisingly, subject attention allocation did not play a major role.
13. Cross-modality averaged delay/latency estimations of Beta and Theta MF region CEPs were found to be 35/65 msec and 55/230 msec, respectively, suggesting different cortical sources of these potentials. Since phase variations induced by the cross-modality stimulus were unaffected by the MF region of the intra-modality stimulus and were uncoupled from the magnitude variations, a serially-connected, "Beta"- "Theta" cortical afferent system model could be deduced. In this model, the magnitude variation dependency on intra-modality parameters could imply the existence of selective, inter-sensory inhibitory pathways (negative feedbacks).

The motivation for this research was to develop an evoked potential methodology for non-invasively monitoring the auditory and visual sensory channel engagement and interaction (AxV) in humans. Parameter-space characterization of the AxV process has never been attempted before. Results obtained in this investigatory study can be utilized in many existing disciplines and promote new research directions: providing further understanding of human sensory channel transfer functions and sensory information integration, investigating the unaccounted for intra-subject unisensory Event Related Cortical Potential (ERCP) variability by applying an exhaustive multisensory input stimulus, facilitating the effectiveness of audio-visual trainers, monitoring sensory channel engagement and alerting against overloading tasks that might deteriorate human-

operator performance, and designing more effective and efficient man-machine communication channels.

This study is a necessary first step in fulfilling the above desired goals. Presently, an integrative sensory-system model needs to be formulated and the dependency between evoked potential and behavior outcomes must be established.

REFERENCES

- Andreassi, J.L. and Greco, J.R. Effects of bisensory stimulation on reaction time and the evoked cortical potential. Physiol. Psychol. 3(2):189-194, 1975.
- Aunon, J.I. and Sencaj, R.W. Comparison of different techniques for processing evoked potentials. Med. & Biol. Eng. & Comput. 16:642-650, 1978.
- Celesia, G.G. Organization of auditory cortical areas in man. Brain. 99:403-414, 1976.
- Childers, D.G. Evoked responses: Electrogenesis, models, methodology and wavefront reconstruction and tracking analysis. Proc. I.E.E.E. 65(5):611-626, 1977.
- Childers, D.G. and Perry, N.W. Alpha-like activity in vision. Review. Brain Res. 25:1-20, 1971.
- Childers, D.G., Bloom, P.A., Arroyo, A.A., Roucos, S.E., Fischler, I.S., Achariyapaopan, T. and Perry, N.W., Jr. Classification of cortical responses using features from single EEG records. I.E.E.E. Trans. Biomed. Eng. BME-29(6):423-438, 1982.
- Ciganek, M.D. Evoked potentials in man: Interaction of sound and light. Electroenceph. Clin. Neurophysiol. 21:28-33, 1966.
- Davis, H., Osterhammel, P.A., Wier, C.C. and Gjerdingen, D.B. Slow vertex potentials: Interactions among auditory, tactile electric and visual stimuli. Electroenceph. Clin. Neurophysiol. 33:537-545, 1972.
- Diamond, A.L. Latency of the steady state visual evoked potentials. Electroenceph. Clin. Neurophysiol. 42:125-127, 1977.
- Donchin, E. and Cohen, M.D. Averaged evoked potentials and intramodality selective attention. Electroenceph. Clin. Neurophysiol. 22:537-546, 1967.
- Erickson, R.P. Parallel 'population' neural coding in feature extraction. In: Schmitt, F.O., Worden, F.G. (Eds.), The Neurosciences: Third Study Program. Cambridge, Massachusetts and London, England: The MIT Press, 1974.

- Euler, M. and Kiessling, J. Frequency-following potentials in man by lock-in technique. Electroenceph. Clin. Neurophysiol. 52:400-404, 1981.
- Fagan, J.E. Jr., Allen, R.G., and Yolton, R.L. Factors contributing to amplitude variability of the steady-state evoked response. Am. J. Optom. & Physiol. Optics. 61(7):453-464, 1984.
- Ford, G.M. , Roth, W.T., Dirks, S.J. and Kopell, B.S. Evoked potentials correlates of signal recognition between and within modalities. Science 181:465-466, 1973.
- Galambos, R., Makeig, S. and Talmachoff, P.J. A 40-Hz auditory potential recorded from the human scalp. Proc. Natl. Acad. Sci. 78(4):2643-2647, 1981.
- Galambos, R. Tactile and auditory stimuli repeated at high rates (30-50 per sec) produce similar event related potentials. Ann. NY. Acad. Sci. 388:722-728, 1982.
- Gebhard, J.W., and Mowbray, G.H. On discriminating the rate of visual flicker and auditory flutter. Am. J. Psychol. 72:521-529, 1959.
- Gevins, A.S. Pattern recognition of human brain electrical activity. I.E.E.E. Trans. Pattern Analysis and Machine Intelligence. 2(5):383-404, 1980.
- Goff, W.R., Allison, T. and Vaughan, H.G., Jr. The functional neuroanatomy of event related potentials. In: Event-Related Brain Potentials in Man Callaway, E., Tueting, P. and Koslow, S.H. (Eds.), Academic Press, New York, San Francisco, London, 1978.
- Hartley, L.R. The effect of stimulus relevance on the cortical evoked potentials. Q. J. Exp. Psychol. 22:531-546, 1970.
- Hillyard, S.A., Picton, T.W. and Regan, D. Sensation, perception and attention: analysis using ERPs. In: Event-Related Brain Potentials in Man Callaway, E., Tueting, P. and Koslow, S.H. (Eds.), Academic Press, New York, San Francisco, London, 1978.
- Horst, R.L. and Donchin, E. Beyond averaging.II.Single trial classification of exogenous event-related potentials using stepwise discriminant analysis. Electroenceph. Clin. Neurophysiol. 48:113-126, 1980.
- Junker A.M. Personal communication. 1984.
- Junker, A.M. and Peio, K.J. In search of visual-cortical describing function. A summary of work in progress. Proc. of 20th Ann. Conf. on Manual Control. NASA conf. publication 2341, Vol II: 37-54, 1984.
- Jasper, H.H. The ten-twenty electrode system of the International Federation. Electroenceph. Clin. Neurophysiol. 10:371-375, 1958.
- Kaufman, L. and Price, R. The detection of cortical spike activity at the human scalp. I.E.E.E. Trans. Biomed. Eng. BME-14(2):84-90, 1967.
- Kay, R.H. Hearing of modulation in sounds. Physiological Reviews. 62(3):894-975, 1982.

- Knox, G.W. Investigation of flicker and fusion: IV. The effect of auditory flicker on the pronouncedness of visual flicker. J. Gen. Psychol. 33:145-154, 1945.
- Koles, Z.J. and Flor-Henry, P. Mental activity and the E.E.G.: Task and workload related effects. Med. & Biol. Eng. & Comput. 19:185-194, 1981.
- Levine, D.A., Elashoff, R., Callaway III, E., Payne, D. and Jones, R.T. Evoked potential analysis by complex demodulation. Electroenceph. Clin. Neurophysiol. 32:513-520, 1972.
- Levison, W.H., Junker, A.M. and Kenner K. Descriptive linear modeling of steady-state visual evoked response. Proc. of 21st Ann. Conf. on Manual Control. Ohio state U., Columbus, Ohio 17-19, 1985.
- Lewis, G.W. and Froning, J.N. Sensory interaction, brain activity, and reading ability in young adults. Intern. J. Neuroscience. 15:129-140, 1981.
- Loveless, N.E., Brebner J. and Hamilton P. Bисensory presentation of information. Psychol. Bull. 73(3):161-199, 1970.
- Maruyama, K. Effect of intersensory tone stimulation on absolute light threshold. Tohko. Psychol. Folia. 17:51-81, 1959.
- Maruyama, K. Contralateral relationship between the ears and the halves of the visual field in sensory interaction. Tohko. Psychol. Folia. 19:81-92, 1961.
- McGillem, C.D. and Aunon, J.I. Measurements of signal components in single visually evoked brain response. I.E.E.E. Trans. Biomed. Eng. BME-24(3):232-241, 1977.
- McGillem, C.D. and Aunon, J.I. New Techniques for Measuring Single Brain Potentials Air Force Office of Scientific Research (NL), Report Number AFOSR-TR-82-0901, TR-EE 83-51, 1983.
- McGillem, C.D. and Aunon, J.I. Detection, Estimation, and Multidimensional Processing of Single Evoked Potentials Air Force Office of Scientific Research (NL), Report Number AFOSR-F49620-83-1C-0031, 1985.
- Moise, S.L., Jr. Development of Neurophysiological and Behavioral Metrics of Human Performance Report Number AFAMRL-TR-80-39, Brain Research Institute, U. of California, Los Angeles, California, 1980.
- Moise, S.L., Jr. An Investigation of the Use of Steady-State Evoked Potentials for Human Performance and Workload Assessment and Control Air Force Office of Scientific Research, Final Report for Contract F49620-83-C-0102, 1985.
- Morrell, L.K. Sensory interaction: Evoked potential observations in man. Exp. Brain. Res. 6:146-155, 1968.
- Nelson, J.I., Seiple, W.H., Kupersmith, M.J. and Carr, R.E. Lock-in techniques for the swept stimulus evoked potential. J. Clin. Neurophysiol. 1(4):409-436, 1984.
- Oglove, J.C. Effect of auditory flutter on the visual critical flicker frequency. Can. J. Psychol. 10:61-68, 1956.

- Perry, N.W. and Childers, D.G. The Human Visual Evoked Response Charles C. Thomas (Publishers), Springfield Illinois, U.S.A., 1961.
- Rees, A. Neurophysiological Aspects of Frequency and Amplitude Modulated Sound Analysis Ph.D. Thesis, Oxford, 1981.
- Regan, D. Some characteristics of steady-state and transient responses evoked by modulated light. Electroenceph. Clin. Neurophysiol. 20:238-248, 1966.
- Regan, D. Evoked Potentials in Psychology, Sensory Physiology and Clinical Medicine Chapman and Hall Ltd. London, 1972.
- Regan, D. Steady-state evoked potentials. J. Opt. Soc. Am. 67(11):1475-1489, 1977.
- Regan, D. Comparison of transient and steady-state methods. Ann. NY. Acad. Sci. 388:45-71, 1982.
- Regan, D. and Cartwright, R.F. A method of measuring the potentials evoked by simultaneous simulation of different retinal regions. Electroenceph. Clin. Neurophysiol. 28:314-319, 1970.
- Regan, D. and Spekreijse, H. Auditory-visual interactions and the correspondence between perceived auditory space and perceived visual space. Perception 6:133-138, 1977.
- Reits, D. Cortical Potential in Man Evoked by Noise Modulated Light Ph.D. Thesis, U. of Utrecht, 1975.
- Rickards, F.W. and Clark, G.M. Steady state evoked potentials to amplitude-modulated tones. In: Evoked Potentials II. The Second International Evoked Potentials Symposium. Nodar, R.H. and Barber, C. (Eds.), Butterworth Publishers, Boston, 1984.
- Rodenburg, M., Verweij, C. and van den Brink, G. Analysis of evoked responses in man elicited by sinusoidally modulated noise. Audiology 11:283-289, 1972.
- Schechter, G. and Buchsbaum M. The effects of attention and individual differences on the average evoked potentials. Psychophysiol. 10(4):392-340, 1973.
- Sencaj, R.W., Aunon, J.I. and McGillem, C.D. Discrimination among visual stimuli by classification of their evoked potentials. Med. & Biol. & Eng. & Comput. 17:391-396, 1979.
- Smith, W.M. Visual recognition: facilitation of seeing by hearing. Psychonomics Science. 2:157-158, 1965.
- Spekreijse, H. Analysis of EEG Response in Man (Evoked by sine wave modulated light), Dr. W. Junk Publishers, The Hague, 1966.
- Spekreijse, H., Estevez, O. and Reits, D. Visual evoked potentials and the physiological analysis of visual processes in man. In: Visual Evoked Potentials in Man: New Developments Desmedt, J.E. (Ed.), Clarendon Press, Oxford, 1977.

- Spekreijse, H. and Reits D. Sequential analysis of the visual evoked potential system in man; nonlinear analysis of a sandwich system. Ann. NY. Acad. Sci. 388:72-97, 1982.
- Squires, Q.C. and Donchin E. Beyond averaging: The use of discriminant functions to recognize event related potentials elicited by single auditory stimuli. Electroenceph. Clin. Neurophysiol. 41:449-459, 1976.
- Squires, N.K., Donchin, E., Squires, K.C. and Grossberg S. Bisensory stimulation: Inferring decision related processes from the P300 component. J. Ex. Psychol.: Hum. Percep. Perform. 33:299-315, 1977.
- Stapells, D.R., Linden, D., Suffield, J.B., Hamel G. and Picton, T.W. Human auditory steady state potentials. Ear and Hearing 5(2):105-113, 1984.
- Sterman, N.B. Measurement and Modification of Sensory System EEG Characteristics During Visual-Motor Performance Air Force Office of Scientific Research (NL), Contract/Grant Number AFOSR 82-0335, 1984.
- Sterrit, G.M., Camp, B.W. and Lipman, B.S. Effects of early auditory deprivation upon auditory and visual information processing. Percept. Motor. Skills. 23:123-130, 1966.
- Sumby, W.H. and Pollack, I. Visual contribution to speech intelligibility in noise. J. Acoust. Soc. Am. 26:212-215, 1954.
- van der Tweel, L.H. and verduyn Lunel, H.F.E. Human visual responses to sinusoidally modulated light. Electroenceph. Clin. Neurophysiol. 18:587-598, 1965.
- Vaughan, H.G., Jr. The neural origins of human event-related potentials. Ann. NY. Acad. Sci. 338:125-138, 1982.
- Vidal, J.J. Real-time detection of brain events in EEG. Proc. I.E.E.E. 65(5):633-641, 1977.
- Walsh, J.K. Evoked brain responses to auditory and visual stimuli of equal subjective magnitude. Percep. & Psychophysics. 26(5):396-402, 1979.
- Walter, W.G. The convergence and interaction of visual, auditory, and tactile responses in human nonspecific cortex. Ann. NY. Acad. Sci. 112:320-361, 1964.
- de Weerd, J.P.C. A posteriori time-varying filtering of averaged evoked potentials. Biol. Cybern. 41:211-222, 1981.
- de Weerd, J.P.C. and Kap, J.I. A posteriori time-varying filtering of averaged evoked potentials. Biol. Cybern. 41:223-234, 1981.
- Wilson, G.F. and O'Donnell, R.D. Human Sensitivity to High Frequency Sine Wave and Pulsed Light Stimulation as Measured by The Steady State Cortical Evoked Response Air Force Aerospace Medical Research Laboratory, Report Number AFAMRL-TR-80-133, 1981.

Wood, C.C. and Wolpaw, J.R. Scalp distribution of human auditory potentials. II. Evidence for overlapping sources and involvement of auditory cortex. Electroenceph. Clin. Neurophysiol. 54:25-38, 1982.

Yolton, R.L., Allen, R.G., Goodsin, R.A., Schaefer, D.L. and Decker, W.D. Amplitude variability of the steady-state visual evoked response (VER). Am. J. Optom. & Physiol. Optics. 60(8):694-704, 1983.

GENERAL REFERENCES

Begleiter, H. (Ed.) Evoked Brain Potentials and Behavior Plenum Press. New York and London, 1979.

Callaway, E., Tueting, P. and Koslow, S. Brain Event-Related Potentials in Man New York: Academic Press, 1978.

Desmedt, J.E. (Ed.) Attention, Voluntary Contraction and Event Related Cerebral Potential Basel; Munich; Paris; London; New York; Sydney: S. Karger, 1977.

Jung, R. (Ed.) Central Processing of Visual Information A: Integrative Functions and Comparative Data from Handbook of Sensory Physiology Series, Springer-Verlag: Berlin, Heidelberg, New York, 1973.

Keidel, W.D. and Neff, W.D. (Eds.) Auditory System: Anatomy Physiology (Ear) from Handbook of Sensory Physiology Series, V/1, Springer-Verlag: Berlin, Heidelberg, New York, 1974.

Masterton, R.B. (Ed.) Sensory Integration Plenum Press, 1978.

Walsh, L.W.T. Photometry Constable & Company LTD (Publisher), London, 1953.

Appendix A. Summary of Individual Responses

SUMMARY OF INDIVIDUAL RESPONSES

NAME=AM SIG=AUDIO

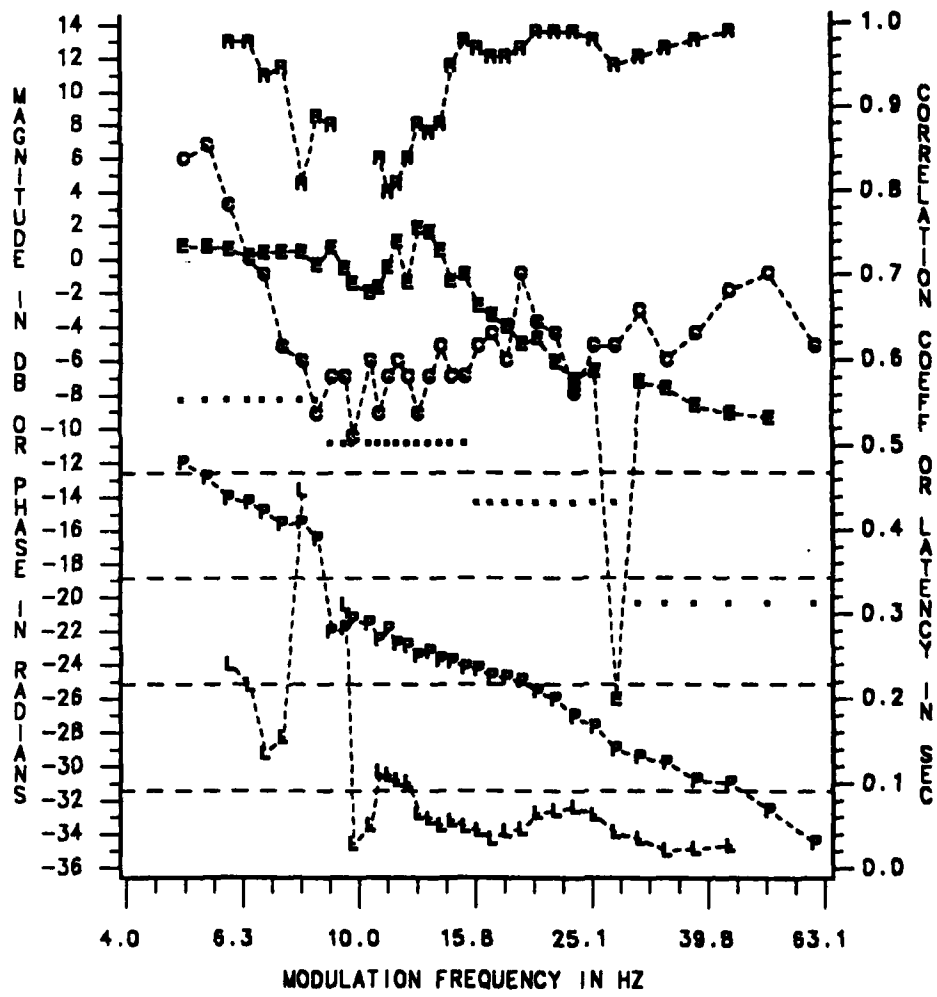


FIGURE II 4.11 : RECORDED FROM CZ-A1 (AUDIO) AND OZ-A1 (VISUAL) SITES. CEP(C),
EEG(E), AND NOISE LEVEL (DOTTED LINE) MAGNITUDES IN DB. CEP
PHASE(P) IN RADIANS, LATENCY(L) IN SEC AND LATENCY RELIABILITY
(R, 1 IS THE HIGHEST, ONLY R>0.71 VALUES ARE DISPLAYED).
L (REGRESSION COEFF/6.29) AND R (CORRELATION COEFF) VALUES
WERE ESTIMATED FROM A 5 PHASE-POINT-WIDE SLIDING WINDOW.

SUMMARY OF INDIVIDUAL RESPONSES

NAME=AM SIG=VISUAL

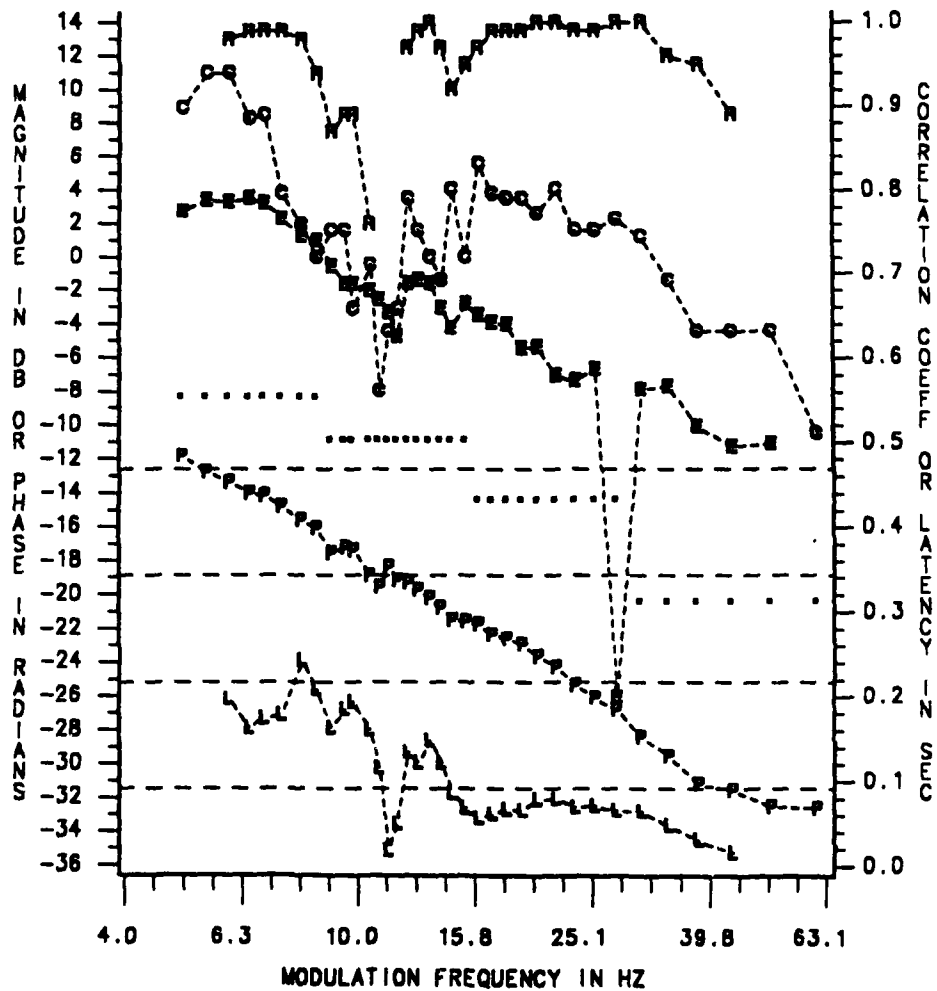


FIGURE II 4.11 : RECORDED FROM CZ-A1 (AUDIO) AND OZ-A1 (VISUAL) SITES. CEP(C), EEG(E), AND NOISE LEVEL (DOTTED LINE) MAGNITUDES IN DB. CEP PHASE(P) IN RADIANS, LATENCY(L) IN SEC AND LATENCY RELIABILITY (R, 1 IS THE HIGHEST, ONLY R>0.71 VALUES ARE DISPLAYED). L (REGRESSION COEFF/6.28) AND R (CORRELATION COEFF) VALUES WERE ESTIMATED FROM A 5 PHASE-POINT-WIDE SLIDING WINDOW.

SUMMARY OF INDIVIDUAL RESPONSES

NAME=CR SIG=AUDIO

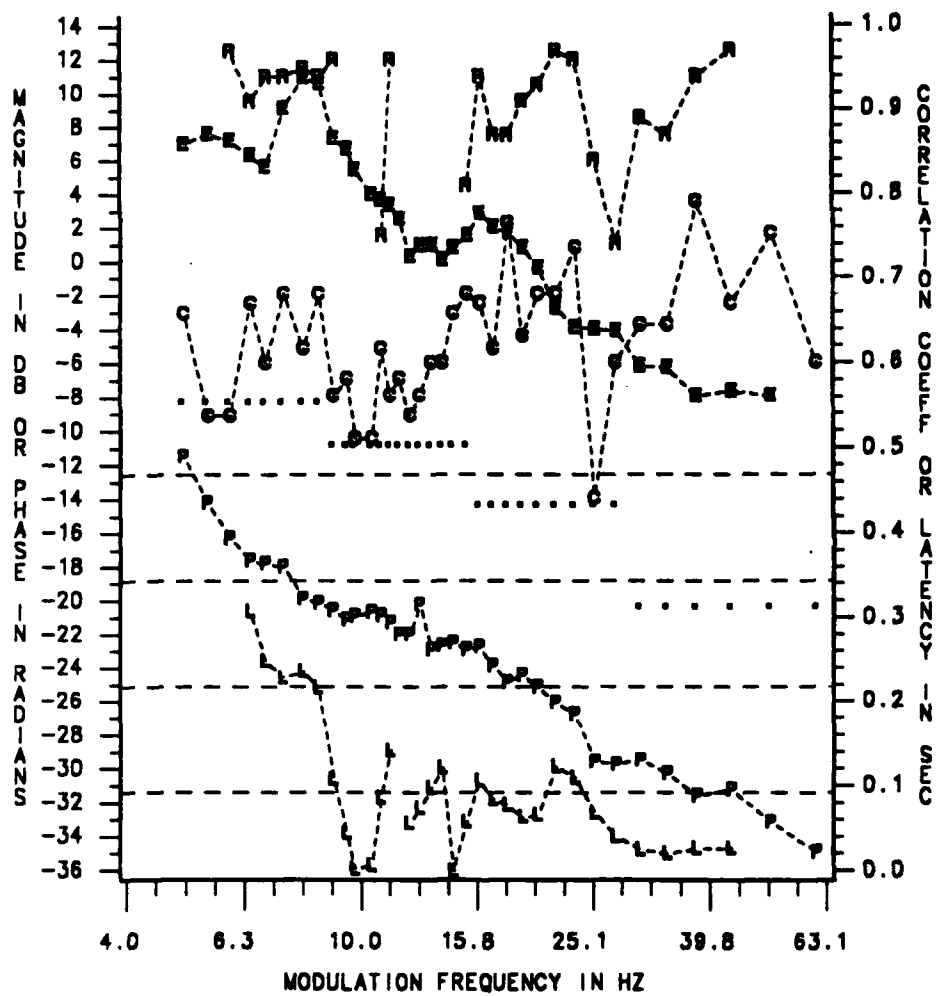


FIGURE II 4.11 : RECORDED FROM CZ-A1 (AUDIO) AND OZ-A1 (VISUAL) SITES. CEP(C),
EEG(E), AND NOISE LEVEL (DOTTED LINE) MAGNITUDES IN DB. CEP
PHASE(P) IN RADIANS, LATENCY(L) IN SEC AND LATENCY RELIABILITY
(R, 1 IS THE HIGHEST, ONLY R>0.71 VALUES ARE DISPLAYED).
L (REGRESSION COEFF/0.29) AND R (CORRELATION COEFF) VALUES
WERE ESTIMATED FROM A 6 PHASE-POINT-WIDE SLIDING WINDOW.

SUMMARY OF INDIVIDUAL RESPONSES

NAME=CR SIG=VISUAL

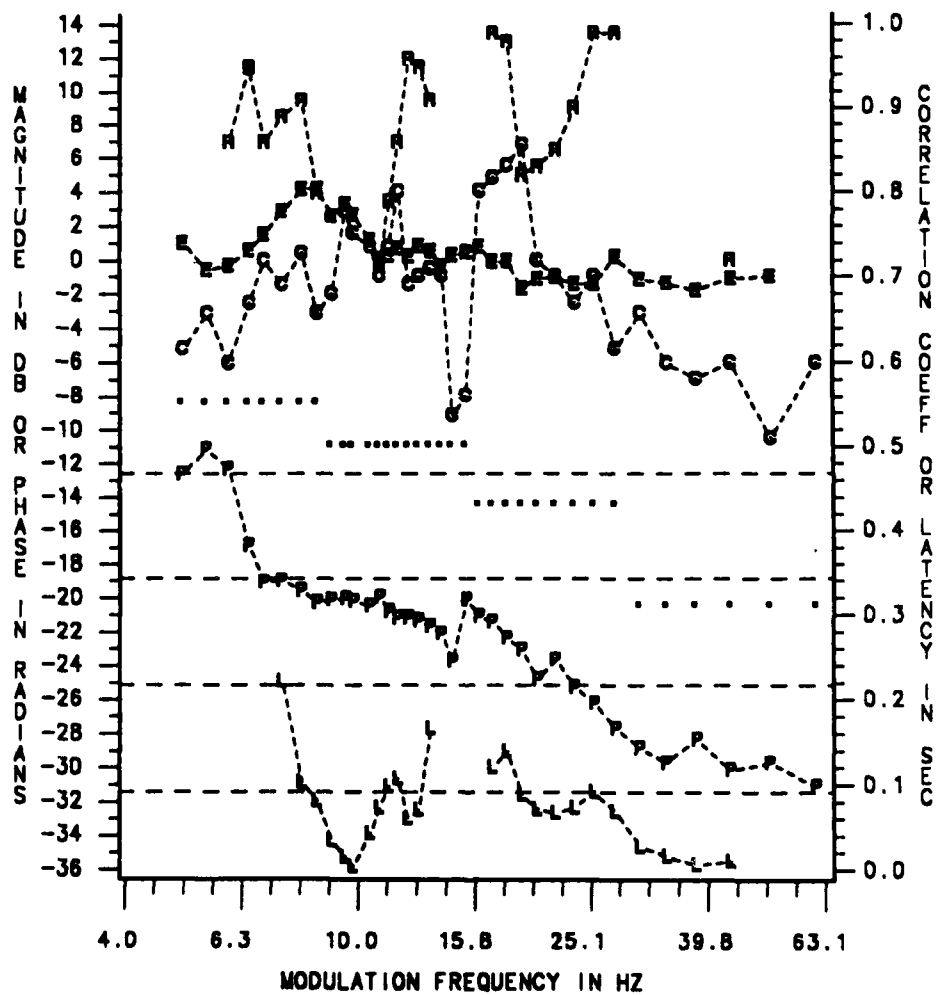


FIGURE II 4.11 : RECORDED FROM CZ-A1 (AUDIO) AND OZ-A1 (VISUAL) SITES. CEP(C),
 KEP(E), AND NOISE LEVEL (DOTTED LINE) MAGNITUDES IN DB. CEP
 PHASE(P) IN RADIANS, LATENCY(L) IN SEC AND LATENCY RELIABILITY
 (R, 1 IS THE HIGHEST, ONLY R>0.71 VALUES ARE DISPLAYED).
 L (REGRESSION COEFF/6.29) AND R (CORRELATION COEFF) VALUES
 WERE ESTIMATED FROM A 5 PHASE-POINT-WIDE SLIDING WINDOW.

SUMMARY OF INDIVIDUAL RESPONSES

NAME=EW SIG-AUDIO

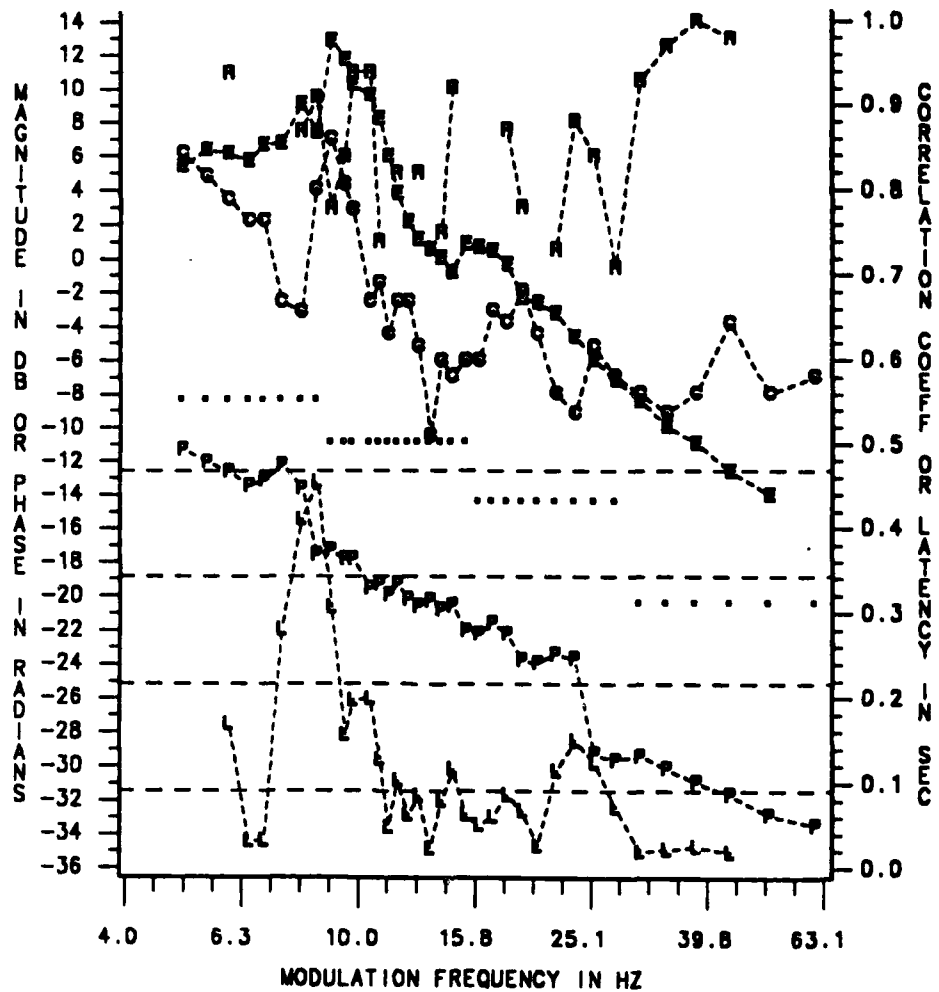


FIGURE II 4.11 : RECORDED FROM CZ-A1 (AUDIO) AND OZ-A1 (VISUAL) SITES. CEP(C),
EEG(E), AND NOISE LEVEL (DOTTED LINE) MAGNITUDES IN DB. CEP
PHASE(P) IN RADIANS, LATENCY(L) IN SEC AND LATENCY RELIABILITY
(R, 1 IS THE HIGHEST, ONLY R>0.71 VALUES ARE DISPLAYED).
L (REGRESSION COEFF/6.29) AND R (CORRELATION COEFF) VALUES
WERE ESTIMATED FROM A 5 PHASE-POINT-WIDE SLIDING WINDOW.

SUMMARY OF INDIVIDUAL RESPONSES

NAME=EW SIG=VISUAL

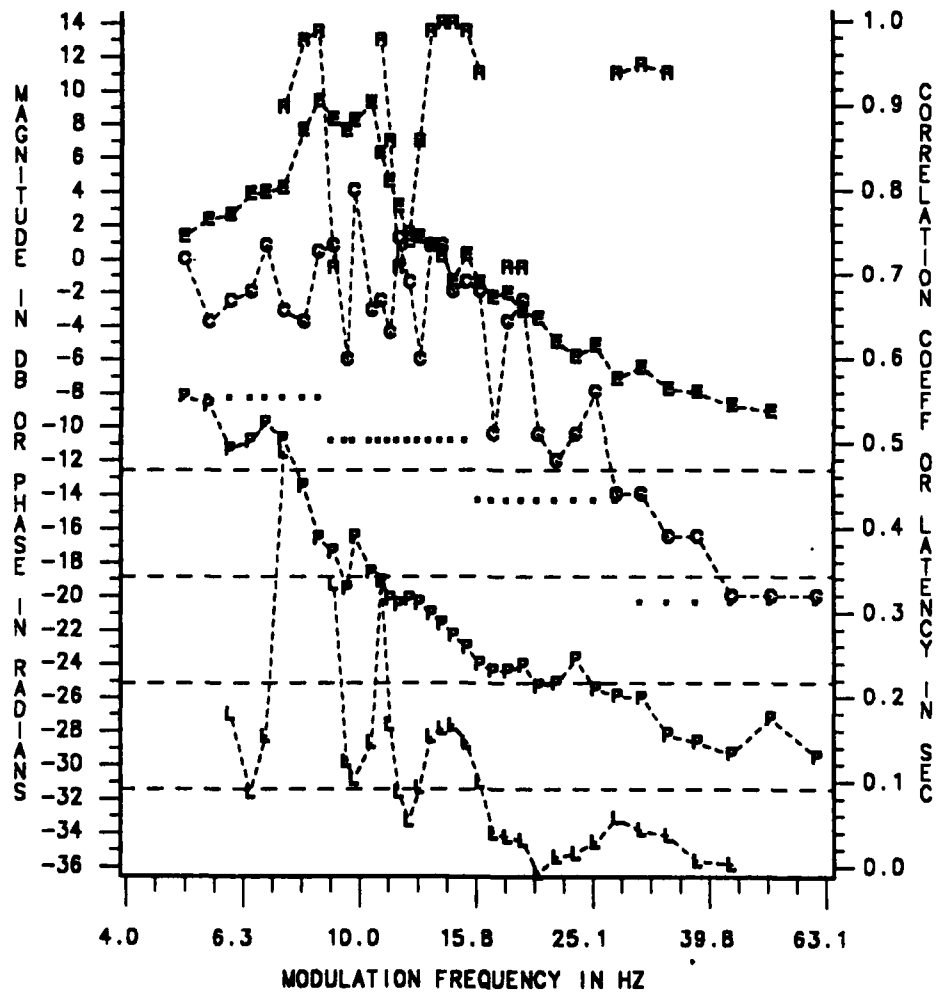


FIGURE II 4.11 : RECORDED FROM CZ-A1 (AUDIO) AND OZ-A1 (VISUAL) SITES. CEP(C),
EEG(E), AND NOISE LEVEL (DOTTED LINE) MAGNITUDES IN DB. CEP
PHASE(P) IN RADIANS, LATENCY(L) IN SEC AND LATENCY RELIABILITY
(R, 1 IS THE HIGHEST, ONLY R>0.71 VALUES ARE DISPLAYED).
L (REGRESSION COEFF/8.29) AND R (CORRELATION COEFF) VALUES
WERE ESTIMATED FROM A 5 PHASE-POINT-WIDE SLIDING WINDOW.

SUMMARY OF INDIVIDUAL RESPONSES
NAME=KC SIG=AUDIO

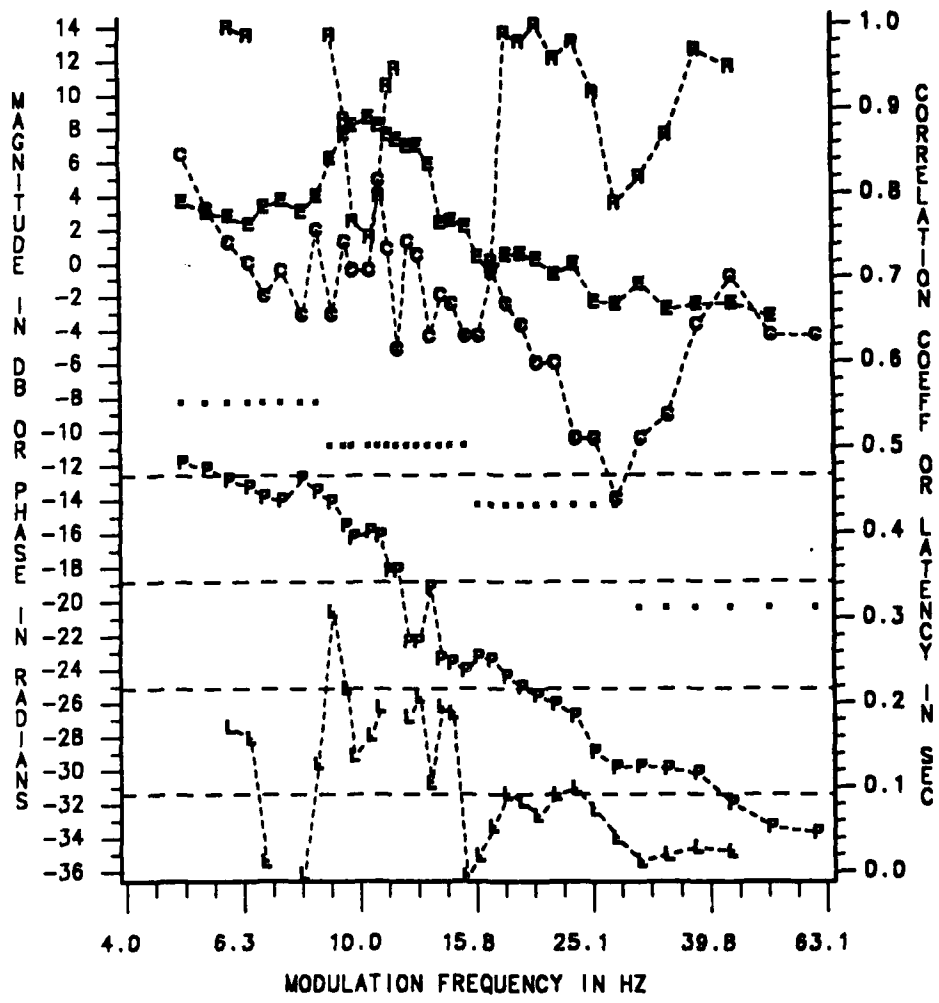


FIGURE II 4.11 : RECORDED FROM CZ-A1 (AUDIO) AND OZ-A1 (VISUAL) SITES. CEP(C),
EEG(E), AND NOISE LEVEL (DOTTED LINE) MAGNITUDES IN DB. CEP
PHASE(P) IN RADIANS, LATENCY(L) IN SEC AND LATENCY RELIABILITY
(R, 1 IS THE HIGHEST, ONLY R>0.71 VALUES ARE DISPLAYED).
L (REGRESSION COEFF/6.29) AND R (CORRELATION COEFF) VALUES
WERE ESTIMATED FROM A 5 PHASE-POINT-WIDE SLIDING WINDOW.

SUMMARY OF INDIVIDUAL RESPONSES

NAME=KC SIG=VISUAL

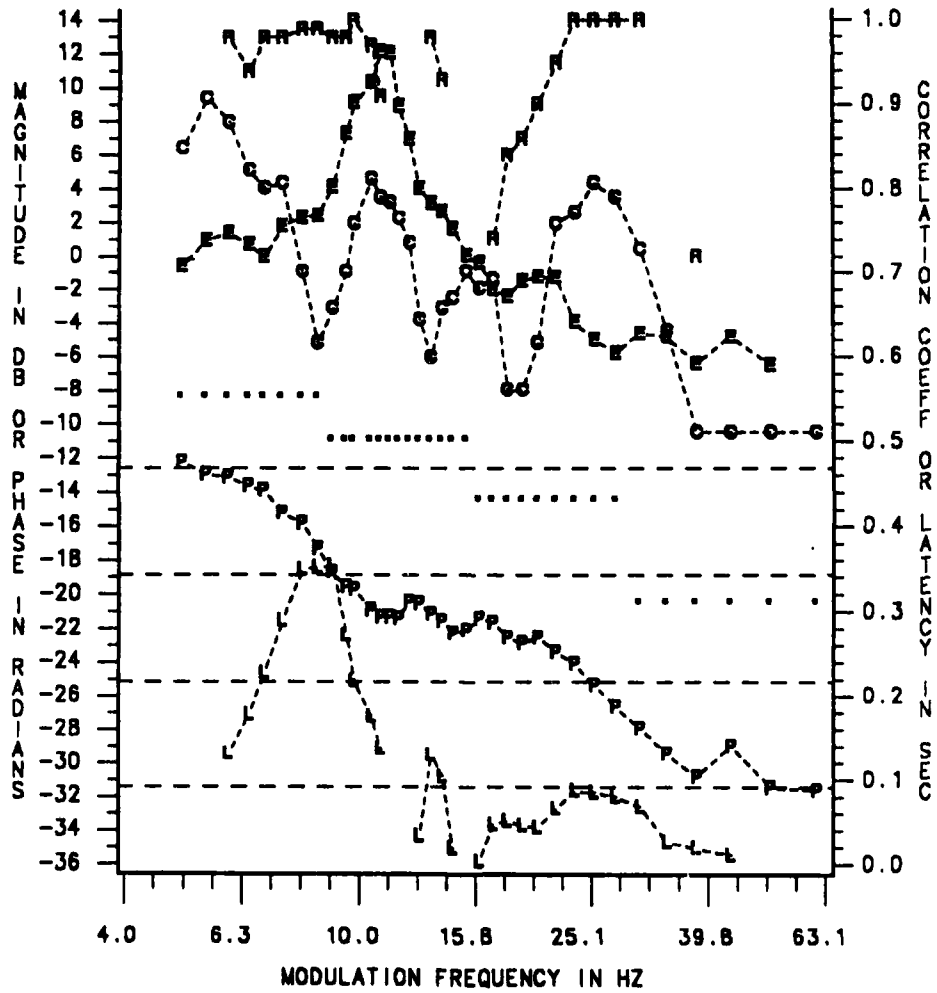


FIGURE II 4.11 : RECORDED FROM CZ-A1 (AUDIO) AND OZ-A1 (VISUAL) SITES. CEP(C), EEG(E), AND NOISE LEVEL (DOTTED LINE) MAGNITUDES IN DB. CEP PHASE(P) IN RADIANS, LATENCY(L) IN SEC AND LATENCY RELIABILITY (R, 1 IS THE HIGHEST, ONLY R>0.71 VALUES ARE DISPLAYED). L (REGRESSION COEFF/8.29) AND R (CORRELATION COEFF) VALUES WERE ESTIMATED FROM A 5 PHASE-POINT-WIDE SLIDING WINDOW.

SUMMARY OF INDIVIDUAL RESPONSES

NAME=MR SIG=AUDIO

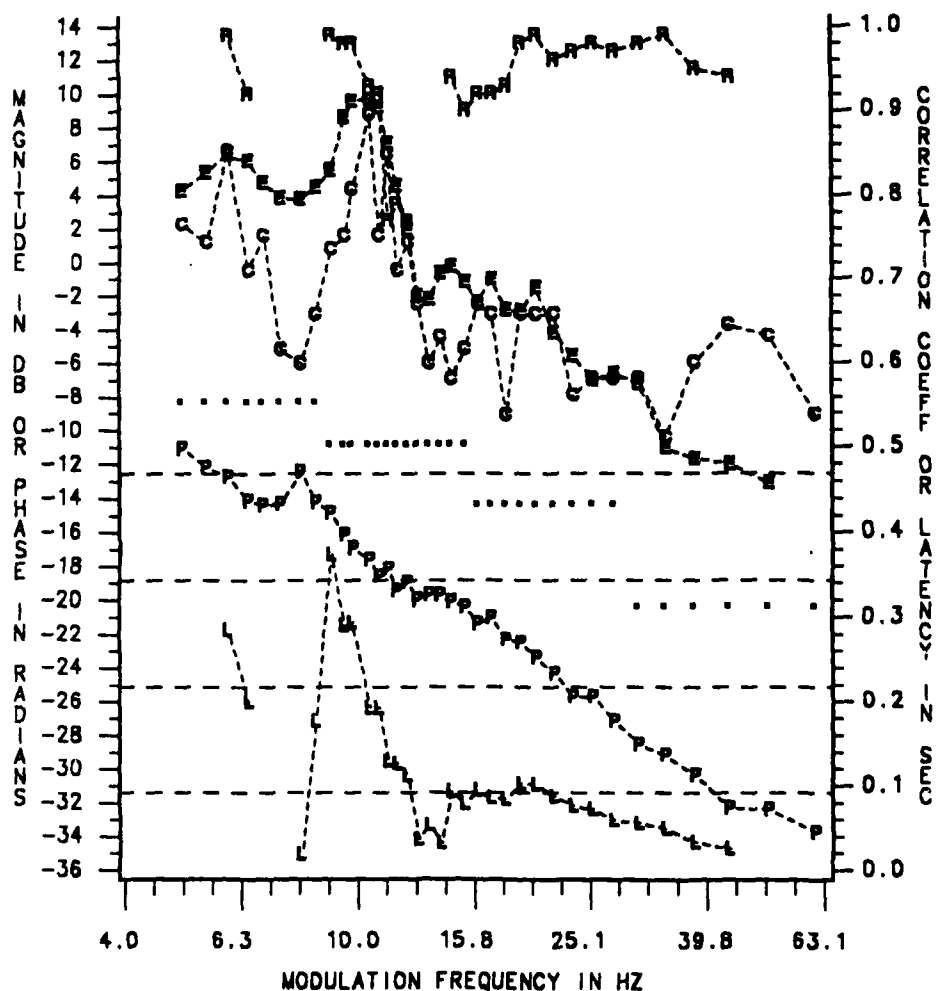


FIGURE II 4.11 : RECORDED FROM CZ-A1 (AUDIO) AND OZ-A1 (VISUAL) SITES. CEP(C),
EEG(E), AND NOISE LEVEL (DOTTED LINE) MAGNITUDES IN DB. CEP
PHASE(P) IN RADIAN, LATENCY(L) IN SEC AND LATENCY RELIABILITY
(R, 1 IS THE HIGHEST, ONLY R>0.71 VALUES ARE DISPLAYED).
L (REGRESSION COEFF/6.29) AND R (CORRELATION COEFF) VALUES
WERE ESTIMATED FROM A 5 PHASE-POINT-WIDE SLIDING WINDOW.

SUMMARY OF INDIVIDUAL RESPONSES

NAME=MR SIG=VISUAL

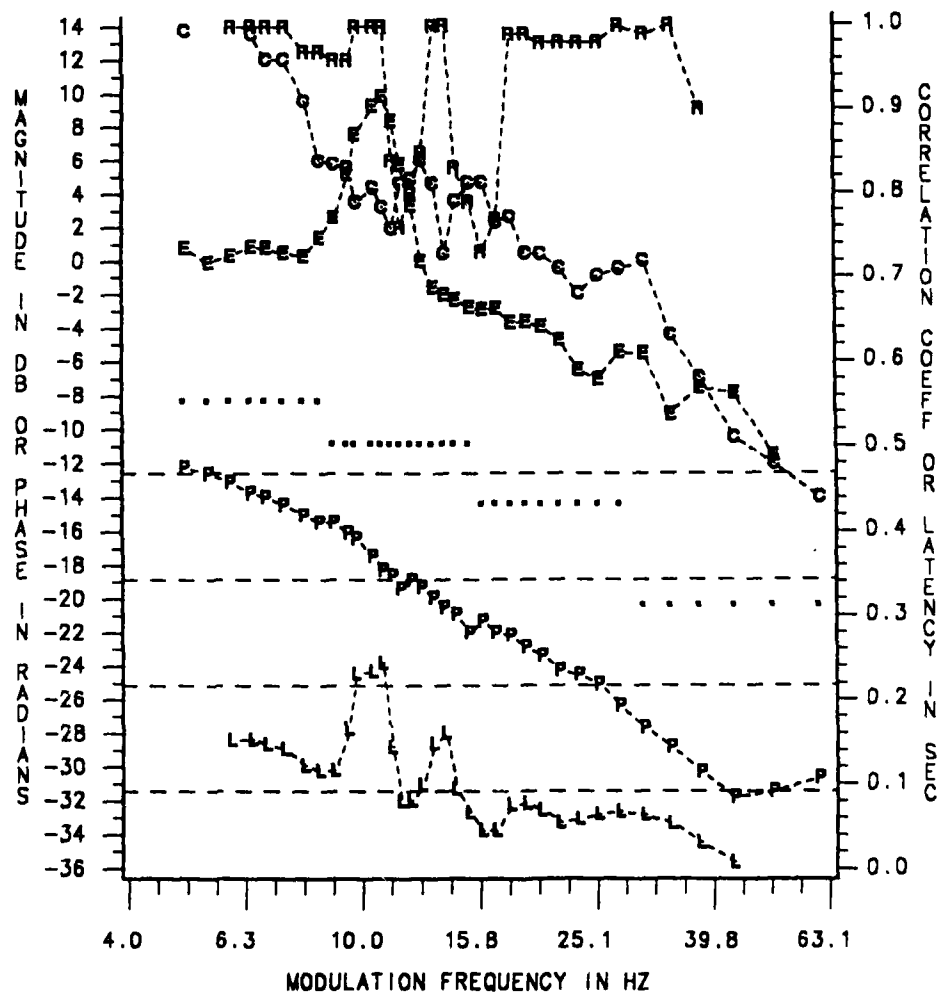


FIGURE II 4.11 : RECORDED FROM CZ-A1 (AUDIO) AND OZ-A1 (VISUAL) SITES. CEP(C), EEG(E), AND NOISE LEVEL (DOTTED LINE) MAGNITUDES IN DB. CEP PHASE(P) IN RADIANS, LATENCY(L) IN SEC AND LATENCY RELIABILITY (R, 1 IS THE HIGHEST, ONLY $R > 0.71$ VALUES ARE DISPLAYED). L (REGRESSION COEFF/6.29) AND R (CORRELATION COEFF) VALUES WERE ESTIMATED FROM A 5 PHASE-POINT-WIDE SLIDING WINDOW.

SUMMARY OF INDIVIDUAL RESPONSES

NAME=PM SIG=AUDIO

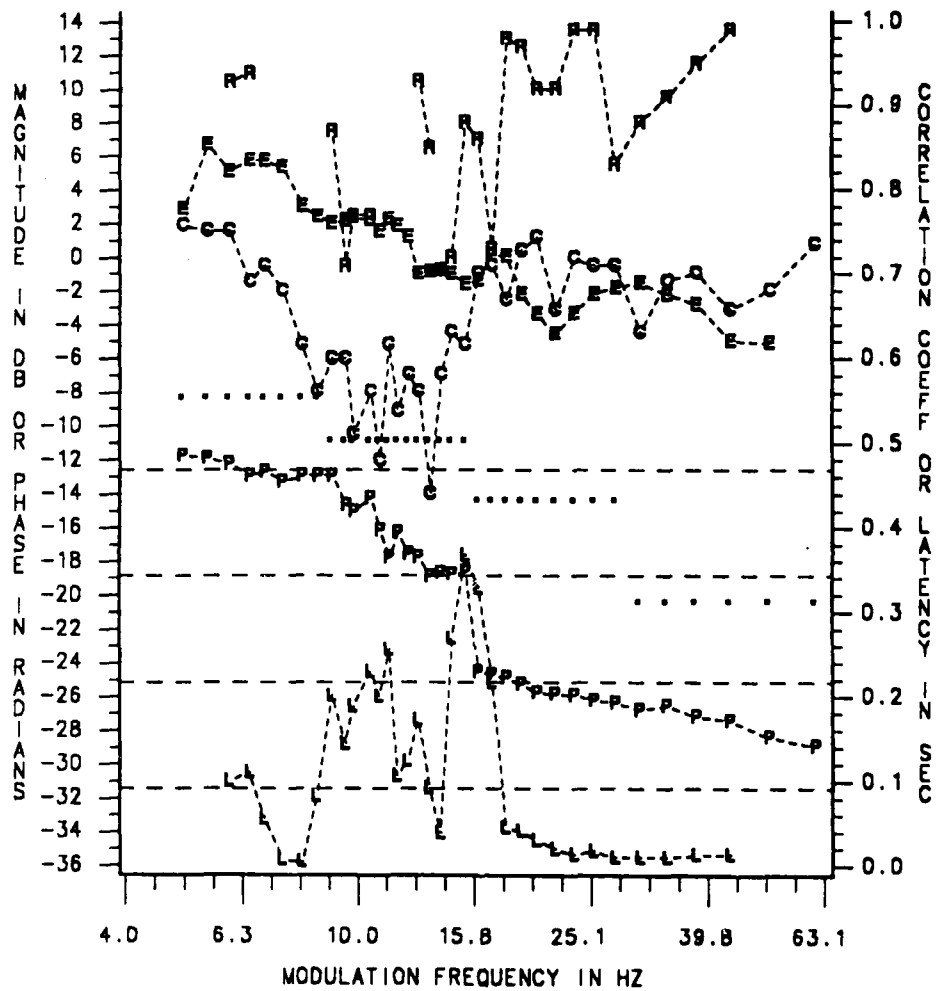


FIGURE II 4.11 : RECORDED FROM CZ-A1 (AUDIO) AND OZ-A1 (VISUAL) SITES. CEP(C), EEG(E), AND NOISE LEVEL (DOTTED LINE) MAGNITUDES IN DB. CEP PHASE(P) IN RADIAN, LATENCY(L) IN SEC AND LATENCY RELIABILITY (R, 1 IS THE HIGHEST, ONLY $R > 0.71$ VALUES ARE DISPLAYED). L (REGRESSION COEFF/6.29) AND R (CORRELATION COEFF) VALUES WERE ESTIMATED FROM A 5 PHASE-POINT-WIDE SLIDING WINDOW.

SUMMARY OF INDIVIDUAL RESPONSES

NAME=PM SIG=VISUAL

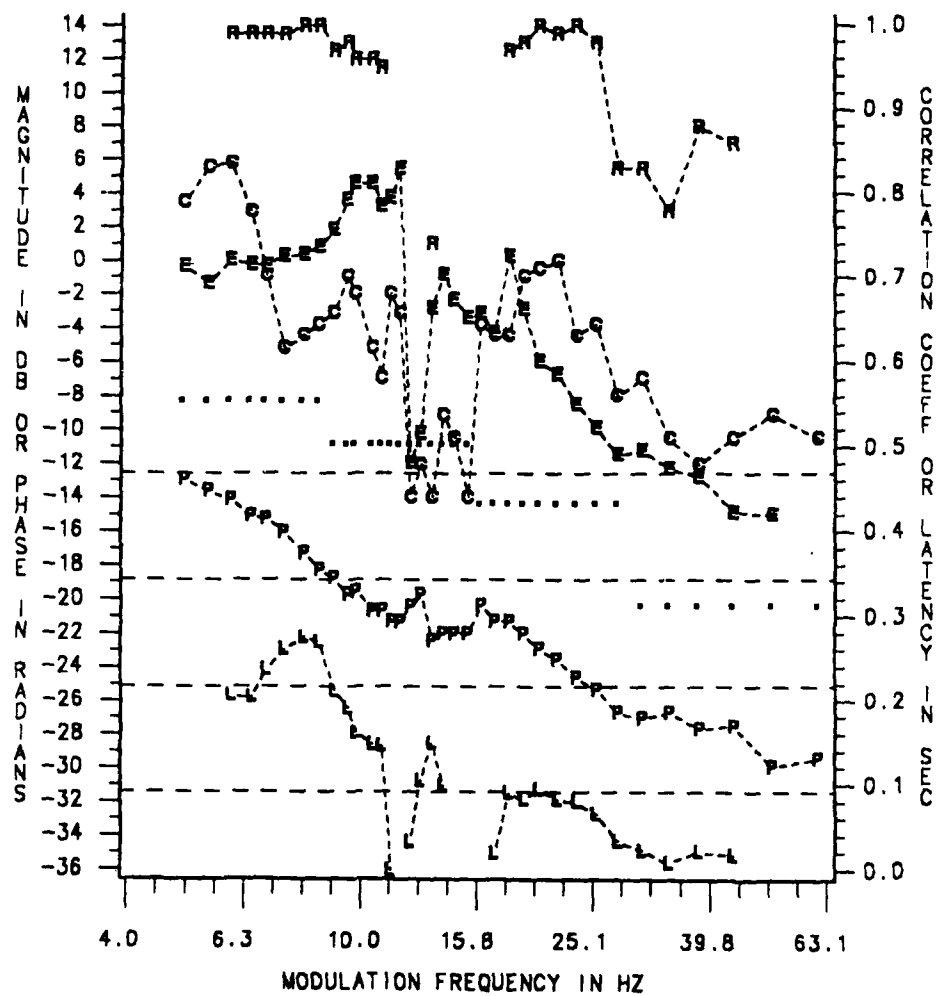


FIGURE II 4.11 : RECORDED FROM CZ-A1 (AUDIO) AND OZ-A1 (VISUAL) SITES. CEP(C),
 EEG(E), AND NOISE LEVEL (DOTTED LINE) MAGNITUDES IN DB. CEP
 PHASE(P) IN RADIANS, LATENCY(L) IN SEC AND LATENCY RELIABILITY
 (R, 1 IS THE HIGHEST, ONLY R>0.71 VALUES ARE DISPLAYED).
 L (REGRESSION COEFF/8.29) AND R (CORRELATION COEFF) VALUES
 WERE ESTIMATED FROM A 5 PHASE-POINT-WIDE SLIDING WINDOW.

SUMMARY OF INDIVIDUAL RESPONSES
NAME=RT SIG=AUDIO

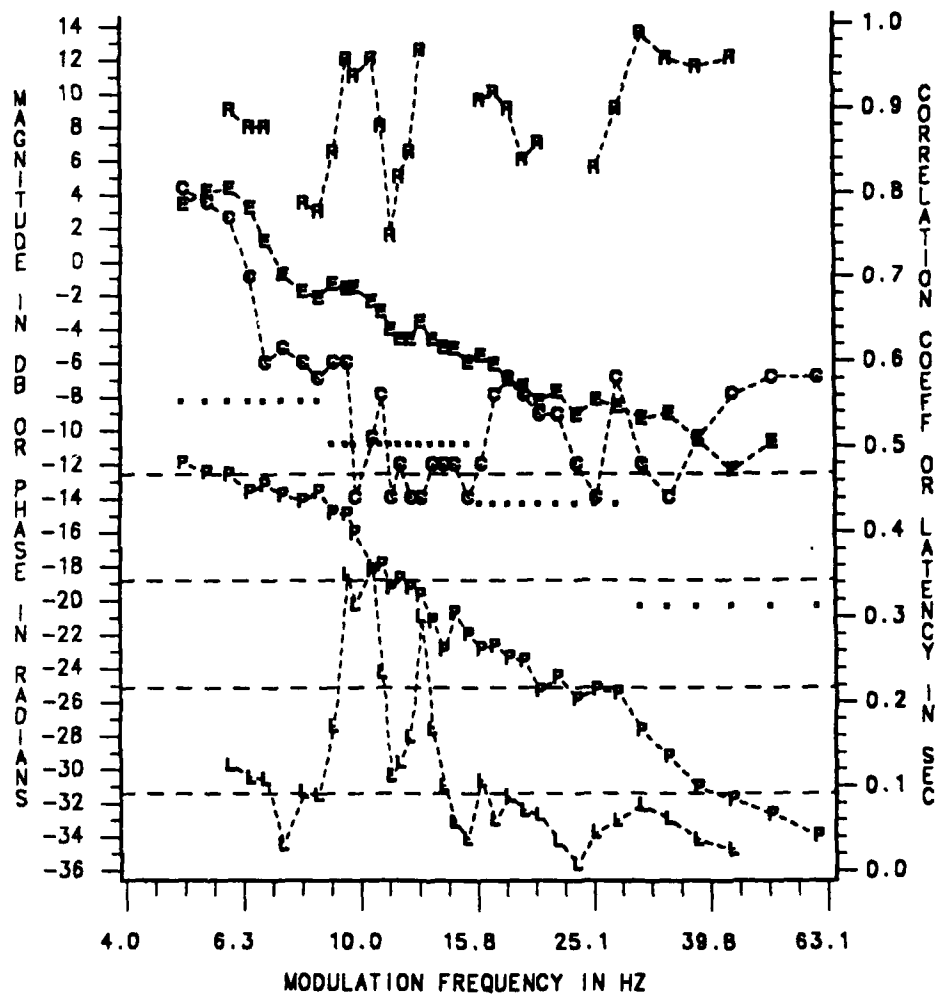


FIGURE II 4.11 : RECORDED FROM CZ-A1 (AUDIO) AND OZ-A1 (VISUAL) SITES. CEP(C),
EEG(E), AND NOISE LEVEL (DOTTED LINE) MAGNITUDES IN DB. CEP
PHASE(P) IN RADIANS, LATENCY(L) IN SEC AND LATENCY RELIABILITY
(R, 1 IS THE HIGHEST, ONLY $R > 0.71$ VALUES ARE DISPLAYED).
L (REGRESSION COEFF/6.29) AND R (CORRELATION COEFF) VALUES
WERE ESTIMATED FROM A 5 PHASE-POINT-WIDE SLIDING WINDOW.

SUMMARY OF INDIVIDUAL RESPONSES

NAME=RT SIG=VISUAL

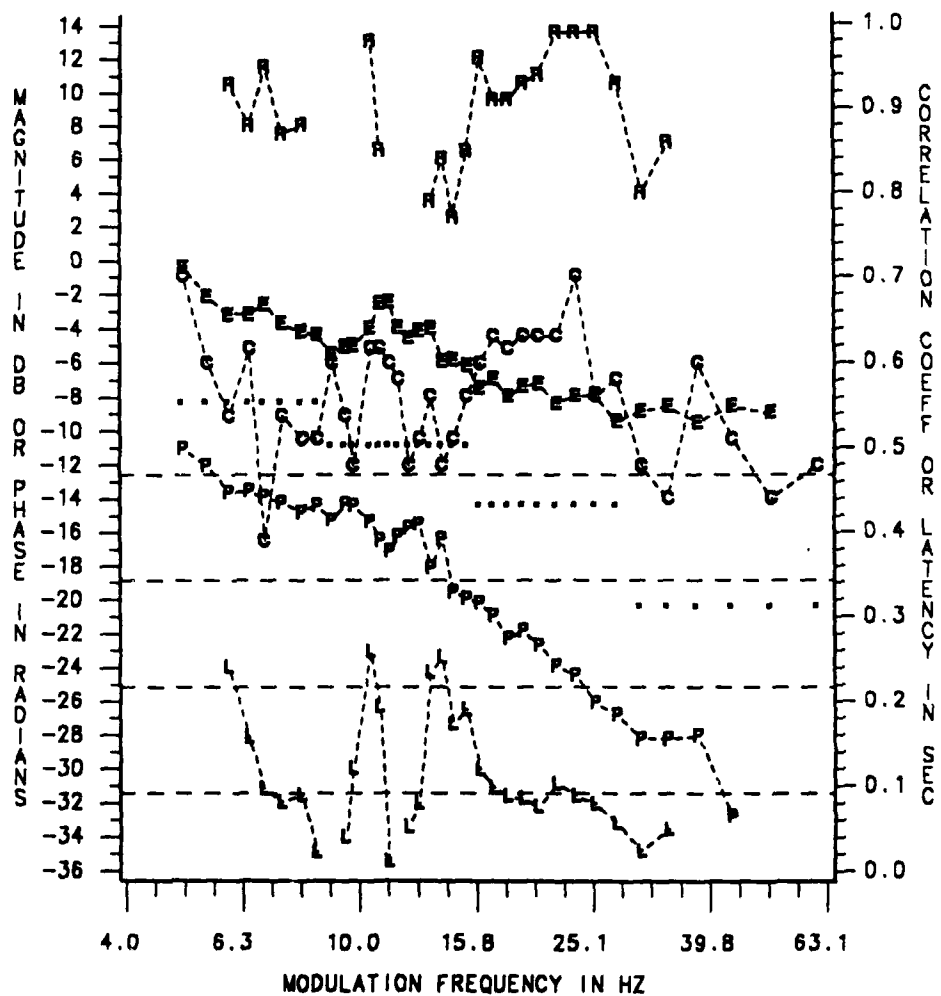


FIGURE II 4.11 : RECORDED FROM CZ-A1 (AUDIO) AND OZ-A1 (VISUAL) SITES. CEP(C), EEG(E), AND NOISE LEVEL (DOTTED LINE) MAGNITUDES IN DB. CEP PHASE(P) IN RADIANS, LATENCY(L) IN SEC AND LATENCY RELIABILITY (R, 1 IS THE HIGHEST, ONLY R>0.71 VALUES ARE DISPLAYED). L (REGRESSION COEFF/6.29) AND R (CORRELATION COEFF) VALUES WERE ESTIMATED FROM A 6 PHASE-POINT-WIDE SLIDING WINDOW.

SUMMARY OF INDIVIDUAL RESPONSES

NAME=SC SIG=AUDIO

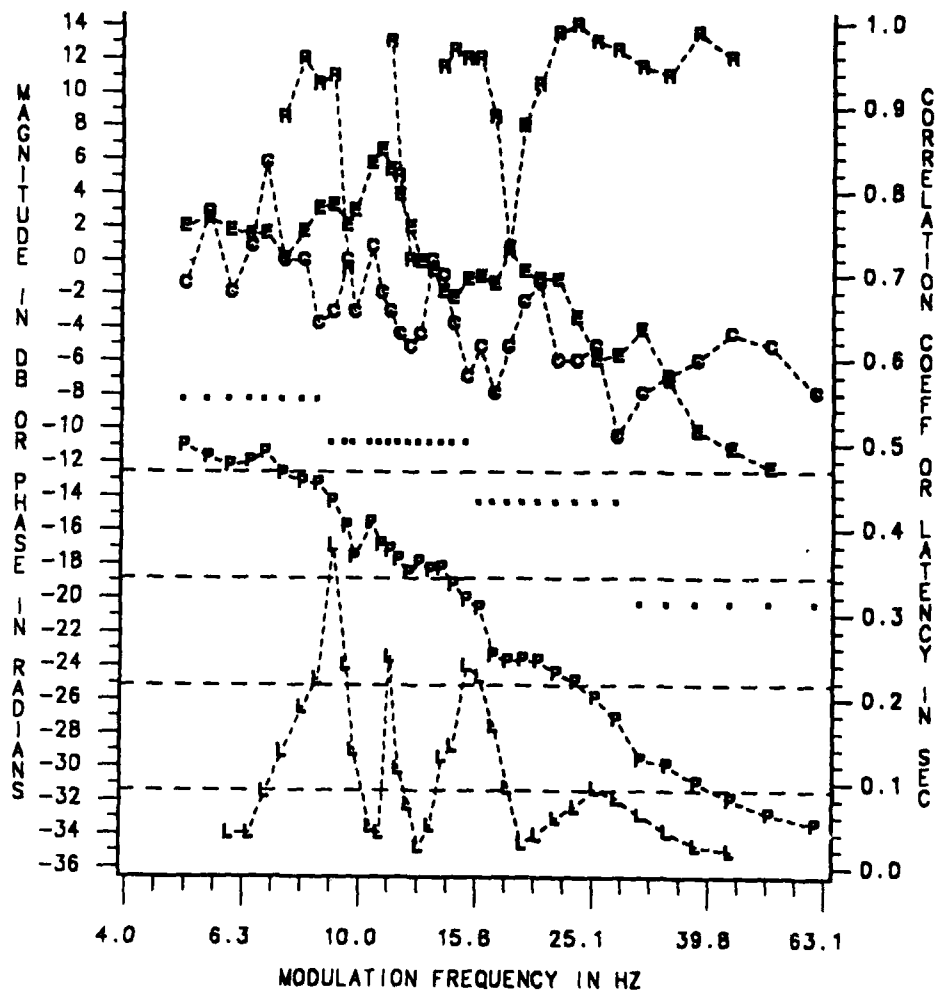


FIGURE II 4.11 : RECORDED FROM CZ-A1 (AUDIO) AND OZ-A1 (VISUAL) SITES. CEP(C),
EEG(E), AND NOISE LEVEL (DOTTED LINE) MAGNITUDES IN DB. CEP
PHASE(P) IN RADIANS, LATENCY(L) IN SEC AND LATENCY RELIABILITY
(R, 1 IS THE HIGHEST, ONLY R>0.71 VALUES ARE DISPLAYED).
L (REGRESSION COEFF/6.29) AND R (CORRELATION COEFF) VALUES
WERE ESTIMATED FROM A 5 PHASE-POINT-WIDE SLIDING WINDOW.

SUMMARY OF INDIVIDUAL RESPONSES

NAME=SC SIG=VISUAL

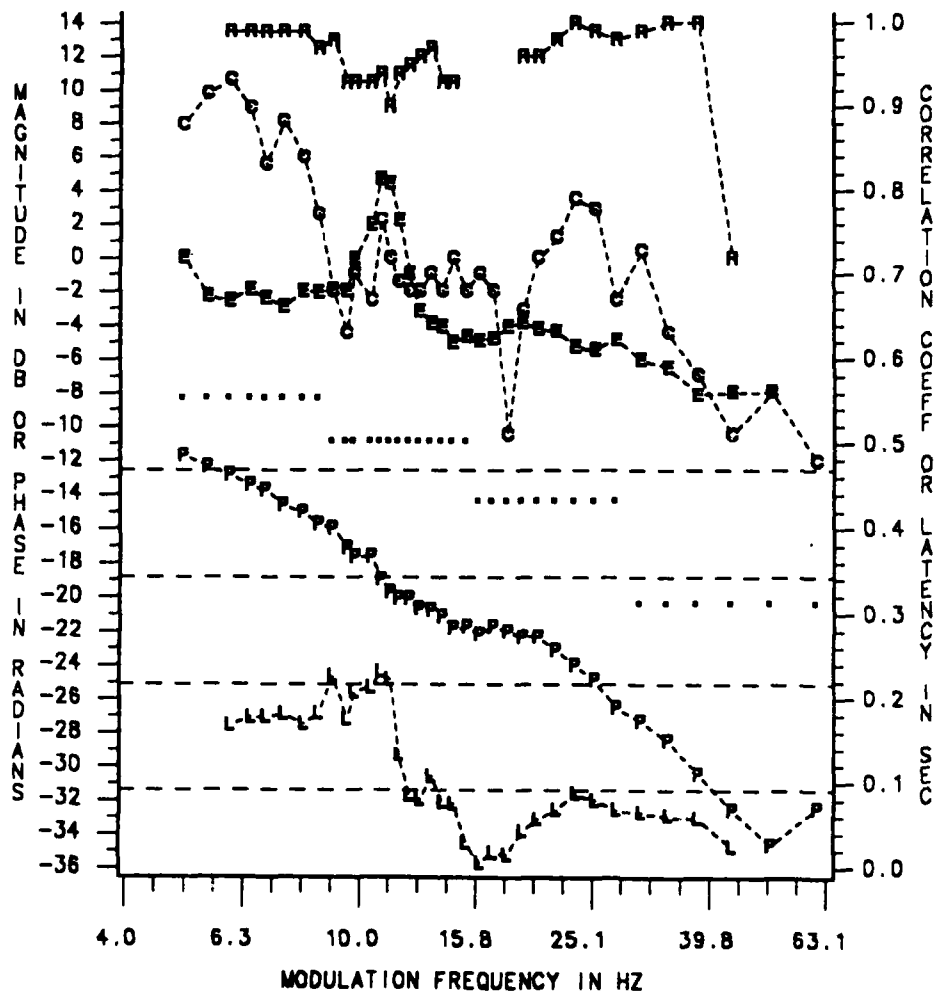


FIGURE II 4.11 : RECORDED FROM CZ-A1 (AUDIO) AND OZ-A1 (VISUAL) SITES. CEP(C),
EEG(E), AND NOISE LEVEL (DOTTED LINE) MAGNITUDES IN DB. CEP
PHASE(P) IN RADIAN, LATENCY(L) IN SEC AND LATENCY RELIABILITY
(R, 1 IS THE HIGHEST, ONLY R>0.71 VALUES ARE DISPLAYED).
L (REGRESSION COEFF/6.29) AND R (CORRELATION COEFF) VALUES
WERE ESTIMATED FROM A 5 PHASE-POINT-WIDE SLIDING WINDOW.

SUMMARY OF INDIVIDUAL RESPONSES

NAME=TN SIG=AUDIO

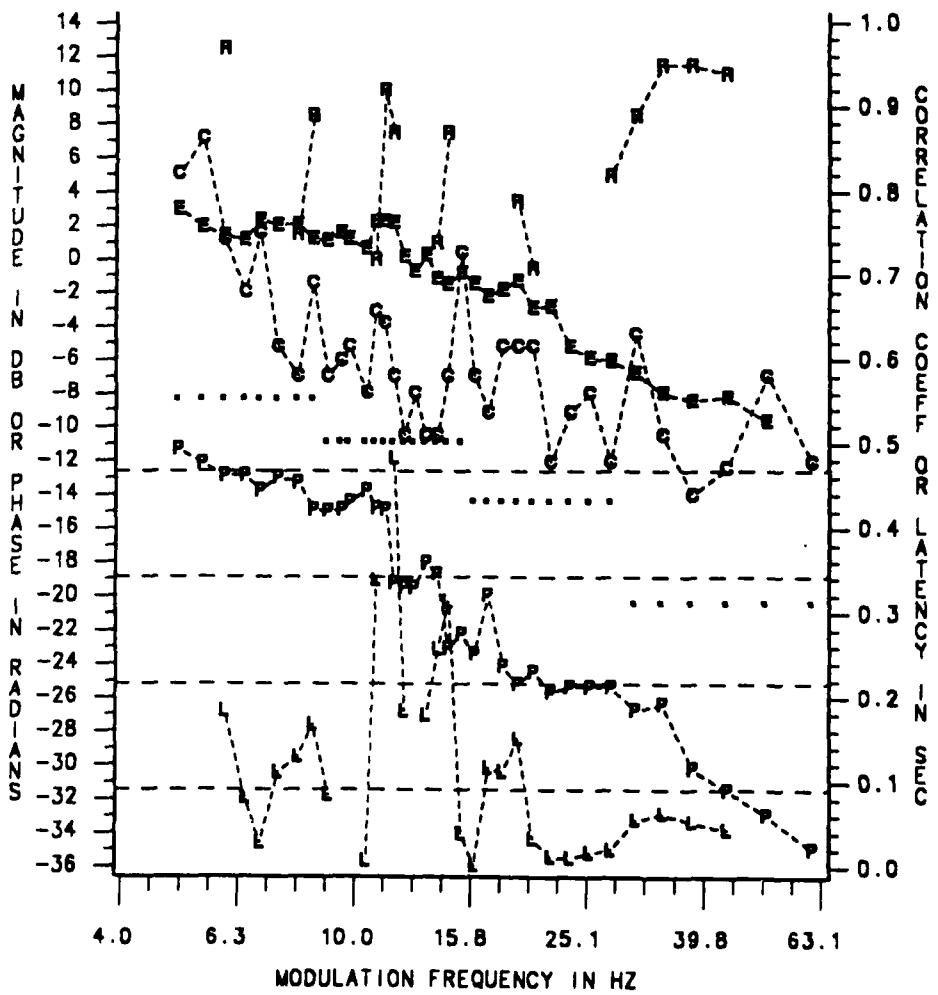


FIGURE II 4.11 : RECORDED FROM CZ-A1 (AUDIO) AND OZ-A1 (VISUAL) SITES. CEP(C),
EEG(E), AND NOISE LEVEL (DOTTED LINE) MAGNITUDES IN DB. CEP
PHASE(P) IN RADIANS, LATENCY(L) IN SEC AND LATENCY RELIABILITY
(R, 1 IS THE HIGHEST, ONLY R>0.71 VALUES ARE DISPLAYED).
L (REGRESSION COEFF/6.29) AND R (CORRELATION COEFF) VALUES
WERE ESTIMATED FROM A 5 PHASE-POINT-WIDE SLIDING WINDOW.

SUMMARY OF INDIVIDUAL RESPONSES

NAME=TN SIG=VISUAL

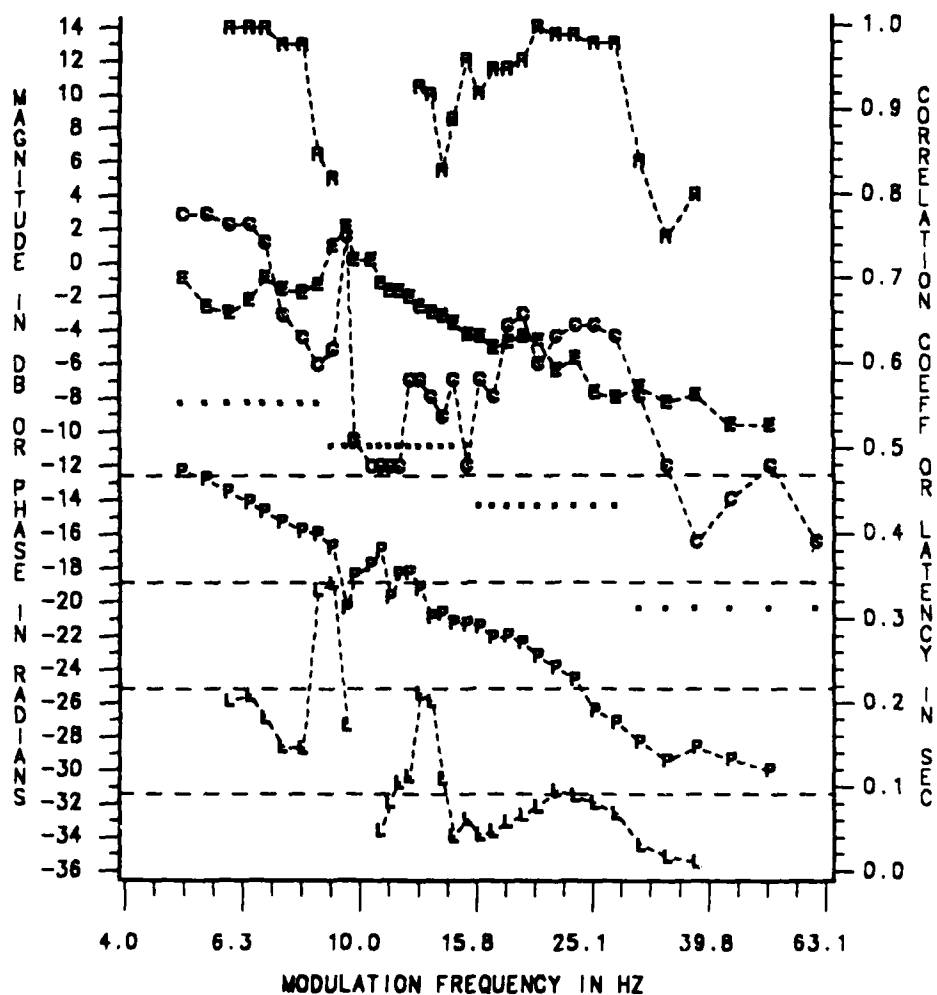


FIGURE II 4.11 : RECORDED FROM CZ-A1 (AUDIO) AND OZ-A1 (VISUAL) SITES. CEP(C), EEG(E), AND NOISE LEVEL (DOTTED LINE) MAGNITUDES IN DB. CEP PHASE(P) IN RADIAN, LATENCY(L) IN SEC AND LATENCY RELIABILITY (R, 1 IS THE HIGHEST, ONLY R>0.71 VALUES ARE DISPLAYED). L (REGRESSION COEFF/6.29) AND R (CORRELATION COEFF) VALUES WERE ESTIMATED FROM A 5 PHASE-POINT-WIDE SLIDING WINDOW.

Appendix B. Alphabetic List of Abbreviations

A	: auditory
AM	: amplitude modulat/ion
ANOVA	: analysis of variance
AP	: action potential
ATT	: attention or attended-to
AVD	: audio visual delay
AxV	: auditory-visual interaction
BI	: bimodal
BPF	: band-pass filter
BW	: bandwidth
CEP	: continuous evoked potential
CF	: cross-modal stimulus modulation frequency
CFF	: critical flicker frequency
CI	: cross-modal stimulus intensity
CMRR	: common-mode rejection ratio
CV	: coefficient of variability
DA	: differential amplifier
DAC	: digital-to-analog converter
DISC	: discrete
ECG	: electrocardiogram
EEG	: electroencephalogram
EMG	: electromyogram
EP	: evoked potential
ERCP	: event related cortical potential
FM	: frequency modulat/ion
FREQ	: frequency
GATE	: stimulus on/off signal
HL	: hearing level
HM	: "home made" device
HPF	: high-pass filter
IMI	: inter-modality interval
INT	: intensity
IPI	: inter-pattern interval
ISI	: inter-stimulus interval
IV	: independent variable
LIA	: lock-in amplifier
LPF	: low-pass filter
M	: absolute, compensated or relative magnitude
MANOVA	: multiple analysis of variance
MF	: modulation frequency

MOD	: stimulus number of modalities
MSE	: mean square error
MTF	: modulation transfer function
N	: number of elements
NAME	: subject code
NAT	: not-attended-to
NL	: magnitude noise level
NS	: not significant
P	: probability or absolute, compensated or relative phase
Q	: quality (filter sharpness) factor
R	: correlation coefficient
REF	: reference MF signal
REF*	: REF + the ac-coupled GATE signal
RMS	: root mean square
RMSE	: root mean square error
RT	: reaction time
S	: stimulus duration
SD	: standard deviation
SF	: intra-modal stimulus modulation frequency
SI	: intramodal stimulus intensity
SE	: standard error
SIG	: stimulus and CEP modality or electrical signal
SL	: sound level
SNR	: signal-to-noise ratio
SPL	: sound pressure level
TC	: time constant
TEP	: transient evoked potential
UNI	: unimodal
V	: visual
VS	: visual stimulator